

**ASSESSING THE STATE-DEPENDENT BEHAVIOR OF  
HUMAN SPINAL MOTONEURONS**

---

A Dissertation  
Submitted to  
the Temple University Graduate Board

---

In Partial Fulfillment  
of the Requirements for the Degree  
DOCTOR OF PHILOSOPHY

---

by  
Christopher Taylor  
May 2023

Examining Committee Members:

Christopher Thompson, PT, PhD, Advisory Chair, Health & Rehabilitation  
Sciences Department

W. Geoffrey Wright, PhD, Health & Rehabilitation Sciences Department

Francesco Negro, PhD, Università degli Studi di Brescia

Shivayogi Hiremath, PhD, Health & Rehabilitation Sciences Department

Laura McPherson, PT, PhD, External Reviewer, Washington University

## ABSTRACT

Spinal motoneurons (MNs) relay neural commands from the brain to the muscles to produce functional movement. However, MNs are more than passive conduits of neural commands; they also shape motor output through alterations in their intrinsic excitability. These alterations allow MNs to modify (e.g., amplify and/or prolong) motor output even in the absence of descending motor commands. How MNs respond to this modulation, under various conditions, is not fully understood. In the scope of this dissertation, we leverage high-density electromyography and motor unit decomposition algorithms to investigate how human MNs behave in (Aim 1) different muscles under similar task demands; (Aim 2) the same muscle under different task demands; and (Aim 3) in response to exogenous neuromodulation. First, in Aim 1 we demonstrate that MN excitability varies across motor pools and, thus, may be functionally tuned to the task and its muscle-specific demands. The results indicate that the MN discharge rates were significantly higher in the first dorsal interosseous, a small hand muscle used for fine motor control. Conversely, higher MN excitability was observed within the tibialis anterior, a lower leg muscle involved in balance and locomotion. Next, in Aim 2 we show that a muscle (i.e., the biceps brachii) with multiple biomechanical functions (e.g., supination and flexion) receives differential synaptic input to perform each action while the MN discharge characteristics remain the same. Finally, in Aim 3 we demonstrate that a single cup of coffee can alter fundamental motor control mechanisms by increasing discharge rate, inter-pulse variability, and excitability through caffeine-induced neuromodulation. Collectively, findings from this dissertation demonstrate the human motor system's tremendous ability to adapt to internal and external states.

## ACKNOWLEDGMENTS

I would like to express my gratitude to my wife, Tessa, for her unwavering patience and support throughout the process of creating this document. Her invaluable writing and editing tutorials over the years have been instrumental in helping me improve my skills. To anyone who may read this document, if it is at all comprehensible, you can thank Tessa for my basic grasp on the English language.

Special thanks to my NMS colleagues, particularly my lab mates Brian Kopicko and Matt Topley, for their support and encouragement throughout this challenging journey we have embarked upon.

I would like to express my gratitude to my committee members. Dr. Thompson, thank you for your continuous guidance and encouragement throughout my graduate student career. Your calming presence helped me stay on track and motivated to explore new ideas. Dr. Negro, thanks for your support and enthusiasm throughout this journey. Your expertise and assistance with analytical techniques and MU decomposition were invaluable to this dissertation. Drs. McPherson and Hiremath, your selfless donation of time and expertise, as well as your timely feedback and suggestions, proved vital to the completion of this project. Dr. Wright, I am grateful for the chance you gave me within the NMS program. Our stimulating academic discussions in and out of the classroom helped shape my scientific curiosity. I feel incredibly fortunate to have had the opportunity to work with all of you and cherish the memories and experiences I have gained in the NMS program.

Thank you!

# TABLE OF CONTENTS

	Page
ABSTRACT.....	ii
ACKNOWLEDGMENTS .....	iii
LIST OF TABLES.....	vii
LIST OF FIGURES .....	viii
CHAPTER 1	
INTRODUCTION AND REVIEW OF THE LITERATURE.....	1
Motoneuron Physiology .....	1
The Motor Unit .....	2
How Movement is Controlled at the Level of the Motor Unit .....	3
Persistent Inward Currents.....	5
Electromyography .....	7
Motor Unit Decomposition .....	8
Measurement of Common Synaptic Input .....	10
Measuring the Excitability of Motoneurons in Humans .....	12
Paired Motor Unit Analysis .....	15
Modulation of Motoneuron Excitability .....	16
Exogenous Modulation of Motoneurons .....	18
Caffeine Background .....	18
Caffeine Pharmacology.....	20
Specific Aims .....	21

Specific Aim 1 .....	22
Specific Aim 2 .....	22
Specific Aim 3 .....	23
 CHAPTER 2	
DIFFERENCES IN HUMAN MOTONEURON EXCITABILITY	
BETWEEN FUNCTIONALLY DIVERSE MUSCLES .....	
	24
Abstract.....	24
Introduction.....	25
Methods.....	27
Results.....	33
Discussion .....	34
 CHAPTER 3	
THE MOTOR COMMAND TO THE BICEPS BRACHII DURING	
DIFFERENT MODES OF ACTIVATION .....	
	39
Abstract.....	39
Introduction.....	40
Methods.....	42
Results.....	52
Discussion .....	55
Conclusion .....	61
 CHAPTER 4	
THE EFFECTS OF CAFFEINE ON HUMAN SPINAL MOTONEURONS .....	
	63
Abstract.....	63

Introduction.....	64
Methods.....	65
Results.....	76
Discussion .....	82
Conclusion .....	93
 CHAPTER 5	
CONCLUSIONS.....	99
Review of Specific Aims .....	99
Summary of Results .....	100
Aim 1 Summary .....	100
Aim 2 Summary .....	101
Aim 3 Summary .....	101
Limitations .....	103
Concluding Remarks .....	105
REFERENCES CITED.....	106
 APPENDICES	
A. RELATIONSHIP BETWEEN CAFFEINE CONSUMPTION AND OUTCOME VARIABLES .....	125
B. EFFECTS OF REPEATED CONTRACTIONS .....	128
C. CAFFEINE CONSUMPTION QUESTIONNAIRE .....	129
D. CHANGE IN STRENGTH OVER TIME .....	130
E. MUSCLE OR DISCHARGE RATE DEPENDENT .....	131

## LIST OF TABLES

Table	Page
1. Table 3.1. Motor Unit and Torque Characteristics.....	51
2. Table 3.2. Tracked Motor Unit Characteristics During HOLDs.....	62
3. Table 4.1. Torque and Torque Variability.....	94
4. Table 4.2. LMEM Marginal Mean Results from TA RAMPs.....	95
5. Table 4.3. LMEM Marginal Mean Results from TA HOLDs.....	96
6. Table 4.4. LMEM Marginal Mean Results from SOL RAMPs.....	97
7. Table 4.5. LMEM Marginal Mean Results from SOL HOLDs.....	98

## LIST OF FIGURES

Figure	Page
1. Figure 1.1. HDsEMG of Bicep.....	10
2. Figure 1.2. Paired Motor Unit Analysis.....	14
3. Figure 2.1. Experimental Setup for TA.....	29
4. Figure 2.2. Raw EMG and MU Spike Trains.....	30
5. Figure 2.3. Delta-F Between FDI and TA.....	32
6. Figure 2.4. TA vs FDI Motor Unit Discharge Characteristics.....	34
7. Figure 3.1. Biceps Flexion RAMP and Delta- F.....	47
8. Figure 3.2. HOLD Trial with Coherence Analysis.....	50
9. Figure 3.3. Delta-F and MaxDR Results.....	52
10. Figure 3.4. Flexion vs Supination Torque Control.....	53
11. Figure 3.5. Flexion vs Supination MU HOLD Results.....	54
12. Figure 4.1. Experimental Design.....	67
13. Figure 4.2. Paired Motor Unit Analysis of Tracked MUs.....	73
14. Figure 4.3. Cardiovascular Response to Caffeine.....	77

15. Figure 4.4. Tracked MU Discharge Characteristics - RAMPs.....	80
16. Figure 4.5. Tracked MU Discharge Characteristics - HOLDS .....	82
17. Figure 4.6. Impact of CAF Consumption on MAP and Delta-F .....	90
18. Figure A.1. Mean Arterial Pressure vs Caffeine Use .....	125
19. Figure A.2. Heart Rate vs Caffeine Use .....	126
20. Figure A.3. Delta-F vs Caffeine Use .....	126
21. Figure A.4. Maximum DR vs Caffeine Use .....	127
22. Figure B.1. Effects of Repeated Contractions on DeltaF.....	128
23. Figure C.1. Caffeine Consumption Questionnaire.....	129
24. Figure D.1. Change in Maximum Strength.....	130
25. Figure E.1. DeltaF Across MaxDR of TA.....	133
26. Figure E.2. DeltaF Across MaxDR of SOL.....	134

## CHAPTER 1

### INTRODUCTION AND REVIEW OF THE LITERATURE.

#### **Motoneuron Physiology**

A motoneuron (or motor neuron; MN) is a type of neuronal cell that carries electrical signals, or impulses, from the central nervous system (CNS) towards the muscles throughout the body to aid in movement. There are two classifications of MNs, based on their location within the CNS: upper and lower (Stifani, 2014).

Upper MNs, are located within the primary motor cortex, the supplementary motor area, and the pre-motor cortex (Purves et al., 2001). Upper MNs have the ability to initiate, modulate, or inhibit the activity of lower MNs, aiding in the control of movement. The axons of upper MNs descend the spinal cord, organized into discrete tracts. The majority of the upper MNs responsible for volitional control of muscle, cross to the contralateral side of the brain stem (i.e., decussation) before ultimately synapsing in the spinal cord with cells of lower MNs, often via interneurons (Kandel et al., 2012).

Lower MNs are located within the brain stem and the ventral horn of the spinal cord. These lower MNs receive a plethora of synaptic information, regulating their output, from neighboring cells including upper MNs, sensory neurons, and interneurons (Lemon, 2008). These lower MNs are then divided into smaller sub-classifications: gamma and alpha MNs.

Gamma MNs innervate intrafusal muscle fibers, which don't contribute to direct musculoskeletal movement but control the sensitivity (gain control) of muscle spindles, which sense how much and how fast a muscle is lengthened or shortened. Gamma MNs,

through the modulation of muscle spindles, allows the nervous system to fine-tune the sensitivity of muscle stretch receptors and thus refine movement control (Eccles, 1964).

Alpha MNs innervate extrafusal muscle fibers, which are the muscle fibers that are responsible for generating force and movement. These are the main neurons that control the contraction of skeletal muscle fibers, they are located in the ventral horn of the spinal cord and send axons to the muscle fibers they innervate. These MNs represent “the final common pathway” for motor commands coming from the brain (Sherrington, 1904). In other words, they receive inputs from upper MNs and all other sources within the spinal cord, integrate them, and send the final motor commands to the muscles and organs they innervate.

For the remainder of this paper, all instances of “MN” are intended to represent spinal alpha motoneurons, except where explicitly mentioned otherwise.

### **The Motor Unit**

A motor unit (MU) is the basic functional unit of the motor system. It consists of a single MN and all of the muscle fibers that it innervates (Adrian & Bronk, 1929). The number of muscle fibers in each MU can vary, based on the type and function of the muscle (or motor pool) it resides within. Furthermore, the number of MNs (and thus MUs) within a particular motor pool can also vary. For example, MUs in muscles used for fine movements, like those controlling the movement of the eye, tend to have fewer muscle fibers per unit than motor units in muscles used for gross movements, like those in the thigh (Heckman & Enoka, 2012). This ratio of muscle fibers innervated by each MN axon is referred to as the innervation ratio and often reflects the functional properties of the parent muscle.

The connection between the axon terminal of the MN and muscle fibers within a MU forms a structure called the neuromuscular junction. This junction provides a relatively large safety factor for the transmission of neural signals, such that the discharge of a MN and the activation of its corresponding muscle fibers have a one-to-one connection (Wood & Slater, 2001). Furthermore, since it is often the case each MN is attached to dozens (if not hundreds) of muscle fibers, when a MN discharges, the corresponding muscle fibers act to amplify this signal (De Luca, 1997). It is through this mechanism, and the propagation of action potentials along the muscle fibers of a MU, that many of the references provided in this dissertation, are able to observe changes with such high-fidelity in the human neuromuscular system (see below section – *Electromyography*). Additionally, because of the inter-connected nature and functional similarities of MNs and their MU's, these terms are often conflated and used interchangeably, despite nuanced anatomical differences.

### **How Movement is Controlled at the Level of the Motor Unit**

To create meaningful movement through the contraction of muscles, MUs regulate force production through two well-established mechanisms: (1) by recruiting more motor units to contribute to a specific task (i.e., *recruitment*); and 2) by increasing the discharge rate of the motor units already active (i.e., *rate coding*) (Henneman, 1957; Milner-Brown et al., 1973; Monster & Chan, 1977). Fortunately, the regulation of these processes is largely based on the intrinsic properties of each type of MN and not left to volitional control.

The control of MUs within a motor pool constitutes a crucial aspect of normal human movement. Henneman's "size principle" governs the order of MU recruitment

based on the fixed physical and electrical properties of the parent motoneuron. Moreover, the discharge rate of a MU is associated with the physical properties of the parent motoneuron, and its variation is proportionate to the level of synaptic input received (Enoka & Duchateau, 2017).

These principles are based on a series of seminal studies, that guided earlier neuromuscular researchers, like Henneman, to investigate regulatory properties of motor control. By measuring the size of MNs, assessed by the size of their extracellular action potentials, Henneman and colleagues (Henneman et al., 1974) demonstrated the “orderly” recruitment of MNs based upon their size. Such that smaller MNs are recruited first, and generally discharge at higher frequencies, than MNs that are recruited later and discharge at much lower frequencies. These properties would later inspire the work of De Luca and Erim (De Luca & Erim, 1994), which termed a model of MU control the “onion skin”. This model is named so for the inverse relationship between firing rates and recruitment order observed when plotted (during symmetrical ramp contractions), resembling the concentric layers of an onion when chopped in half. Further experiments confirmed these initial findings through assessments of additional MN properties such as the conduction velocity of MNs, ratio of rheobase current and the input resistance of MNs (Burke et al., 1973; Clamann et al., 1974; Fleshman et al., 1981; Gordon et al., 1999; Kernell & Zwaagstra, 1981; Olson et al., 1968). In totality, these regulatory properties provide a smooth gradation of force output, in which the progressive recruitment of more MNs provides a steady increase in force.

For nearly half a century, MNs were assumed to act as mere conduits for motor commands sent from the brain to the muscle, relying on these underlying regulatory

properties to regulate force output. However, more recent work (Heckman et al., 2005; Lee & Heckman, 1996) supports the existence of neuromodulatory changes in levels of MN excitability to further explain the full repertoire of MU behavior. These mechanisms allow the MN to augment the motor command, in a non-linear fashion, creating an additional layer of complexity in controlling human movement.

### **Persistent Inward Currents**

Challenging earlier assumptions of highly linear behavior, it is now known that MNs can intrinsically amplify and prolong the synaptic input from the central nervous system (Lee et al., 2003; Lee & Heckman, 1998). These newly discovered properties of MNs are voltage-dependent and regulated by monoamines (*i.e.*, norepinephrine and serotonin) released from the brainstem (Perrier, 2005). The release of monoamines results in intrinsic changes to the excitability of MNs through the activation of persistent inward currents (**PICs**) on the soma and proximal dendrites, which are primarily caused by fast-activating voltage-gated sodium and slow-activating calcium channels (Heckman et al., 2005; Lee & Heckman, 1996). These changes in electrical properties of MNs, as a result of PIC activation, creates a non-linear input-output relationship which complicates typical MN behavior.

Once PICs are activated, they can both accelerate the initial MN firing and contribute to the repetitive firing required for sustained muscle contraction. This amplification observed from PIC activity is proportional to the levels of monoamines present at the MN (Heckman et al., 2005; Lee et al., 2003). As a functional consequence, the MN is able to remain active even after descending synaptic drive has lessened or ceased (Lee & Heckman, 1996). The neuromodulatory effect from fluctuations in

monoamines present, is critical to normal physiological function of MNs (Heckman & Enoka, 2012). In fact, it is estimated that without the effects of monoaminergic neuromodulation, the basal MN activity produces less than 50% of the maximum motor output (Heckman, 1994; Heckman et al., 2008). As a result, understanding the extent to which the human motor system controls PICs is essential to investigate.

Due to the difficulties associated with directly measuring transmembrane currents, the majority of evidence for understanding PIC physiology resides within animal models. For example, within reduced cat and turtle MN experiments (in which the brain stem may be partially severed), the administration of exogenous monoamines can be utilized to elicit hysteresis in MN firing profiles, causing continued activation at levels of depolarizing input that would otherwise be below the threshold for activation (Bennett et al., 1998; Hounsgaard et al., 1988; Hounsgaard & Kiehn, 1989; Lee & Heckman, 1996). This extra current and resulting hysteresis are provided in large part by the activation of PICs.

Unfortunately, unlike the animal model, direct observation of PIC activity in human MNs is not yet possible. However, it is possible to infer underlying cellular process from the discharge of pairs of individual MUs because of the one-to-one relationship between the MN's action potential and resultant action potential of the associated muscle fibers (Duchateau & Enoka, 2011). These inferences are possible due to electromyography.

In addition to providing an essential role in the regulation of normal motor control, there is new evidence suggesting disruptions in the regulation of monoamines (and PIC behavior) may lead to clinically significant symptomology in a wide range of

disease conditions including stroke, spinal cord injury, and amyotrophic lateral sclerosis (ElBasiouny et al., 2010; McPherson et al., 2008; Murray et al., 2010). The effects of drugs which act on the monoaminergic system (that regulate PICs), provide an alluring genre of research which is underexplored (Udina et al., 2010).

## **Electromyography**

Electromyography (EMG) is a useful tool to aid in observing the neuromuscular system. Essentially, EMG acts similarly to a voltmeter that an electrician might use when conducting house repairs, to measure the presence of electrical currents in wires. In neuromuscular science, EMG is able to measure the depolarization and hyperpolarization (changes in voltage) that occur along the surface of the muscle fiber membrane (sarcolemma), during muscular contractions (Vigotsky et al., 2018). These changes in voltage are due to the motor unit action potentials (MUAP) propagating along the sarcolemma, as a result of the parent MN firing. Through these observations, each MUAP corresponds to the discharge of a MN, creating a metaphorical window through which we can observe the human nervous system.

The interpretation of electrophysiological signals from muscle and MNs have been utilized for nearly a century (Adrian & Bronk, 1929). Many early experiments utilized invasive forms of EMG (intramuscular EMG, iEMG), in which a small needle electrode would be inserted into the muscle belly and the input-output dynamics of MNs and muscle contraction could be observed. Surface EMG (sEMG) allows for these recordings to be captured non-invasively, through the skin. The use of both iEMG and sEMG have allowed for massive insight into motor control, however, each have methodological and technical limitations that have been well documented (De Luca,

1997; Farina, 2006; Vigotsky et al., 2018). In short, iEMG provides a high fidelity view of MUAP and MU activity, however, it is spatially restricted to a very small volume of tissue next to the recording needle (Duchateau & Enoka, 2011). It is common for iEMG to only record from a single MU at a time. Furthermore, iEMG is an invasive procedure requiring the insertion of a needle through the skin of the participant. While pain during this procedure is limited, this often becomes prohibitive to use within vulnerable subject populations, requires additional ethical approval, and requires the use (and training of) sterile medical techniques. Contrarily, sEMG captures a relatively large volume of electrical signals through the skin but is much less selective, less sensitive, and is prone to noise (Farina, 2006). Furthermore, the interpretation of sEMG amplitude is fairly limited because of the inability to differentially determine rate coding from recruitment in force generating (Vigotsky et al., 2018). Because of these methodological limitations, accurately assessing the non-linear behavior of MUs (and MNs) is difficult with the use of conventional EMG techniques.

### **Motor Unit Decomposition**

Recent advancement in technology now allows for a new approach to accurately observe the behavior of MUs. High-density surface EMG (HDsEMG), multi-channel (commonly 10 to 128+ channels) electrode arrays, are being used in conjunction with EMG decomposition algorithms to observe the concurrent activity of dozens of active MUs (Thompson et al., 2018) (See Figure 1.1). EMG decomposition algorithms apply various types of signal component analysis, which require multiple EMG observations to accurately identify unique MU activity (Farina & Holobar, 2016). A version of convolutive blind source separation is commonly utilized for this purpose (Holobar et al.,

2010; Negro et al., 2016). This technique, not unique to neuromuscular science, attempts to extract a unique, individual, signal from a mixture of multiple signals. Through the temporal and spatial identification of MUAP waveforms across the multi-channel array, unique MUs (and thus MNs) are able to be tracked with a high degree accuracy throughout the duration of an experiment. Furthermore, it is possible to accurately identify the same MU at a much later time, for example during follow up experiments (Del Vecchio et al., 2020; Martinez-Valdes et al., 2017).

Utilizing these new techniques, it is possible to observe the behavior of the motor system with much higher fidelity. Furthermore, the ability to observe large populations of concurrently active MUs, not just single unit recordings, offers the possibility for much greater insight into the non-linear properties of MNs and the synaptic control of them (Muceli et al., 2015).

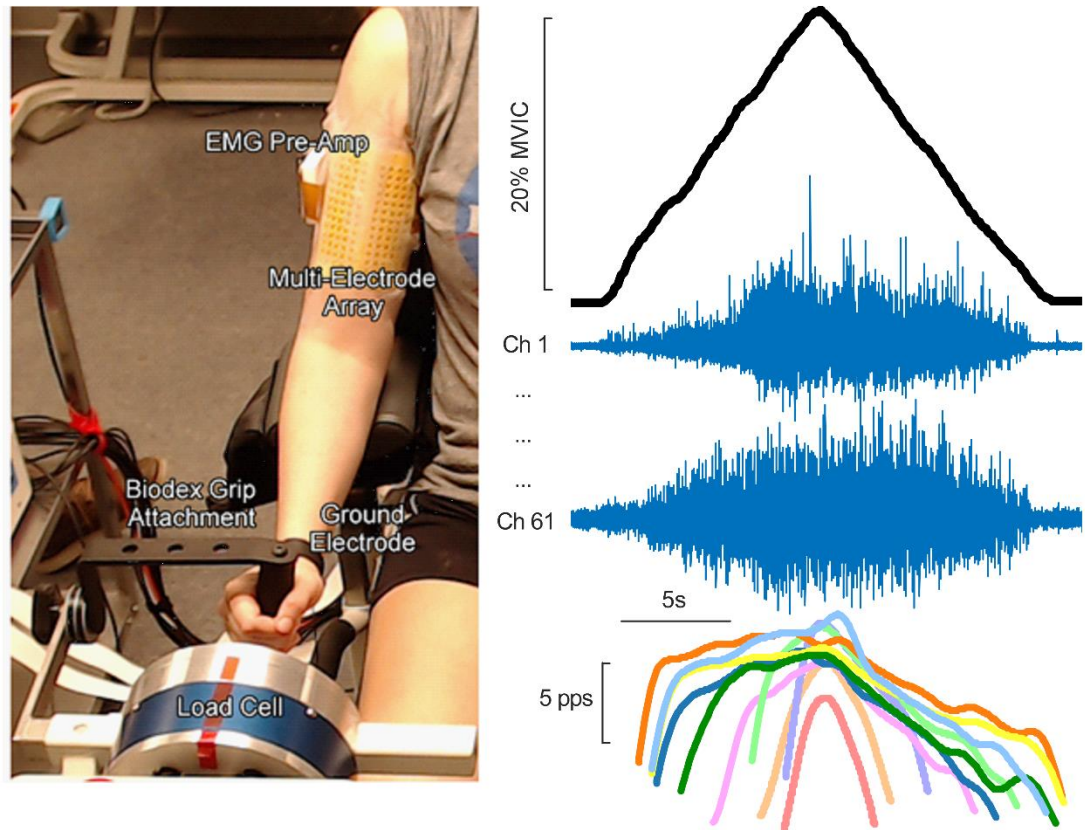


Figure 1.1. HDsEMG of Bicep. Left: Example of a common experimental setup; 64-channel high-density surface electromyography arrays located on the anterior surface of the biceps brachii, with a manipulandum attached to a load cell to measure forces and torques. Right: Bold black line represents torque feedback. Light blue lines represent surface EMG from 2 available channels of one HDsEMG array during a “ramp” shaped, flexion contraction. Bottom Right: Smoothed instantaneous discharge times from 10 decomposed motor units of the same contraction.

### Measurement of Common Synaptic Input

By leveraging HDsEMG and MU decomposition algorithms, it is possible to observe common fluctuations in MN discharge, which can indicate modulation from descending synaptic inputs (Farina & Negro, 2015). Intra-muscular coherence analysis allows for the estimation of the common synaptic input to a single motor pool, through the inspection of the discharge characteristics of individual MNs within that same muscle. Specifically, coherence provides a value of the correlation in the frequency of

synaptic inputs shared between pools of MNs within a single muscle (Laine et al., 2015; Zaback et al., 2022). To facilitate comparisons across subjects and conditions, coherence values are typically converted to standard Z-scores, and the area under the curve of physiologically relevant frequency bins are used for statistical analysis (e.g., Delta band 0-5Hz, Alpha band 5-15Hz, Beta band 15-35Hz).

Although there is a comprehensive understanding of the anatomical factors involved in force production in human muscles, the process of how MNs transform synaptic information into neural commands for muscles is still not fully understood. The main reason for this discrepancy is the difficulty of making *in vivo* observations of these neurons in humans. However, coherence analysis provides a non-invasive opportunity to observe these behaviors during naturalistic voluntary muscular contractions. Previous investigations suggest that alterations in low-frequency coherence (Delta band), also known as common drive (De Luca & Erim, 1994), may be directly related to the control of voluntary force output and can reflect changes in force variability (Castronovo et al., 2015; Farina & Negro, 2015; Negro et al., 2009). Alterations in Beta band coherence may be due to specific input from the motor cortex, pyramidal tract neurons, and/or other task-specific motor information such as grip aperture adjustments (Baker et al., 1997; Kilner et al., 1999; Wang et al., 2020; Yang et al., 2009). Furthermore, Alpha band alterations may represent changes in multimodal input from various cortical and spinal sources (McAuley & Marsden, 2000; McKiernan et al., 2000). This technique provides valuable insights into estimating synaptic input into the motor pool, allowing for comparisons within and between experimental conditions.

## **Measuring the Excitability of Motoneurons in Humans**

Understanding the full repertoire of MNs requires demystifying the non-linear behavior that they often display. One large influence on non-linear firing behavior in MNs is related to changes in MN excitability through the activation of PICs (Lee & Heckman, 1999). Measuring and quantifying these effects in humans has been difficult. Other studies have relied on measuring MN excitability in humans through the use of an electrical-stimulation induced spinal reflex, known as the H-reflex (Kalmar & Cafarelli, 1999; Knikou, 2008). This indirect measure of MN excitability is performed by providing an exogenous electrical stimulation of a peripheral nerve and recording the subsequent motor output with EMG (Pierrot-Deseilligny & Mazevet, 2000).

The H-reflex is similar to the traditional “tendon-tap” (stretch) reflex, routinely used in medical exams, and can be used to study the excitability and reflex pathways of MN and its afferent input. However, unlike the stretch reflex, the H-reflex bypasses the muscle spindles, providing further investigative capabilities of the monosynaptic reflex arc. The H-reflex can also be used to assess the function of the spinal cord and peripheral nerves, and evaluate the effects of various interventions, such as spinal cord injury, nerve injury, and certain diseases, on the nervous system (Palmieri et al., 2004). Typically, this proxy measure is quantified by calculating the amplitude of the resultant EMG waveforms, as well as other derivations of similar measures (Funase et al., 1994).

In addition to its investigative clinical use, the H-reflex has also been utilized by researchers as a proxy measure to quantify MN excitability. However, this technique has numerous limitations when trying to infer specific mechanisms and interpretations related to MN excitability (Misiaszek, 2003; Palmieri et al., 2004). Most notably, the H-reflex is an electrically induced reflex arc that does not naturally occur within the human body,

limiting its ability to generalize its interpretation to naturalistic motor control of MNs. Further, there is a common misconception that the H-reflex is derived purely from the stimulation of Ia afferents, projecting monosynaptically onto the parent MN, and the resultant H-reflex accurately represents MN excitability (Knikou, 2008; Misiaszek, 2003; Palmieri et al., 2004). It has been demonstrated that oligosynaptic inputs and presynaptic modifications readily contribute to alterations of H-reflex amplitude (Burke et al., 1984; Pierrot-Deseilligny et al., 1981). Lastly, while H-reflex amplitude can be altered by state changes in motor pool excitability, this relationship is not mutually exclusive, and misunderstanding these nuanced limitations may lead to erroneous interpretations of quantifying MN excitability in humans (Knikou, 2008; Misiaszek, 2003; Palmieri et al., 2004).

## Paired Motor Unit Analysis

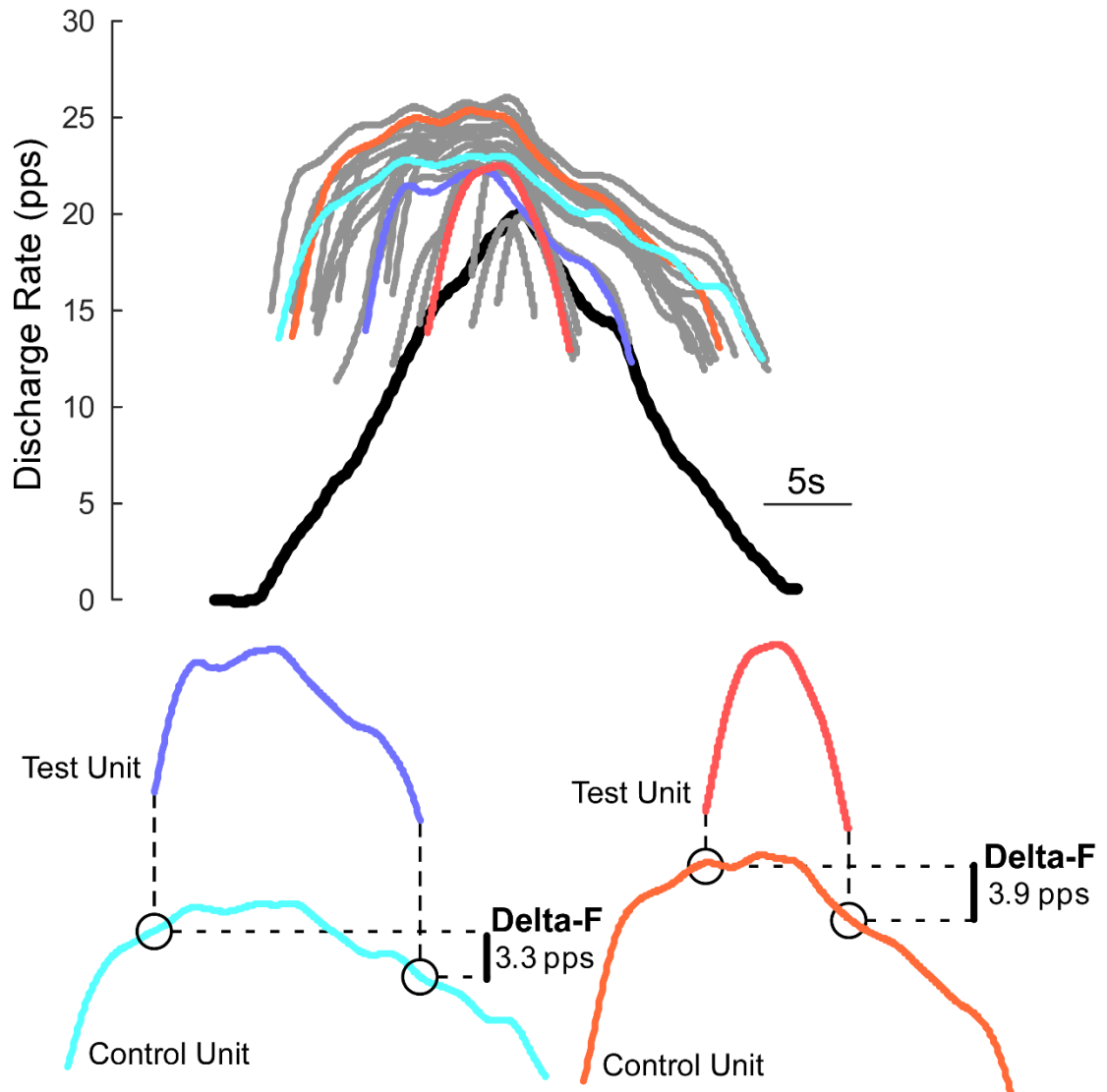


Figure 1.2. Paired Motor Unit Analysis. Top: Torque (black) and all available decomposed motor units (grey). Bottom: Two examples of test and control units utilized for the paired motor unit analysis (Delta-F).

## Paired Motor Unit Analysis

During a series of experiments investigating the non-linear behavior of MNs in humans, Gorassini and colleagues (Gorassini et al., 2002a, 2002b), introduced a new technique for estimating the effects of PICs in human MNs. This new technique, the “paired motor unit analysis” (i.e., Delta-F;  $\Delta F$ ), provides the ability to estimate the contribution and amplitude of PICs on the activation of MUs. This technique involves recording the discharge activity of (at least) two MUs during a triangular-shaped, symmetrical, “ramp” contraction (See Figure 1.2). Then, the time at which a higher threshold MU (aka. “test unit”) is recruited and derecruited is found and normalized to the firing frequency of a low-threshold MU (aka. “control” unit). Then, the difference in discharge rate of the low-threshold MU, at the time when the higher MU is recruited and subsequently de-recruited, is calculated as  $\Delta F$ . Under high levels of PIC activity (and thus excitability), in a case where increased values of  $\Delta F$  may be observed, the synaptic current needed to reach threshold will be lowered and a lower derecruitment threshold will be observed and the change in discharge rate (i.e.,  $\Delta F$ ) will be calculated. It is through these methods that Gorassini (Gorassini et al., 2002a) first estimated that PICs are responsible for ~40% of the rate modulation in MUs during these contractions, exemplifying their functional significance. Heckman and colleagues (Heckman et al., 2009) would later claim this number to be an underestimation of true PIC amplitude.

Since its inception, the  $\Delta F$  calculation, has been validated in numerous studies (Gorassini et al., 2004; Heckman et al., 2009; Powers et al., 2008). Until recently,  $\Delta F$  calculations were performed largely through the use of iEMG on humans and animal models, and only included a small number of MU comparisons. However, with the utilization of non-invasive, HDsEMG arrays and MU decomposition techniques the

number of valid motor unit comparisons possible has increased significantly. By utilizing HDsEMG in humans, we are now able to measure  $\Delta F$ , not only at single MU level, but at the level of entire populations of MUs (motor pools). These population measures of human MN discharge provide us with a new means to quantify the distribution of excitability within motor pools, across motor pools, and in response to exogenous neuromodulation.

### **Modulation of Motoneuron Excitability**

The modulation of MN excitability is largely influenced by monoamines (*e.g.*, serotonin and norepinephrine) through the activation of PICs. The resulting PICs can enhance synaptic currents by fivefold (Heckman & Enoka, 2012), resulting in profound functional implications. However, the inability to readily observe these fluctuations in human subjects has limited its understanding and significance. The innovations in HDsEMG and MU decomposition algorithms now allow for the quantification of PIC amplitude (Gorassini et al., 2002a) and better understanding of the non-linear behavior of MNs.

Previous electrophysiological studies, utilizing decerebrate feline and rat models, have demonstrated larger PIC magnitudes in extensor motor pools, than flexor motor pools (Cotel et al., 2009; Hounsgaard et al., 1988). These preliminary reports demonstrate the potential for PIC activity to vary between motor pools. More recently, Wilson and colleagues (2015) observed similar findings in humans, utilizing the paired-motor unit analysis technique (Gorassini et al., 2002a). Similarly, our preliminary studies have shown significant variation in MN excitability between functionally-different motor pools within the same subjects (Taylor et al., 2020). Further, we suggest that there may

be a functional distribution of PIC activity, across motor pools, that may aid in task- and function-dependent motor control. For example, the estimated PIC amplitude of a postural-support muscle may be much greater than that of a muscle responsible for fine-motor control. This potential disparity in PIC amplitude, across motor pools, could aid the motor system in achieving functionally specific goals. Additionally, these mechanisms could act to reduce the computational load on the nervous system, by allowing motor pools with repetitive or tonic activity patterns (such as muscles necessary for posture control or locomotion) to remain activated after descending synaptic drive has lessened or ceased. Such theories may offer additional insight to classical motor control questions (Bernstein, 1966).

In addition to motor-pool dependent disparities in PIC activity, it is possible for PIC amplitude to fluctuate within the same motor pools, in response to varying monoaminergic drive. The activity of the brain stem nuclei from which monoaminergic inputs arise is highly state-dependent (Aston-Jones et al., 2000), raising the possibility that this system can regulate the amplitude of PICs to suit the specific demands of a given task. State-dependent fluctuations in human PIC activity, through alterations in neuromodulatory input, have only recently been demonstrated through the use of powerful stimulant drugs (Udina et al., 2010) and through meditative, whole-body relaxation practice (Mesquita et al., 2022). These pioneering studies represent the first to utilize these novel methods in humans, however, our understanding of the extent to which monoaminergic input is regulated during normal motor behavior is limited and demands further investigation.

## **Exogenous Modulation of Motoneurons**

The extent to which PICs can be modified exogenously, in humans, is unknown. Although, a number of studies have investigated this question in terminal animal models (Harvey et al., 2006; Hounsgaard et al., 1988; Lee & Heckman, 1999), however, analogous experiments in humans have not been possible until non-invasive measures have become available.

One recent study utilizing the  $\Delta F$  approach, has shown that the administration of amphetamine significantly increased MN excitability in humans (Udina et al., 2010). The authors believe the observed alterations in PIC, from amphetamine, are largely due to its effects as a central nervous system stimulant. Specifically, through the volumetric release of the monoamines: serotonin and norepinephrine. Both of these monoamines have a prominent effect on MNs by activating PICs, which can evoke non-linear MU behavior. Similarly, other studies have shown that increasing basal levels of these monoamines, through the administration of orally ingested caffeine, also has the potential to evoke non-linear MU behavior in the form of a self-sustained discharge of MUs (Walton et al., 2002). In a similar study Walton and colleagues (2003), also demonstrated the propensity for orally ingested caffeine to increase recorded H-reflex, suggesting caffeine's effects modify the excitability of human MNs.

## **Caffeine Background**

Caffeine has garnered increased attention in the field of human physiology with a plethora of studies demonstrating its ergogenic potential. For example, studies have shown caffeine has the ability to improve cognitive ability (Ruxton, 2008), short-term memory (Bättig & Buzzi, 1986), physical endurance (Doherty et al., 2004; Doherty &

Smith, 2005; Warren et al., 2010), muscular strength (Grgic et al., 2018, 2019; Grgic & Pickering, 2019), and exercise tolerance (Meyers & Cafarelli, 2005).

At typical doses, caffeine acts as a stimulant on the central nervous system. Achieving these effects by acting as a competitive antagonist to adenosine, which elicits its benefits for wakefulness and alertness (Fisone et al., 2004). Additionally, caffeine can evoke the release of excitatory monoaminergic neurotransmitters, including norepinephrine and serotonin (Berkowitz & Spector, 1971). These monoaminergic neurotransmitters are of particular interest as they can modulate MN excitability through the activation of PICs in spinal MN, which aid in the amplification and prolongation of synaptic input to the MN (Bennett et al., 1998; Hounsgaard et al., 1988; Hounsgaard & Kiehn, 1989; Lee & Heckman, 1996).

Caffeine has been proposed to impact not only the central nervous system but also the peripheral neuromuscular system through two primary mechanisms: 1) intracellular mobilization of calcium from the sarcoplasmic reticulum (Bianchi, 1961, 1968; Grgic et al., 2019; Nehlig & Debry, 1994; Wendt & Stephenson, 1983), which increases myofibril sensitivity to calcium (de Beer et al., 1988; Fryer & Neering, 1989), and 2) inhibition of phosphodiesterases, resulting in an increase in cyclic-3',5'-adenosine monophosphate in various tissues, including muscle (Beavo et al., 1970; Butcher & Sutherland, 1962). However, it is important to note that most of these findings have been demonstrated in animal models or *in vitro* studies using relatively high concentrations of caffeine (Graham, 2001; Reggiani, 2021). Therefore, the physiological significance of these studies remains unclear and it is challenging to determine the extent to which these mechanisms of action of caffeine translate to human ergogenic benefits *in vivo*.

While caffeine remains one of the most researched psychoactive drugs openly available to consumers, its effects at the level of the human MN still remains unclear and there remains ambiguity regarding the complete impact of its pharmacodynamics, particularly its effects on human spinal MNs.

### **Caffeine Pharmacology**

Caffeine (1, 3, 7-trimethylxanthine) is a naturally occurring member of the methylxanthine class of compounds. Though caffeine is not an essential nutrient, it is one of the most commonly consumed stimulants world-wide due to its abundant presence in food products as well as over-the-counter and prescription drugs (Fulgoni et al., 2015; Graham, 2001). After ingestion, caffeine is rapidly absorbed into the bloodstream, reaching peak serum concentration in less than two hours (Kaplan et al., 1997). Though "generally recognized as safe", (FDA Act Section 201) toxic effects (including tachycardia and ventricular arrhythmia) have been reported; however, these effects are almost exclusively observed at exceptionally large doses, starting at approximately 1,200 mg. A life-threatening dose of caffeine is typically estimated at between 10,000 and 14,000 mg (Kaplan et al., 1997; Nawrot et al., 2003). While caffeine content varies in different products, a typical 8-ounce cup of ground coffee contains approximately 100 mg of caffeine; therefore, to reach the toxic dose, roughly 50–100 ordinary cups of coffee would have to be consumed. The dosage for the current study (aim 3), a single-dose oral administration of 3 mg/kg (~210 mg for a 70kg participant), is well below the toxic dose, within the FDA's recommendation for daily use, and approximately the average dose of caffeine found in a "Starbucks Grande Brewed Coffee" (260 mg).

## **Specific Aims**

Once thought to be a passive follower of descending neural commands, the motoneuron (MN) which controls muscular contractions, is now known to behave in a non-linear and state-dependent manner. These non-linear and state-dependent properties are largely due to the activation of persistent inward currents (PICs), as a result of changes in monoamines (serotonin and norepinephrine). Recent advancements in technology (HDsEMG and decomposition algorithms) now permit the study of entire populations of MNs in humans. These observations can be done non-invasively and with a high degree of fidelity, unlocking a new window through which to observe the human nervous system. Despite the vital role PICs play in controlling motor output, the mapping of PICs and their non-linear behavior is underexplored in human motor pools.

A comprehensive understanding of these non-linear behaviors is essential to directing a complete understanding of the human motor system, as older theoretical models of motor control do not account for their interactions. Furthermore, developing a full understanding of human MNs may guide diagnostic, prognostic, and therapeutic implications for neuromotor pathology with known PIC disruptions.

In a series of three experiments, the current work aims to assess the influence of PICs on the behavior of human spinal MNs. Specifically, how human MNs behave in response to muscle-, task-, and neuromodulation-dependent state changes.

### *Specific Aim 1*

**Assess human spinal motoneuron behavior and excitability within functionally varying motor pools.** Hypothesis 1A: Maximal motor unit discharge rate within the first dorsal interosseous motor pool will differ from the tibialis anterior motor pool. Hypothesis 1B: Motoneuron excitability will differ between the first dorsal interosseous motor pool and the tibialis anterior motor pool.

Rationale: The known peripheral properties of the muscular system exhibit significant variation depending on the muscle in question, such as its size, shape, and pennation angle. We suggest that the behavior of neurons controlling these muscles also varies significantly between muscles.

### *Specific Aim 2*

**Observe alterations in neuromotor control of a single motor pool in response to varying volitional motor commands.** Hypothesis 2A: Motoneuron excitability within the biceps brachii motor pool will remain invariant, despite different volitional motor commands (i.e., flexion and supination). Hypothesis 2B: Intra-muscular coherence within the biceps brachii motor pool will differ between flexion and supination motor commands.

Rationale: We propose that modifications in the synaptic input to the motor pool may be a more suitable mechanism than changes in the excitability of motor neurons for controlling task-specific alterations required in a multi-functional muscle.

### *Specific Aim 3*

**Assess the effects of exogenous neuromodulation on the human spinal motoneurons.** Hypothesis 3A: Motoneuron excitability will increase after the administration of orally ingested caffeine (3mg/kg) during a double-blind randomized control trial with inactive-placebo control. Hypothesis 3B: Intra-muscular coherence will decrease after the administration of orally ingested caffeine (3mg/kg) during a double-blind randomized control trial with inactive-placebo control.

Rationale: Previous studies have shown that the administration of caffeine leads to an increase in the release of epinephrine and serotonin, which we believe will result in an increase in the intrinsic excitability of MNs. Moreover, we anticipate that any observed behavioral response to caffeine will stem from these intrinsic changes at the level of the MN rather than from an increase in the synaptic input to the motor pool from other sources, as measured by intra-muscular coherence.

## CHAPTER 2

### DIFFERENCES IN HUMAN MOTONEURON EXCITABILITY BETWEEN FUNCTIONALLY DIVERSE MUSCLES

#### **Abstract**

Spinal motoneurons (MN) transmit neural commands from the brain to the muscles they innervate and, as a result, produce functional movement. However, MNs are not simply passive conduits of these command and, instead, actively shape motor output through alterations in intrinsic excitability. We hypothesize that the excitability of MNs is not fixed across the body; instead, MNs are functionally tuned to the tasks they control. Here, we investigate this mapping of MN excitability across motor pools. High-density surface electromyography of the tibialis anterior (TA) and first dorsal interosseous (FDI) was recorded from four neurologically intact participants while they performed low-level, isometric contractions. The data were decomposed into underlying motor unit action potentials and paired motor unit analyses were subsequently performed on these spike trains to quantify MN excitability ( $\Delta F$ ). 1,638 motor unit spike trains were extracted across all contractions. Mann-Whitney U test revealed that all subjects (4/4) had significantly higher maximal discharge rates in FDI, 19.13 [17.62 – 20.59] pps, when compared to the TA, 13.08 [11.51 – 15.46] pps. All subjects (4/4) had a higher  $\Delta F$  in the TA (4.22 [2.89 – 5.61] pps) than the FDI (3.62 [1.23 – 4.94] pps), with 3/4 reaching statistical significance. Our findings suggest that the discharge rate and intrinsic excitability of human MNs differs across TA and FDI motor pools during similar isometric tasks. These results support the notion that motor pools are functionally tuned to their environmental demands.

## **Introduction**

Spinal motoneurons (MN) are the conduits for volitional movement in humans, communicating motor commands from the brain through the spinal cord to muscle fibers (Heckman & Enoka, 2012). The motor system is organized such that a single MN and the muscle fibers it controls (i.e., motor unit; MU) represents the smallest functional unit of the motor system. Two accepted mechanisms explain the way by which the human nervous system controls force output: 1) by recruiting more motor units to contribute to the task; 2) by increasing the discharge rate of those motor units already active (Adrian & Bronk, 1929; Monster & Chan, 1977). These mechanisms have been well-explored and suggest a highly linear, rigidly organized, model for the regulation of motor unit activity (Henneman, 1957; Milner-Brown et al., 1973). However, recent evidence (Conway et al., 1988; Crone et al., 1988; Hounsgaard et al., 1988) has shown that MNs do not simply act as a passive follower of the brain, but instead, are regulated by complex intrinsic properties that may cause nonlinear changes to motor unit behavior. This active role of the MN in the generation of muscle force and ultimately movement is largely unaccounted for in our current models of motor control and understanding of pathologies of the neuromotor system.

These intrinsic properties of MNs are regulated via monoamines (i.e., norepinephrine and serotonin) released from the brainstem (Perrier, 2005). The released monoamines result in intrinsic changes to the excitability of MNs through the activation of persistent inward  $\text{Ca}^{2+}$  and  $\text{Na}^{+}$  currents (PICs) on the soma and proximal dendrites (Heckman et al., 2003). The functional consequence of this is to allow the MN to remain active even after descending synaptic drive has lessened or ceased (Crone et al., 1988; Lee & Heckman, 1996). A classic example of this is a current clamp recording from a

spinal motoneuron from an animal, which is provided a triangular injection of current and hysteresis is observed in the discharge of the neuron (Bennett et al., 1998). That is to say, more current is needed to initiate discharge than is needed to maintain repetitive discharge – this extra current and resulting hysteresis is provided in large part by the activation of PICs. It has been proposed that these channels are more prominent in postural muscles, to support the tonic activation of muscles (Wilson et al., 2015).

Direct observation of transmembrane currents of human MNs is not yet possible. But because the neuromuscular junction is a high-fidelity synapse where each MN action potential results in an action potential of the associated muscle fibers, we can infer underlying cellular process from the discharge of individual motor units (Thompson et al., 2018; Wood & Slater, 2001). Further, our utilization of non-invasive, high-density surface electromyography (HDsEMG) arrays and decomposition techniques (Negro et al., 2016) allows us to quantify the concurrent discharge of a large amount (in some cases >40) of individual human motor units. Such population measures of human MN discharge provides us with a new means to quantify the distribution of human spinal MN excitability across motor pools (Gorassini et al., 2002).

Here, we map the excitability of human spinal MNs within and across motor pools in the upper and lower extremity. We hypothesize that the excitability of MNs is not fixed across the body, but rather is functionally tuned to the tasks they control. We hypothesis that a MN that innervates a key postural muscle of the lower extremity (TA) will have greater intrinsic excitability compared to a MN that innervates an intrinsic muscle in the hand (FDI). Understanding the diverse repertoire of mechanisms available for the central nervous system to control motor output may provide insight for future

therapeutic interventions for individuals with neuromotor pathology (El Basiouny et al., 2010; McPherson et al., 2008; Murray et al., 2010).

## **Methods**

**Participants.** Four individuals (2 females, mean age  $26.5 \pm 4.98$ ) with no known neuromuscular impairments were recruited for this study. All subjects self-reported right hand and foot dominance and provided written informed consent prior to participation. All procedures were approved by the Institutional Review Board at Temple University.

**Experimental Design.** To investigate the behavior of MNs within and across motor pools of the upper and lower extremity, two experimental sessions were implemented on non-consecutive days. Each experiment consisted of data collection from a single muscle. Similar protocols were conducted during both experimental sessions, with the muscle being tested first randomly assigned. To quantify the discharge characteristics and estimated excitability of individual MNs, we utilized a series of slow ramping isometric muscular contractions in which the force output could be slowly modulated over time in a consistent manner. During this time, we recorded the MN activity with HDsEMG.

**Experimental setup - tibialis anterior (TA).** Prior to the experimental session, the skin over the dominant-side (i.e., right) tibialis anterior (TA) was shaved, abraded with high-grit sandpaper, and cleansed. One 64-channel high-density electrode array (8mm inter-electrode distance, 5 columns x 13 rows, ELSCH064NM2; OT Bioelettronica; Turin, Italy) was coated with conductive adhesive paste (AC Cream; Spes Medica; Genova, Italy) and placed on the skin over the muscle, covering the largest portion of the muscle belly, and secured with medical tape (3M Transpore; St. Paul, MN).

Specifically, the medial border of the TA HDsEMG array was placed parallel with and aligned to the anterior tibial crest, the center of the array was positioned on the largest part of the muscle belly approximately in the upper 2/3 of the lower right leg. Participants were seated in an isokinetic dynamometer (Biodex; Shirley, NY) and secured with straps across the torso and upper leg in a comfortable position of 60-90° hip flexion and 15° knee flexion. The ankle was secured to a footplate achieving 15° degrees of plantarflexion and affixed to a six degrees of freedom load cell (JR3; Woodland, CA). The ankle's axis of rotation was centered to the load cell in this position (See Figure 2.1). Real-time feedback of torque output was provided on a TV monitor positioned directly in front of the participant to assist task performance.

**Experimental setup - first dorsal interosseous (FDI).** In a similar manner as described above, the skin over the dominant-side (i.e., right) first dorsal interosseous (FDI) was prepared and one 64-channel high-density electrode array (4mm inter-electrode distance, GR04MM1305; OT Bioelettronica; Turin, Italy) was placed on the skin over the largest portion of the muscle belly, parallel to the muscle fiber direction with the distal end of the array extending to the second metacarpophalangeal joint on the right hand, and then secured with medical tape. Participants were seated in a comfortable position in a chair facing an exam table. Chair height was adjusted such that their arms were resting in a neutral position on the exam table (forearm pronated, such that the palms were facing down). The tested hand was positioned against a rigid block on the exam table with fingers fully extended and thumb abducted 90° away from the index finger. This position enabled the participants to exert abduction force with their index finger into the rigid block without moving the rest of their hand or fingers. Real-time

feedback of FDI EMG was provided on a TV monitor, positioned directly in front of the participant, to assist task performance.

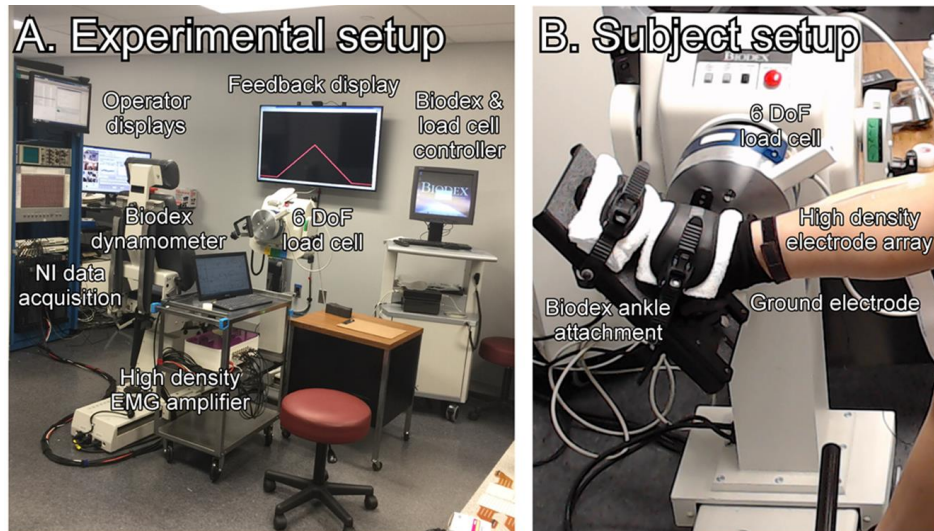


Figure 2.1. Experimental Setup for TA. **A)** Laboratory setup during data collection. Subject is seated in Biodex facing the feedback display. **B)** Sagittal view of the ankle during data collection for the TA. The axis of rotation of the ankle is lined up with the center of the load cell.

**Experimental protocol.** At the beginning of each experimental session, participants performed three maximal volitional isometric contractions (MVIC) of the tested muscle, waiting at least two minutes between attempts, to establish a baseline of performance. For the purpose of EMG decomposition and subsequent motor unit analysis, participants were asked to produce a symmetrical time-varying isolated joint torque up to a fixed percentage (20%) of their MVIC and at a consistent rate of torque development. Participants performed three sets of three isometric contractions for each muscle tested. To mitigate the effects of fatigue, 10 seconds of rest between contractions and 2 minutes of rest between sets was imposed.

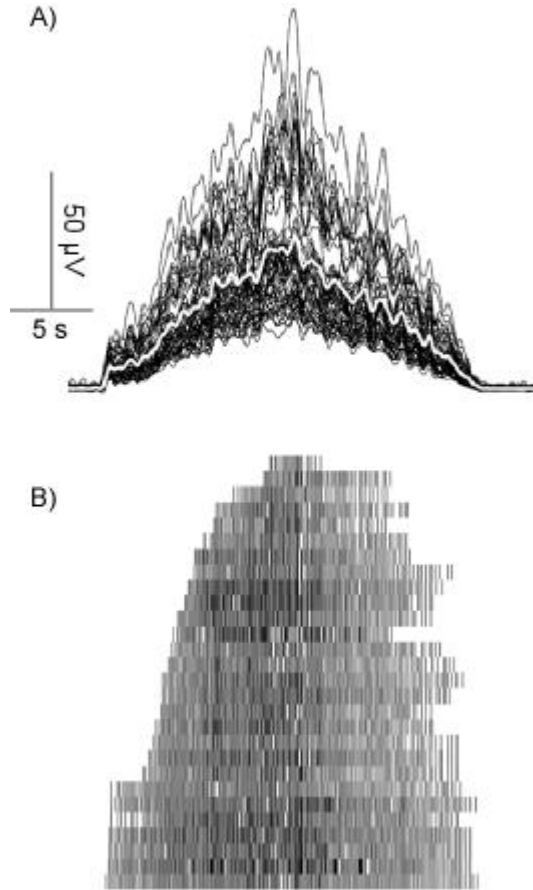


Figure 2.2. Raw EMG and MU Spike Trains. Representative data from the TA of one individual. **A)** Surface EMG is collected from 64 channel surface EMG during an isometric ramp contraction. **B)** Surface EMG recordings are decomposed into their corresponding motor unit action potentials; 28 motor units from the TA are shown here.

**Data Collection.** During isometric contractions, HDsEMG data was recorded using the OTBioLab software (OT Bioelettronica; Turin, Italy). Torque was baseline corrected and filtered using a 20 Hz low pass filter, this signal was used for visual feedback of task performance during the TA contractions. A single channel of EMG was isolated, amplified, rectified, and smoothed using a  $\sim 500$  ms root mean square filter, and then utilized for visual feedback of task performance during the FDI contractions. EMG

was filtered at 20-900 Hz and collected at 2048 Hz using a 16-bit A/D converter (OT Bioelettronica; Turin, IT), simultaneously with the torque data.

**Motor unit decomposition and analysis.** HDsEMG array recordings were decomposed offline into the discharge of individual motor units using a blind source separation algorithm (Figure 2.2.; Negro et al., 2016). This algorithm has been extensively validated and provides an accurate method for decomposing motor unit spike trains (Thompson et al., 2018). For each participant, individual isometric contractions were isolated. Thereafter, each spike train was identified and convolved with a 2-second hanning window. From these windowed spike times, the maximum discharge rate of each MN was calculated

**Measurement of intrinsic motoneuron excitability ( $\Delta F$ ).** PICs act to augment and prolong the activity of motor units. To estimate the magnitude of these effects, we measured the prolonged activity of motor units through the use of slow, symmetrically ramping (up to 20% MVIC and back down), isometric muscle contraction. If there were no appreciable nonlinear properties of these MNs, the time at which a motor unit was recruited and derecruited would be perfectly equal and symmetrical on the up- and down-slope of the triangular contraction. However, if there are increases in the excitability of spinal motoneurons (as such is the case with increased PIC magnitude), motor units would have an observable hysteresis, in which a motor unit would remain active long after it was expected to de-recruit. Because we are unable to directly assess the synaptic input to a motor pool from the nervous system, this paired motor unit technique was utilized (Gorassini et al., 2002). Specifically, the recruitment and derecruitment time of a higher threshold unit was found and compared to the estimated synaptic current (i.e., the

firing frequency of a lower threshold motor unit).  $\Delta F$  is calculated by finding the difference in discharge rate of the lower threshold unit between these two time points. In instances where  $\Delta F$  is greater, a larger hysteresis will become observable between the time at which a higher threshold unit is recruited and derecruited (see Figure 2.3). To limit the amount of erroneous comparisons only pairs that met the following criteria were accepted: 1) less than 1 second between the first discharge of the lower threshold unit and the first discharge of the higher threshold unit, 2) an increase of at least 0.5 pps in the lower threshold unit following the recruitment of the higher threshold unit to ensure a lack of saturation, and 3) to ensure common synaptic drive underlying the rate modulation of both units, only pairs with a rate-rate  $r^2$  value of greater than 0.7 were considered suitable pairs (Gorassini et al., 2004).

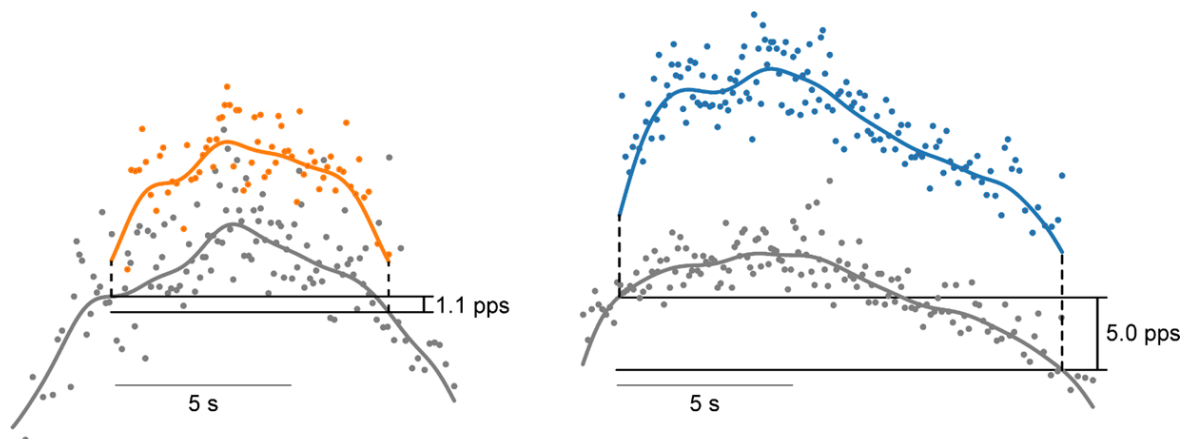


Figure 2.3. Delta-F Between FDI and TA. Exemplary data from the paired motor unit analysis technique for the FDI (left) and TA (right); lower threshold motor units (gray) from the same contraction are paired with higher threshold units for analysis (FDI in orange; TA in blue). Here,  $\Delta F$  is greater in the TA (right; 5.0 pps), as such, a larger hysteresis is observable, and the higher threshold motor unit remains active for much longer when compared to its paired lower threshold motor unit (Pulses per second; pps).

**Statistical Analysis.** Normality of the data was tested with the Shapiro-Wilk test and revealed non-normal distributions for  $\Delta F$  and maximal firing rate. Thus, Mann-

Whitney U tests were used to compare the  $\Delta F$  and maximal firing rate within each subject between the TA and FDI. A Bonferroni correction was applied to account for multiple comparisons. All statistical analyses were performed using MATLAB 2017b (MathWorks, Natick, USA) and significance was accepted at the  $p$  value  $\leq 0.05$ . Results are reported as median and [first quartile – third quartile].

## Results

Each of the four subjects completed three sets of three contraction in both the TA and FDI for a total of 72 contractions. Figure 2.2 shows an example of a single contraction in which the HDsEMG signals are overlaid above the decomposed discharge times. The TA contractions were performed at 18.4% [15.8 – 22.1] maximal EMG amplitude while FDI contractions were performed at 23.8% [21.1 – 27.7] maximal EMG amplitude. From these signals, a significant difference in the number of MUs yielded per contraction is observed between the TA (15.5 [12 - 21]) and FDI (5.5 [4 - 7];  $p = .006$ ). All subjects (4/4) had a significantly higher maximum discharge rates in the FDI than in the TA (all  $p < 0.01$ ). This ranged from a 15.1% to a 67.5% increase in discharge rate of the FDI as compared to the TA (Figure 2.4a).

To conduct the paired motor unit analysis, suitable motor unit pairs in each contraction were found (see methods). Figure 2.3 shows an example of the  $\Delta F$  analysis in pairs of motor units from the TA and FDI, note the greater hysteresis in the TA. This resulted in a median of 42 [11 - 101] pairs in the TA and 6 [4 - 16] pairs in the FDI per contraction. When pooling these values, all subjects (4/4) had a higher  $\Delta F$  in the TA (4.22 [2.89 – 5.61] pps) than FDI (3.62 [1.23 – 4.94] pps), with 3/4 reaching statistical significance (Figure 2.4b).

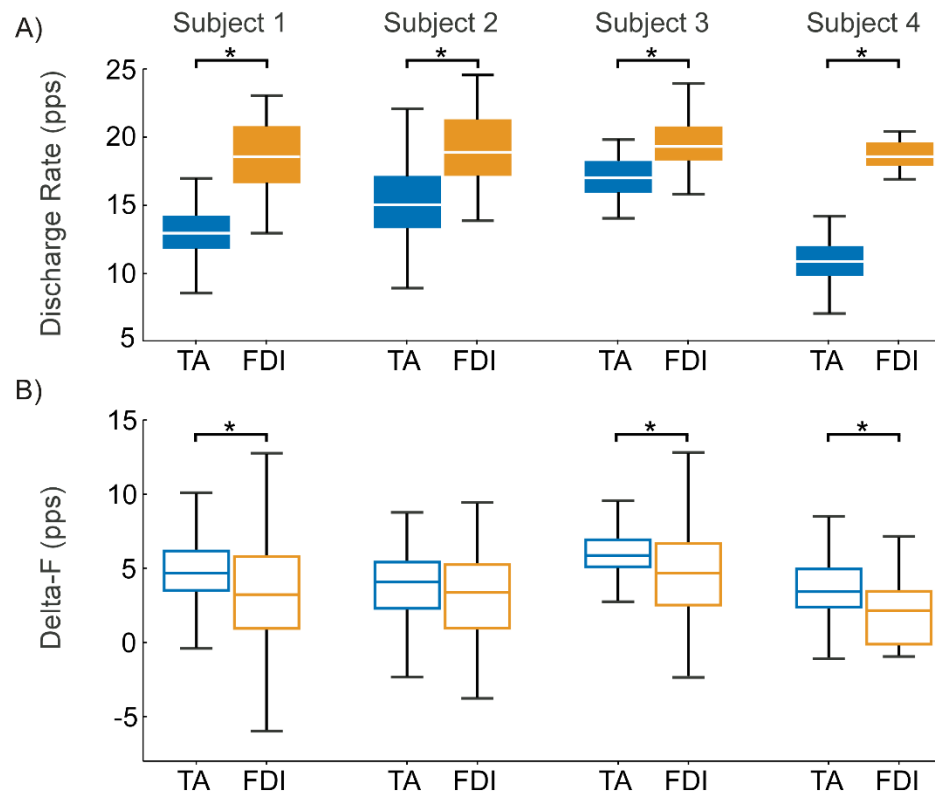


Figure 2.4. TA vs FDI Motor Unit Discharge Characteristics. Individual data (subjects 1-4) for maximal discharge rate (top row, filled boxes) and  $\Delta F$  (bottom row, empty boxes). (\*) Represents significant differences between TA (blue) and FDI (orange).

## Discussion

The discharge patterns and intrinsic excitability of human MNs are different across functionally diverse motor pools. These findings indicate that the FDI preferentially utilizes higher discharge rates than the TA to achieve the same relative level of effort. Furthermore, using the paired motor unit ( $\Delta F$ ) approach, we observe the intrinsic excitability of human MNs is higher in the TA than in the FDI.

Two functionally diverse muscles appear to be controlled in fundamentally different ways by the CNS to achieve task dependent outcomes. This evidence supports the notion that motor pools are functionally tuned to their environmental demands. While

others have observed state-dependent changes in the motor system through neuromodulation (Wei et al., 2014), none have yet assessed the baseline organization and relative sensitivity of these motor pools (TA and FDI) in humans. Because of the nonlinear ways in which PICs can augment motor unit behavior, it may be possible that the nervous system may utilize these organizational differences to transform the motor command between motor pools, to facilitate complex motor tasks. For example, the TA, predominantly a postural control muscle, is utilized constantly for stability and locomotion. As such, its MNs may have a biophysical benefit to higher levels of excitability ( $\Delta F$ ), this would lower the effective activation threshold of the motor pool to assist in repetitive tasks. In contrast, the FDI is almost exclusively utilized for fine control in grasping. As such, its MNs may benefit from a reduced level of excitability when executing controlled, fine motor tasks, in which prolonged MN activation may increase the difficulty of controlling a precise movement.

In addition to differences in intrinsic MN excitability, during slow time varying isometric contractions the FDI preferentially utilizes higher discharge rates than the TA to achieve the same relative level of effort. The difference in maximal discharge rates could reflect further organizational differences between the TA and FDI. Others have reported similar findings in the characteristics and discharge rates of the TA (Connelly et al., 1999) and FDI (Seki & Narusawa, 1996). While the absolute size and maximal force output of the TA and FDI muscles may greatly vary, the use of a normalized task (20% MVIC) acts to diminish these differences and alone are not likely responsible for the observed differences. However, relative differences in the amount of MNs (and the number of muscle fibers in each motor unit), between these two motor pools could result

in varying force-generating capabilities (Lawrence & De Luca, 1983) and, as a result, require divergent control strategies. The current data is consistent with previous work suggesting the FDI uses a rate-modulation (as opposed to recruitment) based strategy for increasing force (Seki & Narusawa, 1996). Taken together, the data suggest that distinct organizational differences exist between the TA and FDI motor pools.

It is important to note that consequent to the calculations involved in estimating intrinsic MN excitability with the paired motor unit method, the  $\Delta F$  value cannot exceed the peak discharge of the motor pool under observation. Thus, it is possible that the observed  $\Delta F$  findings in the TA were *underestimated* by their inherently lower discharge rates when compared to the FDI (with a higher discharge rate and lower  $\Delta F$  value). It is possible the differences between motor pools may be even larger without this limitation. This would be more of a concern if both the peak discharge rate and the  $\Delta F$  measure trended in the same direction, regardless this should be considered in its future use in comparing values across motor pools.

This method of HDsEMG analysis generates an extraordinary amount of data per subject (in some cases hundreds of data points, per muscle, per contraction), in which important biophysical signals and individual variation may be lost when collapsing the data across subjects. Further, within the same subject, the TA and FDI may not have had the same number of representative data samples recorded in each motor pool. To address this unequal sampling, unpaired tests of statistical inference were chosen to assess changes within subjects. Additionally, due to a multitude of reasons including subcutaneous fat, anatomical differences, and signal noise, not all subjects yielded similar numbers of motor unit spike trains after decomposition. For example, subject 2 (female)

yielded a total of 145 motor unit comparisons for the paired motor unit analysis compared to subject 4 (male) who yielded 847. Similar sex-related differences in motor unit decomposition yield have been previously observed (Taylor et al., 2022). This disparity in motor unit comparisons may account for the non-significant increase in TA  $\Delta F$  in subject 2 (see Figure 2.4b). Future efforts should aim to improve motor unit spike train yield and to provide further rigor in statistical inference testing with this unique data collection method.

Motor unit decomposition methods in HDsEMG, such as the ones employed in this study, present multiple advantages in data collection over the lifespan in populations with neuromuscular pathology. Fine-wire EMG, in which a needle is inserted percutaneously into the muscle belly to temporarily place metal wires for direct recording and electrostimulation, is commonly used for diagnosis and prognosis across a range of neuromuscular pathologies, including amyotrophic lateral sclerosis (ALS) and peripheral nerve lesions (e.g., obstetric brachial plexus injury). However, the invasiveness of these procedures creates discomfort for vulnerable populations, deters patients from serial studies, requires trained clinician oversight, and presents analytical limitations (Bashford et al., 2020). Instead, noninvasive HDsEMG techniques can be employed, creating opportunities for remote testing in outpatient facilities, or even patients' homes, without the resources needed in a hospital or laboratory setting. The noninvasive nature of the HDsEMG collection allows for longer recording periods with minimal discomfort and often yielding magnitudes more data (Del Vecchio et al., 2020; Farina et al., 2010). Furthermore, fine-wire EMG, despite high levels of focal fidelity, cannot provide information about the entire motor pool during contractions. As a result, fine-wire EMG

is unable to distinguish between individual MN activity and the behavior of the entire motor pool. This valuable spatial information is easily gathered utilizing surface HDsEMG recordings and can help to discriminate between spontaneous action potentials which can be used to assess their various origins, especially important in the ALS population (Jahanmiri-Nezhad et al., 2014; Kleine et al., 2012).

These findings demonstrate a crucial extension of earlier experiments exploring the non-linear role of MNs in the animal model (Bennett et al., 1998; Hounsgaard & Kiehn, 1989). Future work should aim to replicate the work of fine-wire experiments in mapping MN behavior across a variety of tasks (e.g. changes in posture, intensities, and varying rest intervals) and motor pools (Enoka, 2019). Mapping PIC activity and developing a comprehensive understanding of MN behavior may have important implications for the diagnosis, prognosis, and treatment of neuropathologies, including ALS, spinal cord injury, and stroke.

## CHAPTER 3

### THE MOTOR COMMAND TO THE BICEPS BRACHII DURING DIFFERENT MODES OF ACTIVATION

#### **Abstract**

It is unclear how the nervous system regulates the activation of spinal motoneurons for muscles with more than one biomechanical function. The biceps brachii, with the ability to perform elbow flexion and supination, offers a unique opportunity to observe functional changes in the motor unit behavior. Here, we record the discharge of 588 motoneurons (10 subjects) from the biceps brachii during contractions with two different modes of activation, isometric elbow flexion and supination, at similar levels of intensity. The results show alpha (5-15Hz) and beta (15-35Hz) band coherence differed between supination and flexion ( $p < 0.001$ ). However, motoneuron discharge rate, variability, and excitability remained similar across the modes of activation. These data show different sources of synaptic drive may regulate the activation of biceps during distinct modes of volitional activation, while the excitability of the motor pool remains invariant. Changes in synaptic drive suggest the motor command to the biceps motor pool may contain information regarding limb movement and kinematics.

## **Introduction**

Human movement is a result of the graded activation of spinal motoneurons, which ultimately integrate motor commands from the nervous system to create volitional movement (Duchateau & Enoka, 2011). Spinal alpha motoneurons that synapse onto muscle fibers, a motor unit (MU), represent the smallest functional element of motor output. Traditionally, it has been thought that MUs are uniformly and homogeneously innervated within a motor pool, receiving similar levels of synaptic input, and regulated largely by the size of their parent motoneuron (*i.e.*, Size Principle) (De Luca & Erim, 1994; Henneman & Mendell, 1981). However, recent evidence for the existence of discrete task- and function-dependent behavior of MUs within a motor pool complicates these previous notions (de Souza et al., 2017; Herrmann & Flanders, 1998; Holtermann et al., 2010; Holtermann & Roeleveld, 2006; Jensen & Westgaard, 1997; McMillan & Hannam, 1992; G. M. Murray et al., 1999; Paton & Brown, 1994; Staudenmann et al., 2013; Wolf et al., 1993). Further, if MUs within the same motor pool do behave differently depending on task performed, it is feasible that these MUs may modify their output through multiple mechanisms, especially for muscles that have more than one biomechanical function.

The biceps brachii, a multi-function muscle, acts across the shoulder and elbow to perform two discrete actions; elbow flexion and supination of the forearm, despite a single point of insertion on the radial tuberosity (Athwal et al., 2007). These qualities, along with its ease of access for surface electromyography (EMG), lend the biceps brachii to be uniquely suited to the study of function-dependent changes in the neural control of motor pools. Others have provided evidence for functionally tuned and task-dependent behavior of MUs within the biceps brachii (Denier van der Gon et al., 1985;

ter Haar Romeny et al., 1984; van Zuylen et al., 1988). The aforementioned studies have utilized combinations of fine-wire intramuscular EMG and surface EMG to capture motor unit activity during various biomechanical tasks, however, none have attempted to simultaneously quantify the synaptic input into the motor pool and the level of motoneuron excitability during such tasks; both may be able to alter the neural control of motor units within the motor pool.

Overt changes to the synaptic input to motoneurons is an obvious mechanism toward task-dependent MU behavior. However, changes in motoneuron excitability may also be partially responsible for modifications in task-dependent MU behavior of the same motor pool. Changes in motoneuron excitability are driven through fluctuations in monoaminergic drive, facilitating the activation of persistent inward currents (PIC), that act to prolong and amplify the synaptic drive to the motoneuron (Hounsgaard et al., 1988; Lee & Heckman, 1996). Further, it has been proposed that PICs may fluctuate in response to state-dependent and task-dependent behaviors (Heckman et al., 2009; Hynstrom et al., 2007). However, our understanding of the extent to which monoaminergic drive, and thus motoneuron excitability, is regulated within a single motor pool is limited. The flexibility of this neuro-modulatory system, and its involvement in state-dependent modulation of MU behavior, make it a valid candidate to investigate its potential to modify motor commands for multi-function muscles.

While direct observation of spinal motoneurons in humans is not yet possible, our approach (Taylor et al., 2022; Thompson et al., 2018), utilizing noninvasive, high-density surface electromyography arrays (HDsEMG) and motor unit decomposition techniques (Negro et al., 2016), allows us to quantify the concurrent discharge of a large amounts of

individual motoneurons. Here, we record the discharge of many motor units from the biceps brachii during two modes of activation, elbow flexion and forearm supination, at similar levels of intensity. Such an approach allows us to quantify spinal motoneuron excitability and discharge characteristics within the biceps brachii. We hypothesize spinal motoneuron excitability will remain invariant to changes in the type of functional task performed, however, the estimates of common synaptic input will differ between flexion and supination of the elbow, within the biceps brachii motor pool.

## **Methods**

**Participants.** Ten neurologically intact individuals (4 females) were recruited for this study. All participants gave written informed consent prior to participation. All self-reported right-hand dominance. All had indicated that they experienced no musculoskeletal injuries within the past six months and were free from pain. Neurological deficits or prescription medications were criteria for exclusion. All procedures were approved by the Institutional Review Board at Temple University (Protocol # 23971).

**Experimental Set-up.** To quantify motor unit discharge characteristics of the biceps brachii during two functionally distinct tasks, we utilized HDsEMG electrode arrays. Prior to the experimental session, the skin over the short head of the right biceps brachii was shaved, abraded with high-grit sandpaper, and cleansed. One 64-channel high-density electrode array (8mm inter-electrode distance, 5 columns x 13 rows, ELSCH064NM2; OT Bioelettronica; Turin, Italy) was coated with conductive adhesive paste (AC Cream; Spes Medica; Genova, Italy) and placed on the skin over the right biceps brachii and secured with medical tape (3M Transpore; St. Paul, MN). Specifically,

the medial border of the HDsEMG array was aligned vertically in parallel with the medial edge of the short head of the biceps and centered vertically to capture the largest portion of the muscle belly. Participants were seated in an isokinetic dynamometer (Biodex; Shirley, NY) and secured with straps across the torso. The right arm was placed in 90° degrees elbow flexion, upper arm abducted 5° degrees, wrist in neutral position, grasping a padded handle attached to a custom mounted 6 degrees of freedom load cell (JR3; Woodland, CA). A large flat screen TV was mounted directly in front of the participant, approximately 5 ft (1.5 m) from the subject, for real-time visual feedback of their performance.

**Experimental Protocol.** Data for each participant was collected during a single experimental session. Participants were asked to perform two different modes of activation (*i.e.*, elbow flexion and forearm supination) by manipulating the handle attached to the load cell. Real-time visual feedback of torque was provided to the participant throughout each trial to guide their effort. Participants performed three maximal voluntary isometric contractions (MVIC) for both elbow flexion and forearm supination with verbal reinforcement, waiting 2 minutes in between attempts. The MVICs were only deemed reliable if the amount of variance in torque between attempts was  $\leq 5\%$ . If variance was observed greater than this amount additional MVIC attempts were completed until three attempts were within the  $\leq 5\%$  range, then the maximum value achieved was used to normalize force output.

For the purpose of EMG decomposition and subsequent analysis of MU discharge characteristics, participants performed two tasks for each *mode of activation*: 1) isometric ramp contractions (RAMP) and 2) isometric steady-state contractions (HOLD).

The target intensity for RAMP and HOLD contractions was 20% MVIC. During the RAMP contractions, participants were asked to produce a symmetrical rise (10 seconds) and fall (10 seconds) of isolated joint torque up to the target intensity (20% MVIC). Participants followed real-time feedback to modulate their task performance. Participants completed two sets of three repetitions of RAMP contractions with 20 seconds rest between repetitions and at least two minutes between sets. During the HOLD contractions, participants were asked to steadily increase the isolated joint torque (or sEMG) up to the target intensity (20% MVIC) and maintain this contraction for 40 seconds, receiving real-time visual feedback as described previously. Participants completed two HOLD contractions with at least two minutes rest between contractions. Trials for mode of activation were pseudo-randomized to mitigate order- and time-dependent effects.

**Data Collection.** Limb segment length was measured for each participant and isometric joint torque was calculated using a matrix transform based on the position of joint centers relative to the load cell. Torque was baseline corrected and filtered using a 20 Hz low pass filter. EMG was filtered at 20-900 Hz and collected at 2048 Hz using a 16-bit A/D converter (OT Bioelettronica; Turin, IT), simultaneously with the torque data.

**EMG Feedback.** In instances where joint torques were unable to be calculated, or when specific isolation (supination) of a single muscle needed to be encouraged, we substituted a version of the EMG signal for the torque to guide the effort of the contraction (n=2 subjects). Here a single channel (positioned in the center of the array) was chosen to be the feedback signal. The signal was amplified, rectified, baseline corrected, and smoothed using a ~400 ms root mean square filter. This provides a line,

similar to that of the previously described torque feedback, which represents specific muscle activation such that the subject can use this real-time EMG feedback to perform controlled efforts of a specific muscle group. Target intensity in this method, in lieu of force output, was calculated by taking the average EMG amplitude during a 20% torque MVIC flexion HOLD task.

**Motor unit decomposition and processing.** HDsEMG array recordings were decomposed offline into the discharge of individual motor units using a convolutive blind source separation algorithm (Negro et al., 2016). This algorithm has been extensively validated (Thompson et al., 2018) and provides a robust method for decomposing motor unit spike trains. For each spike train, the resulting discharge times were manually inspected using semiautomatic software. A semi-automated motor unit cleaning process was performed by an experienced investigator, to ensure the accurate detection of each spike of each motor unit (Afsharipour et al., 2020; Hassan et al., 2021). All remaining motor unit spike trains were identified and incorporated into the subsequent data set for further analysis.

The estimated MN excitability ( $\Delta F$ ), initial (InitDR), maximum (MaxDR), and final discharge (FinalDR) rates of MUs at target intensities were calculated during RAMP contractions. The mean discharge rate (meanDR), coefficient of variation (CoV) of the inter-spike intervals (ISI), and coherence of each motor unit were calculated from the motor unit data 2 seconds after the start of and 2 seconds prior to the end of the torque plateau from each HOLD contraction, ensuring that only the isolated steady-state firing of each motor unit, during stable torque levels, were considered for analysis.

**Measurement of intrinsic motoneuron excitability ( $\Delta F$ ).** To estimate intrinsic MN excitability, the paired motor unit technique was utilized (Gorassini et al., 2002a). Here, the time at which a higher threshold unit is recruited and derecruited is found and normalized to the firing frequency of a low-threshold motor unit (i.e., the estimated synaptic current). Under high levels of excitability, the synaptic current needed to reach threshold will be lowered and a lower derecruitment threshold will be observed and the change in discharge rate (i.e.,  $\Delta F$ ) will be calculated (Figure 3.1). To ensure accurate representation of PIC amplitude, from  $\Delta F$  calculations, the following restrictions were applied to limit invalid motor unit comparisons: the low threshold (control) unit was recruited at least 1 second before the higher threshold unit, and the low threshold unit was de-recruited at least 1.5 seconds after the high threshold unit (Hassan et al., 2020).

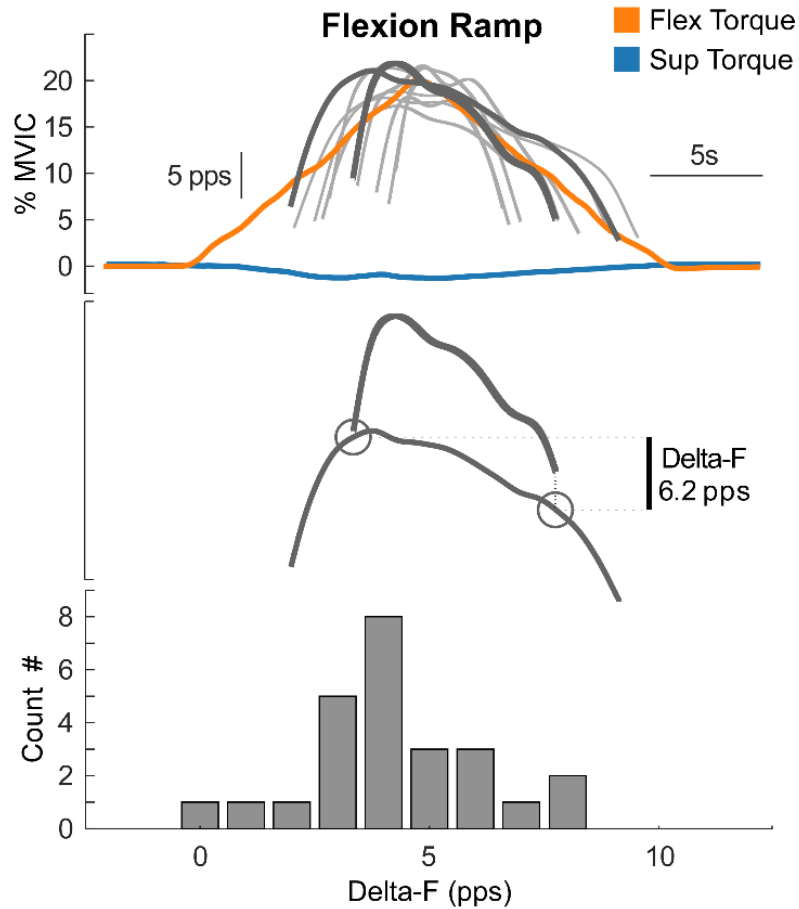


Figure 3.1. Biceps Flexion RAMP and Delta-F. Exemplary data from a single subject during a flexion RAMP contraction. **Top:** 8 unique motor units (grey) along with corresponding flexion and supination torque. **Middle:** a single pair of motor units (dark grey) used in Delta-F calculation. **Bottom:** Histogram of all valid Delta-F comparisons for this trial.

**Measurement of common synaptic input.** To estimate the common synaptic input to motoneurons, we calculated a pooled coherence (Laine et al., 2015) between all unique pairs of simultaneously active motor unit spike trains, within the active motor pool. This technique provides a normalized value of the correlation in the frequency of synaptic inputs shared between the unique pairs of motoneurons. Here, all valid MUs are assessed to ensure sustained repetitive firing throughout the steady-state portion of each

HOLD contraction. Units without sustained repetitive firing during this period were removed and the remaining individual spike trains were concatenated into two long spike trains of consecutive unique pairs. Coherence was then calculated on the two concatenated spike trains in consecutive non-overlapping 1s segments with the cross-spectra of the two uniquely paired units normalized by the pairings combined auto-spectra (Laine et al., 2015; Zaback et al., 2022). To compare these coherence measures across conditions, coherence values at each frequency were converted to standard Z-scores, based on the number of segments contained in the concatenated spike trains and the area under the curve of these Z-scores were calculated in the following frequency bins: Delta band 0-5Hz, Alpha band 5-15Hz, Beta band 15-35Hz.

**Motor unit action potential analysis.** Motor unit action potential (MUAP) waveforms across the array were calculated by spike-triggered averaging the HDsEMG data using the discharge of each motor unit. The peak-to-peak amplitude and median frequency content of the waveforms at each electrode were calculated on these reconstructed MUAPs. Spatial distribution of MUAPs across the array was calculated by identifying the number of channels (out of 64 available), for each MU identified, in which MUAP peak-to-peak amplitude exceeded 50% of each MUAPs maximum peak-to-peak amplitude (Taylor et al., 2022).

**Motor unit tracking.** In an attempt to identify and track the same motor units across modes of activation, all valid and available motor unit action potential (MUAP) waveform profiles, from the single highest MU yield set, within each trial were cross-correlated with the corresponding trial of the opposite mode of activation (i.e., supination HOLD and flexion HOLD). MUAP waveforms across the array were calculated by spike-

triggered averaging the HDsEMG data using the discharge of each motor unit. Normalized cross-correlations higher than 0.85 between MUAPs of two trials were considered a match and were given a unique identifier, tracked across the testing session, and ultimately utilized in the subsequent motor unit analysis methods. On rare occasions, multiple matches with cross-correlation values greater than 0.85 were identified, the highest value of cross-correlation source was selected and all other duplicates were removed from future analysis.

Despite these methods, only 3 MUs (from 2 subjects) during RAMP contractions met the criteria for matching MUAP profiles, whereas 54 MUs (from 10 subjects) were accurately identified during HOLD contractions. The successfully tracked MUs (n=54) within HOLD contractions closely resembled the behavior of untracked MUs (see Table 3.2); however, due to the requirement of multiple unique MUs for accurate paired motor unit analysis (i.e.,  $\Delta F$ ), the resultant tracked MU data from RAMP contractions were not utilized in the final analysis of this study (see - *Discussion*).

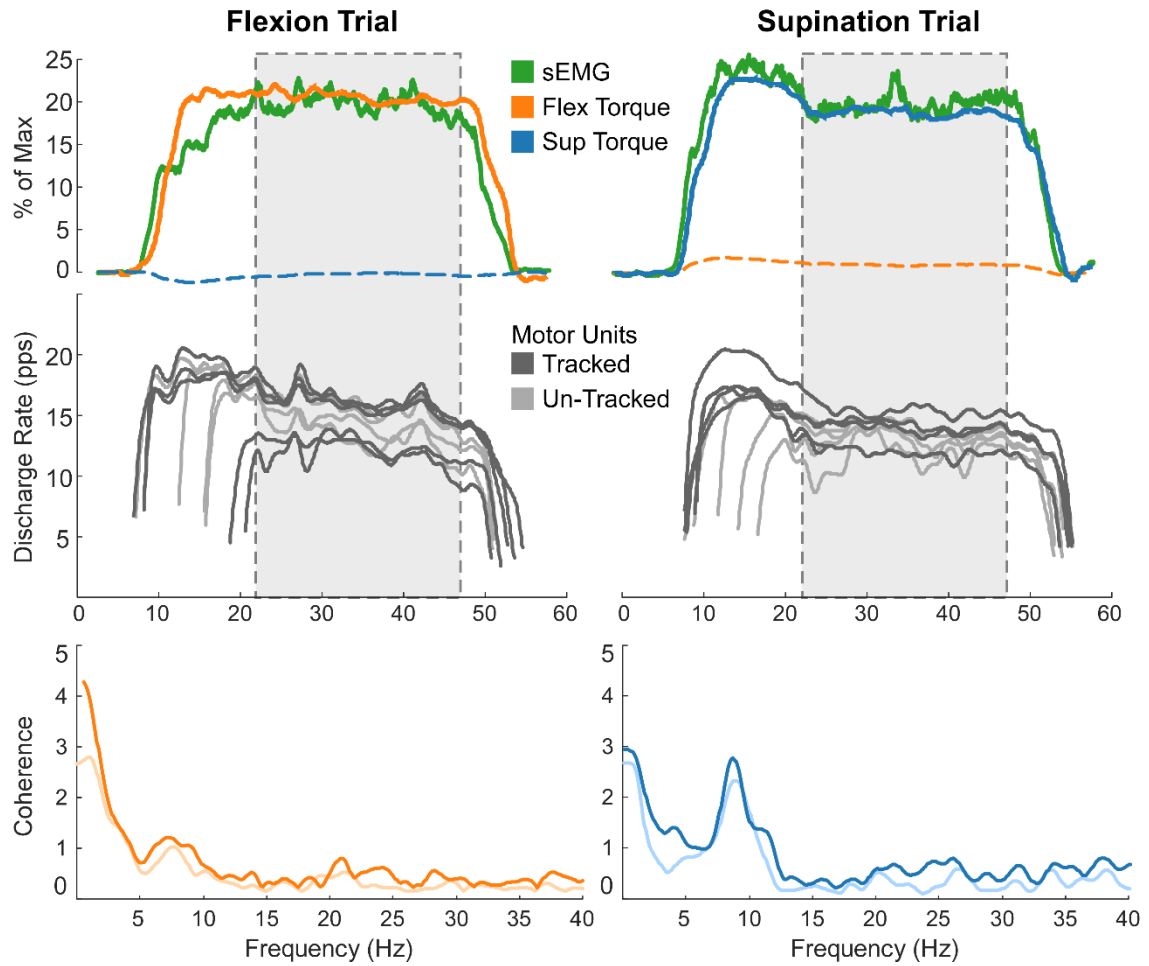


Figure 3.2. HOLD Trial with Coherence Analysis. Exemplary data from a single subject during flexion and supination HOLDS. Top: Rectified and filtered sEMG (green) along with corresponding flexion and supination torque. The light grey dotted-box represents the window within which meanDR, CoV ISI, and Coherence values were captured. Middle: All available motor units yielded within each trial (grey). 5 unique motor units were accurately tracked and identified within both trials (dark grey). Bottom: Coherence analysis results utilizing all available (light) and only tracked motor units (dark).

**Statistical analysis.** All statistical analysis, data manipulation, and visualization were performed using MATLAB 2019b (MathWorks, Natick, USA). The normality of the data was tested with the Shapiro-Wilk test and revealed normal distributions for MU characteristics, torque, and MU yield. A paired t-test was used to compare differences in subject characteristics and MU variables between modes of activation. Bonferroni corrections were applied, and significance was accepted at the  $p \leq$  value 0.05. Results are reported as mean and ( $\pm$  standard deviation)

Table 3.1. Motor Unit and Torque Characteristics

	Flexion	Supination	p-value
MU Yield	6.80 (2.29 $\pm$ )	7.35 (3.35 $\pm$ )	0.55
Initial DR	5.30 pps (0.91 $\pm$ )	5.59 pps (0.68 $\pm$ )	0.16
Max DR	16.84 pps (1.28 $\pm$ )	16.72 pps (1.48 $\pm$ )	0.71
Final DR	4.14 pps (0.99 $\pm$ )	4.12 pps (0.50 $\pm$ )	0.92
$\Delta F$	3.79 pps (1.01 $\pm$ )	3.84 pps (0.70 $\pm$ )	0.85
% MVIC Torque	20.08 % (1.32 $\pm$ )	21.09 % (2.95 $\pm$ )	0.28
Torque CoV	1.54 % (0.37 $\pm$ )	1.73 % (0.21 $\pm$ )	0.20
sEMG Amplitude	44.46 $\mu V$ (13.56 $\pm$ )	42.38 $\mu V$ (10.95 $\pm$ )	0.54
Mean DR	13.85 pps (1.28 $\pm$ )	14.23 pps (1.65 $\pm$ )	0.30
CoV ISI	18.04 % (0.97 $\pm$ )	17.42 % (1.87 $\pm$ )	0.42
Delta Coherence	2.61 (1.13 $\pm$ )	2.64 (1.01 $\pm$ )	0.87
<b>Alpha Coherence</b>	<b>0.77 (0.27<math>\pm</math>)</b>	<b>1.30 (0.43<math>\pm</math>)</b>	<b>&lt;0.001*</b>
<b>Beta Coherence</b>	<b>0.55 (0.15<math>\pm</math>)</b>	<b>0.90 (0.25<math>\pm</math>)</b>	<b>&lt;0.001*</b>
MUAP Distribution	15.44 % (2.95 $\pm$ )	16.72 % (2.8 $\pm$ )	0.08
Mean MUAP p2p Amplitude	218.98 $\mu V$ (79.66 $\pm$ )	231.95 $\mu V$ (78.26 $\pm$ )	0.61
MUAP Median Frequency	114.45 Hz (15.92 $\pm$ )	115.95 Hz (18.23 $\pm$ )	0.46

Table 3.1. Motor Unit and Torque Characteristics. The data described here is for all valid and available motor units, descriptive statistics of tracked motor units can be found below (see Table 3.2.). Abbreviations: Motor unit (MU); Motor unit action potential (MUAP); Discharge Rate (DR); Maximum volitional isometric contraction (MVIC); Coefficient of Variation (CoV); Inter-Spike Interval (ISI); Delta-F ( $\Delta F$ ). Statistically significant (<0.05) p-value (\*).

## Results

**Subject Characteristics.** Ten subjects (4 females) with a mean age of 24.5 ( $\pm$  4.1) and mean estimated body mass index of 26.4 ( $\pm$  3.6) completed 40 trials (20 RAMP and 20 HOLD). A total of 588 motor unit spike trains (284 from HOLDS) were identified over the course of the experiment, in the biceps brachii. There were no significant differences in MU yield between tasks or modes of activation. During maximal volitional attempts subjects produced an average of 47.6 ( $\pm$  12.69) Nm of torque during flexion and 5.94 ( $\pm$  1.86) Nm during supination. Key results are presented in **Table 3.1**.

**RAMPs.** No significant differences were observed between modes of activation for  $\Delta F$  ( $p=0.85$ ), InitialDR ( $p=0.16$ ), MaxDR ( $p=0.71$ ), and FinalDR ( $p=0.92$ ) during RAMP contractions (Figure 3.3).

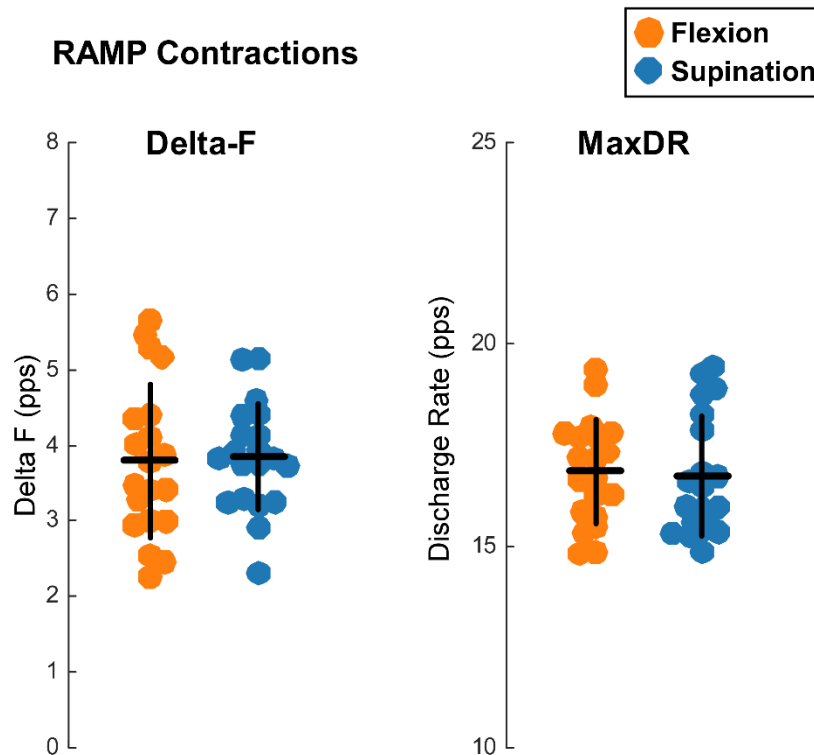


Figure 3.3. Delta-F and MaxDR Results. Individual data (dots) from all trials of RAMP contractions. Black lines represent mean (horizontal) and standard deviation (vertical).

**HOLDS.** On average, there was no significant difference in relative torque ( $p=0.28$ ), torque CoV ( $p=0.20$ ), and sEMG amplitude ( $p=0.54$ ) between modes of activation during HOLD contractions. Furthermore, no significant difference between the mean discharge rate ( $p=0.30$ ) and CoV ISI ( $p=0.42$ ) was observed. However, measures of common synaptic input (coherence) did significantly differ between modes of activation for the alpha ( $p<0.001$ ) and beta bandwidths ( $p<0.001$ ), but not delta bandwidth ( $p=0.87$ ). **Figures 3.4 and 3.5** display the individual data between modes of activation and the consistency of these measures between trials.

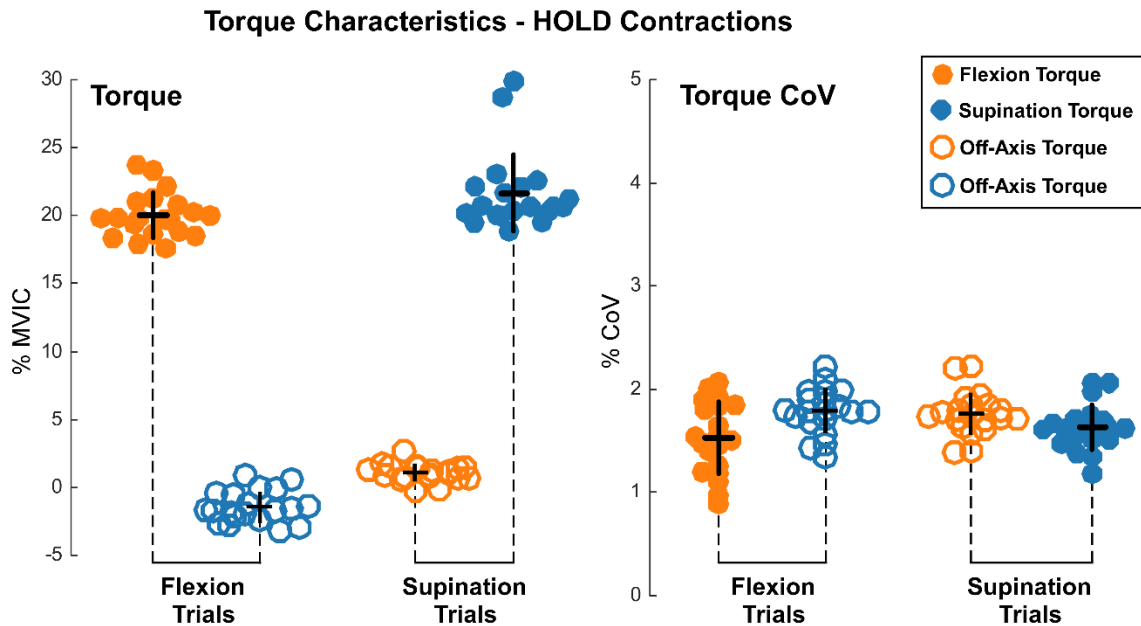


Figure 3.4. Flexion vs Supination Torque Control. Individual means (dots) from all trials of HOLD contractions. Black lines represent mean (horizontal) and standard deviation (vertical). Open circles represent the opposing torque direction of interest (e.g., within flexion trials: solid orange represents flexion torque and blue open circles represent supination off-axis torque).

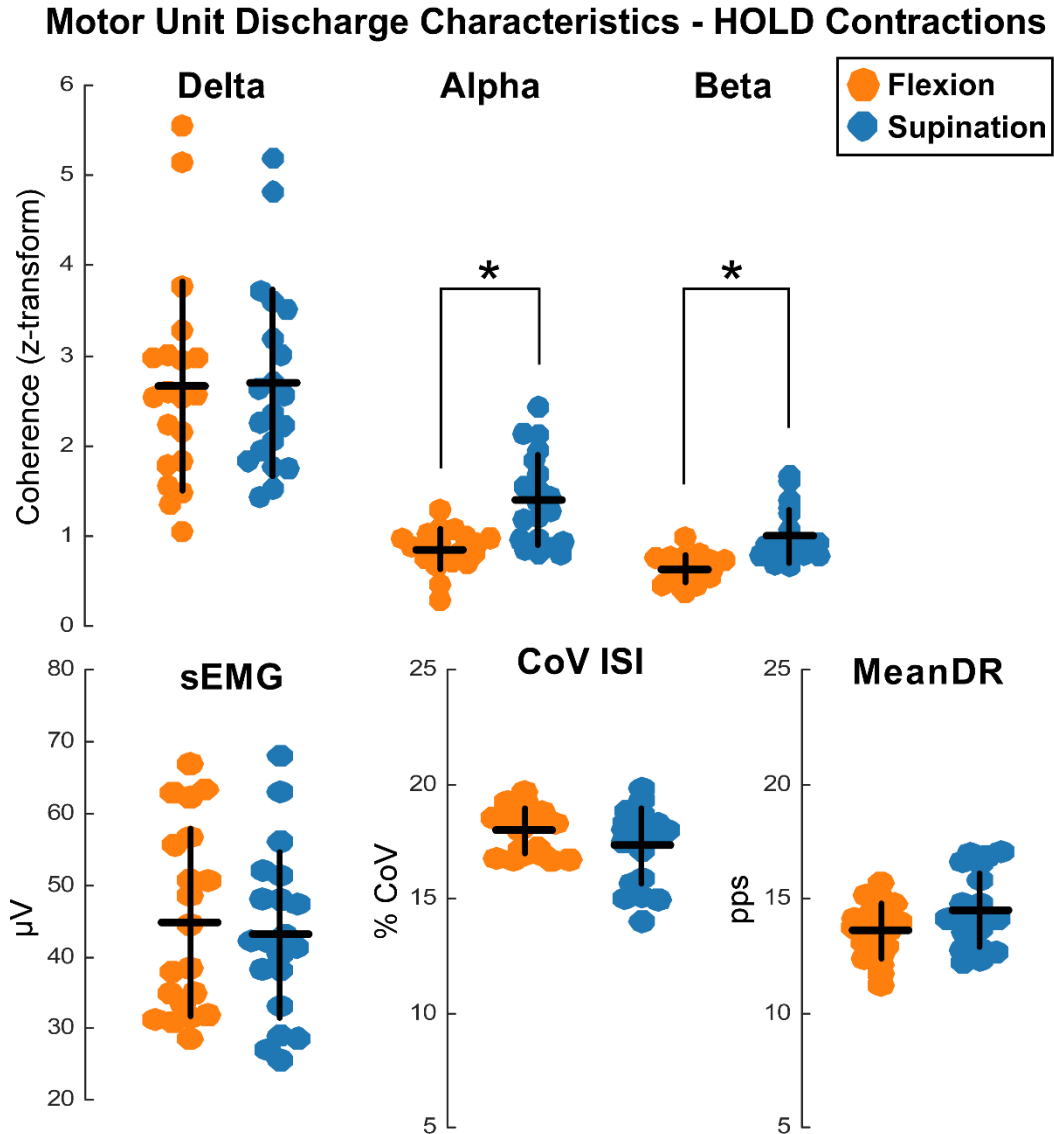


Figure 3.5. Flexion vs Supination MU HOLD Results. Individual means (dots) from all trials of HOLD contractions. Black lines represent mean (horizontal) and standard deviation (vertical). Delta (0-5Hz), Alpha (5-15Hz), and Beta (15-35Hz) band coherence. (\*) represent a statistically significant ( $p < 0.05$ ) difference between flexion and supination conditions.

**Tracked MUs (HOLDs).** 54 unique MUs were tracked across modes of activation. Similar to the un-tracked MU data, no significant difference between mean discharge rate ( $p=0.79$ ) was observed between flexion 13.83 pps ( $\pm 1.15$ ) and supination 13.87 pps ( $\pm 1.01$ ). Further, no significant difference between CoV ISI ( $p=0.66$ ) was

observed between flexion  $17.25 (\pm 1.30)$  and supination  $16.93 (\pm 2.17)$ . However, measures of common synaptic input (coherence) did significantly differ between modes of activation for the alpha (flexion  $0.79 (\pm 0.28)$ , supination  $1.16 (\pm 0.47)$ ;  $p=0.005$ ) and beta bandwidths (flexion  $1.08 (\pm 0.41)$ , supination  $1.50 (\pm 0.55)$ ;  $p=0.003$ ), but not delta bandwidth (flexion  $1.54 (\pm 0.30)$ , supination  $1.51 (\pm 0.28)$ ;  $p=0.74$ ). Individual subject data are presented in **Table 3.2**.

**MUAP morphology.** No significant differences were observed between modes of activation for the normalized MUAP distribution across each HDsEMG array ( $p=0.08$ ), mean MUAP peak-to-peak amplitude ( $p=0.61$ ), and the median MUAP frequency content ( $p=0.46$ ).

## **Discussion**

Here, we recorded the discharge characteristics and estimates of synaptic input to motor units from the biceps brachii during two modes of activation (flexion and supination), at similar levels of intensity. Through the use of HDsEMG and MU decomposition algorithms we observed that the MU discharge rate, inter-spike interval variability, MUAP morphology, torque variability, and estimated MN excitability ( $\Delta F$ ), did not differ between supination and flexion tasks. However, despite homogenous MU discharge characteristics between modes of activation, we observed a significant increase in coherence during supination within the alpha (5-15Hz) and beta (15-35Hz) bandwidths. These data support our hypothesis that the synaptic drive to bicep brachii motoneurons may differ during these modes of activation, however, the excitability and MU discharge characteristics of the motor pool remains invariant to differential functional tasks.

**Motoneuron discharge characteristics.** The biceps brachii, with the ability to perform more than one biomechanical function, offers a unique opportunity to observe functional changes in the MU behavior. Previous studies investigating task- and function-dependent behavior of the biceps brachii, and surrounding muscles, have found evidence for nonuniform muscle activity (ter Haar Romeny et al., 1984; van Zuylen et al., 1988) and spatial inhomogeneity (Holtermann et al., 2005). More recently, Rudroff and colleagues (2010) compared the MU discharge characteristics of the biceps brachii during position-controlled (joint angle) contractions and target-force controlled contractions during two postures (neutral and supinated). Their findings suggest that MUs initially behaved similarly between contraction types (force- and position-control) but were significantly modulated over time by changes in posture (supination). Rudroff and colleagues propose a potential mechanism of these posture-dependent changes may have been the result of alterations in synaptic input to the motor pool, under conditions of increased mechanical difficulty associated with supination, rather than changes in intrinsic properties of motoneurons (Rudroff et al., 2010). Extending these findings, in the current study, we show the underlying MU behavior, estimates of excitability, and torque variability to be invariable to changes in task. However, estimates of common synaptic input significantly differed between modes of activation.

The MU discharge rates and  $\Delta F$  values observed in the present study are consistent with previous findings of the biceps brachii, during similar isometric flexion tasks (Holobar et al., 2010; Mottram et al., 2009; Wilson et al., 2015). Similarly, the quantity of MUs yielded from the biceps brachii, although lower than other motor pools like the tibialis anterior, appears to be similar to previous investigations (Holobar et al., 2010;

Wilson et al., 2015). While the bicep brachii is a convenient muscle for use in EMG experiments, it should be noted that the muscle belly moves a considerable amount (even in isometric tasks) relative to the cutaneous position of each electrode on the array. This movement, as well as muscle fiber morphology (fusiform), may be reasons for lower MU yield when compared to other motor pools.

Changes in motoneuron excitability, driven by fluctuations in monoaminergic drive, may offer the nervous system additional ways to optimize motor control strategies. Previous studies have shown motoneuron excitability (and  $\Delta F$  values) can vary between motor pools (Kim et al., 2020; Taylor et al., 2020; Wilson et al., 2015). Further, differences in excitability between motor pools may offer functional benefits for motor control by altering the synaptic input necessary for specific tasks (Heckman & Enoka, 2012; Lee & Heckman, 1998). For instance, motor pools used for postural support or locomotion, which have higher levels of tonic activity, may benefit from higher levels of excitability to aid in their continued use over long periods of time. However, it is not well understood if similar alterations in motoneuron excitability are utilized to modify motor commands within the same motor pool. Khurram and colleagues (2021) have recently investigated task-dependent changes in  $\Delta F$  values of the tibialis anterior motor pool between seated isometric contractions and unconstrained standing contractions. Their findings suggest  $\Delta F$  values do not change across these two tasks. Similarly, the results of the current study are congruent with these prior findings and extend this notion to the biceps brachii, under two functionally distinct modes of activation.

Spatial inhomogeneity in MU recruitment and MU activity may also have a role in complex motor tasks (Paton & Brown, 1994; Watanabe et al., 2021). Spatially selective

sub-sets of MUs may offer an intuitive control strategy for the muscles with more than one function. However, in contrast to previous notions of spatial inhomogeneity, the current study did not observe differences in MUAP waveform amplitude, frequency content, or relative MUAP size across the HDsEMG array, between modes of activation. Suggesting a homogenous population of MUs were observed between flexion and supination within the current study.

To further explore the potential of spatial differences in MU behavior, the current study also attempted to track unique MUs across trials and modes of activation by correlating the spike-trigger averaged MUAP waveform between each trial type (similar to Martinez-Valdes et al., 2017) (see Methods – *Motor Unit Tracking*). However, given the restrictive nature of this method, the resultant MU yield was inadequate for the analysis of RAMP contractions, specifically recruitment/de-recruitment thresholds and  $\Delta F$  calculations. While successful MU matching attempts were achieved between HOLD contractions (54 MUs identified), MU matching between RAMP contractions (3 MU identified) proved much more difficult (see Table 3.2). This disparity in yield may reflect the difficulties associated with MUAP identification (and MU decomposition yield) during RAMP contractions and not necessarily differences between modes of activation. Others have suggested MU yield and MUAP tracking may be adversely affected by the shorter stable firing duration and changes to the shape of the MUAP during RAMP trials, when compared to HOLDs (Del Vecchio et al., 2020). Despite these difficulties, the successfully tracked MU data from HOLD contractions closely resembled the un-tracked data and no significant differences were observed within the mean MU firing rate or variation of the inter-spike intervals between supination and flexion. Taken together,

these findings demonstrate a lack of spatial inhomogeneity and invariance of MU firing characteristics to differential modes of activation, within the biceps brachii motor pool.

**Differences in coherence.** The aforementioned findings suggest that the motor unit firing behavior and the intrinsic excitability of MNs remain invariable across modes of activation. However, the observed differences in coherence between these tasks suggest that the synaptic input received varies between modes of activation. Furthermore, this may suggest the synaptic input during different modes of activation contains task-specific, kinematic, information required for motor control of a multi-function muscle (Georgopoulos et al., 1982, 1986). Others have characterized changes within intra- and intermuscular EMG coherence of the beta band are driven by the motor cortex and may be task-dependent (Baker et al., 1997; Kilner et al., 1999; Wang et al., 2020; Yang et al., 2009), whereas alpha band changes may represent changes in multimodal input from various cortical and spinal sources (McAuley & Marsden, 2000; McKiernan et al., 2000).

Changes in alpha and beta band coherence may indicate altered synaptic input, however, similar changes in lower frequency bands (delta band) of coherence did not exist between modes of activation. Others have referred to these lower frequencies as common drive (De Luca & Erim, 1994) or the common synaptic input to the motor pool which may be more directly related to the control of voluntary force output (Castronovo et al., 2015; Farina & Negro, 2015). Although the absolute torque generated greatly varied between conditions, each task was performed at similar relative intensities with similar torque variability, which may explain why no differences were observed in delta band coherence.

Hug and colleagues (2021) recently provided evidence for a divergent control strategy across muscles within the same functional group, using similar methods as the current study. They observed task-dependent changes in coherence across muscles of the triceps surae (i.e., soleus, medial and lateral gastrocnemius) during plantarflexion tasks with changes in posture. Suggesting that, despite anatomical and biomechanical similarities, the muscles of this group received differential amounts of common input (Hug et al., 2021). The current study did not quantify changes within surrounding motor pools that may have influence on joint mechanics, such as antagonists and synergists, so it is not possible to infer if the changes in synaptic input are shared across functional movement synergies. Further it may be possible, the observed changes in coherence are a *result of* alterations in higher-level movement synergies between muscles. Nonetheless, the observation of function-dependent intra-muscular alterations in coherence, may support a motor control framework that emphasizes modular control and the flexibility of input to motoneurons (Hug et al., 2023).

**Limitations.** Some limitations of the current study include the lack of varying contraction types and MVIC intensities. Additionally, future studies should record MU behavior from antagonistic and synergistic muscles, to aid in quantifying the motor command of multi-function muscles. Lastly, during flexion tasks, a slight pronation torque was observed. Subjects were not given visual feedback of this secondary (off-axis) torque however, specific verbal instructions were provided at the start of the experiment, to emphasize joint action only in the primary direction for each task. We do not believe this finding alters the overall interpretation of the results as this finding was consistent

within all subjects across the experiment and likely reflects biomechanical constraints and preferences of the elbow joint during flexion.

## **Conclusion**

To our knowledge, we are the first to utilize HDsEMG and decomposition techniques to investigate changes in the task- and function-dependent behavior of MUs within the biceps brachii motor pool. Here, we observed significantly greater intramuscular coherence, during supination, within the alpha (5-15Hz) and beta bands (15-35Hz). These data suggest different sources of synaptic drive may regulate the activation of biceps during distinct modes of volitional activation, while the excitability and MU discharge characteristics of the motor pool remains invariant. These alterations in common synaptic drive, between tasks, suggest the motor command to the biceps motor pool may contain essential information regarding the limb movement.

Table 3.2. Tracked Motor Unit Characteristics During HOLDS

Subject	MU	Flexion				Supination			
		MeanDR	Delta	Alpha	Beta	MeanDR	Delta	Alpha	Beta
1	5	13.84 pps (1.16±)	1.54	0.49	0.91	14.14 pps (1.43±)	1.39	0.76	1.24
2	3	14.23 pps (1.25±)	1.92	0.74	0.99	14.53 pps (0.95±)	1.90	0.68	1.23
3	2	15.11 pps (1.37±)	1.32	0.90	1.73	15.34 pps (1.53±)	1.05	1.58	2.39
4	4	14.11 pps (1.48±)	1.33	0.68	0.80	13.61 pps (0.97±)	1.45	1.15	1.32
5	7	12.91 pps (1.37±)	1.70	0.69	0.81	13.14 pps (1.07±)	1.83	0.64	1.32
6	5	15.71 pps (1.17±)	1.88	1.09	0.79	14.65 pps (1.35±)	1.87	2.05	1.75
7	3	12.74 pps (1.54±)	1.87	1.15	1.88	12.45 pps (1.34±)	1.64	1.44	2.00
8	6	14.02 pps (1.41±)	1.29	1.05	0.83	13.91 pps (1.25±)	1.34	1.47	1.07
9	8	13.94 pps (1.92±)	1.11	0.27	0.81	14.72 pps (2.18±)	1.30	0.83	0.89
10	3	11.71 pps (1.61±)	1.49	0.82	1.17	12.30 pps (2.00±)	1.37	1.02	2.21

Table 3.2. Tracked Motor Unit Characteristics During HOLDS. Descriptive statistics of 46 MUs tracked across both modes of activation from each subject. Abbreviations: Tracked Motor units (MU); pulses per second (pps).

## CHAPTER 4

### THE EFFECTS OF CAFFEINE ON HUMAN SPINAL MOTONEURONS

#### Abstract

Human spinal motoneurons are partially governed by the activation of persistent inward currents that contribute to changes in excitability and elicit lingering effects on the output of motoneurons. Persistent inward currents are regulated by monoamines, such as serotonin. Caffeine, one of the world's most popular performance-enhancing supplements, elicits its ergogenic benefits through stimulating the volumetric release of monoamines. However, little is known on how caffeine may directly affect motoneuron excitability and discharge characteristics. We utilized a double-blind, inactive placebo-controlled, crossover study design (clinical trial: NCT04891393) to examine the effects of caffeine (3 mg/kg) on motoneuron excitability and discharge characteristics. Utilizing high-density electromyography from the right tibialis anterior (TA) and soleus (SOL) muscles of 20 neurotypical adults, we decomposed and tracked 1,452 concurrently active motoneurons during sub-maximal (20%) isometric contractions of the ankle. In the caffeine group, we observed significant changes in mean arterial pressure and heart rate after the consumption of caffeine. Utilizing linear mixed effects models, we observed significant interactions, within the caffeine group, over time, within the TA motor pool for changes in estimated motoneuron excitability, discharge rate, and the variability of inter-spike intervals. However, similar changes within the SOL or placebo groups were not observed. These findings suggest that caffeine differentially affects the discharge characteristics of the TA motoneurons through an increase in excitability and rate coding.

## **Introduction**

Caffeine is one of the world's most popular, and readily available, psychoactive drug (Graham, 2001). Recent national surveys have indicated that 89% of Americans consume caffeine, with average daily users typically consuming two cups of coffee per day (211 mg of caffeine/day) (Fulgoni et al., 2015). Owing to its widespread use and low toxicity (Kaplan et al., 1997; Nawrot et al., 2003), caffeine has garnered increased attention in the fields of human kinesiology and psychology with a plethora of studies demonstrating its ergogenic potential. For example, at typical doses (i.e., 2–10 mg/kg), caffeine has been shown to improve cognitive ability (Ruxton, 2008), short-term memory (Bättig & Buzzi, 1986), physical endurance (Doherty et al., 2004; Doherty & Smith, 2005; Warren et al., 2010), muscular strength (Goldstein et al., 2010; Grgic et al., 2018), and exercise tolerance (Meyers & Cafarelli, 2005). While the effects of caffeine on performance-related outcomes are well-documented, there remains ambiguity regarding the complete impact of its pharmacodynamics, particularly its effects on human spinal motoneurons.

At typical doses, caffeine acts as a stimulant. Caffeine achieves these effects by acting as a competitive antagonist to adenosine, which elicits its benefits for wakefulness and alertness (Fisone et al., 2004). Additionally, caffeine can evoke the release of excitatory monoaminergic neurotransmitters, including norepinephrine and serotonin (Berkowitz & Spector, 1971). These monoaminergic neurotransmitters are of particular interest as they can modulate motoneuron excitability through the activation of persistent inward currents (PIC) in spinal motoneurons, which aid in the amplification and prolongation of synaptic input to the motoneuron (Bennett et al., 1998; Hounsgaard et al., 1988; Hounsgaard & Kiehn, 1989; Lee & Heckman, 1996). The extent to which PICs can be modified exogenously through caffeine consumption in humans is unknown. One

recent study has shown that the use of amphetamine (a drug with a similar, albeit more powerful, mechanism of action) can increase motoneuron excitability in humans (Udina et al., 2010). Others have shown that orally administered caffeine increases the probability of evoking self-sustained discharge of motor units, a known phenomenon of PICs and increased excitability (Walton et al., 2002). While caffeine remains one of the most researched psychoactive drugs openly available to consumers, its effects at the level of the human motoneuron is unclear. Its ubiquitous nature and wide acceptance in exercise and sport science make it imperative to fully understand its effects on the human neuromotor system.

We aim to utilize a double-blind, inactive placebo-controlled, crossover study design to examine the effects of caffeine on motoneuron excitability and discharge characteristics. Using decomposition software and non-invasive, high-density surface electromyography (HDsEMG), we can concurrently track dozens of motoneurons and observe changes in their firing characteristics over time (Negro et al., 2016). We will utilize a paired-motor unit analysis technique to quantify estimated motoneuron excitability (Gorassini et al., 2002a). We hypothesize the ingestion of a 3mg/kg dose of caffeine will increase estimated motoneuron excitability within the tibialis anterior and soleus motor pools.

## **Methods**

**Participants.** Twenty human subjects (10 females, mean age  $27.4 \pm 5.0$  years; mean BMI  $23.2 \pm 2.2$ ) were recruited from the university student and faculty population. Participants reported no known neuromuscular impairments, no known cardiovascular pathology (e.g., hypertension, cardiac arrhythmias), no use of medications with known

effects on spinal motoneuron excitability (e.g., stimulants, selective serotonin reuptake inhibitors), and reported no aversions or allergies to coffee or caffeine. All procedures were approved by the Institutional Review Board at Temple University (Protocol # 26014). All subjects provided written informed consent prior to participation.

**Protocol.** This study design was pre-registered on [clinicaltrials.org](https://clinicaltrials.org) (NCT04891393) on May 11<sup>th</sup>, 2021. Participants and experimenters were blinded to the intervention. An outside researcher not involved in the creation, analysis, or design of the current study, created a randomized blinding matrix containing participant ID number and intervention type, which was stored in a locked file cabinet. This outside researcher measured the caffeine (and placebo) intervention utilizing a commercially available food scale and the intervention was served in individualized microwave-safe cups, labeled with participant ID numbers, for each participant. Experimenters remained blinded to the intervention until all primary data collection, motor unit cleaning, and data-processing steps were completed.

This study utilized oral administration of commercially available instant coffee for human use. A 3 mg/kg dose of caffeine (Starbucks VIA Instant Dark Roast Coffee) was administered as the caffeine intervention (CAF). An equal weight of Starbucks VIA Instant *Decaffeinated* Dark Roast Coffee was administered as an inactive-placebo intervention (DE). The DE intervention may have trace amounts of caffeine (up to 5 mg/serving), however, previous studies have shown that ultra-low doses of caffeine found in decaffeinated coffee (< 20 mg) do not elicit clinically significant changes in physiology (i.e., changes in systolic or diastolic blood pressure > 2 mmHg or changes in

heart rate > 2 bpm) (Ammon et al., 1983; van Dusseldorp et al., 1989). Both coffee interventions were served with water heated to around 140° F.

### Experimental Design

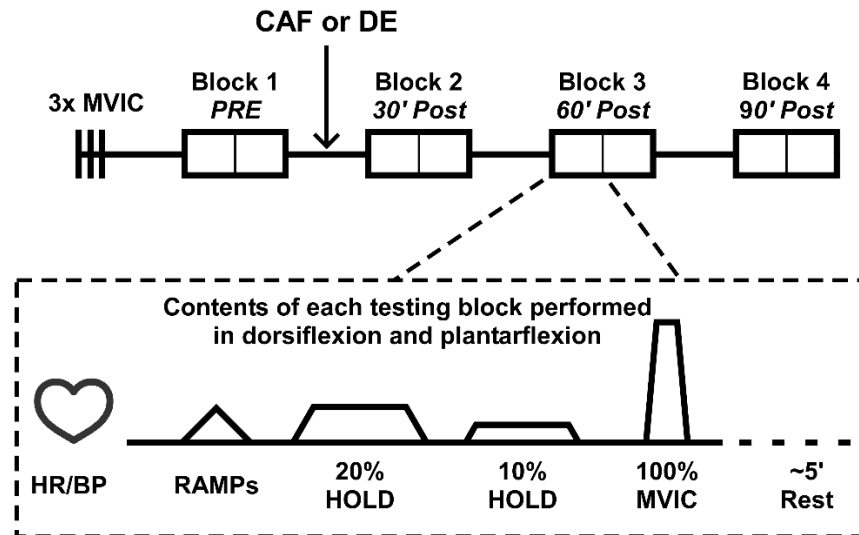


Figure 4.1. Experimental Design. Double-blind, inactive placebo-controlled, crossover study design. Subjects were randomly assigned to perform this experiment under either CAF or DE condition, completing it a second time under the opposite condition. Each testing block was completed in both dorsiflexion and plantarflexion directions.

**Testing sessions.** Each participant attended one pre-screening session prior to enrollment in the intervention arm. This was used to screen participants for inclusion/exclusion criteria, provide informed consent to the study, complete a validated caffeine consumption questionnaire (Bühler et al., 2014), familiarize the participant with the testing apparatus, and to confirm that adequate EMG signal analysis could be performed. Pre-screening and all testing sessions were separated by at least 48 hours to mitigate the effects of fatigue. All sessions were collected within 10 days of the pre-screening session. Participants were randomly assigned to receive either CAF or DE interventions during the subsequent testing sessions. Participants received the opposite

intervention on subsequent sessions (i.e., if a subject received CAF on testing session #1, they received DE on testing session #2).

Testing session #1 was performed on a non-consecutive day following the pre-screening session. Participants completed a total of 4 blocks of testing (see **Figure 4.1**), consisting of a pre-test, 30 minute post-test, 60 minute post-test, and 90 minute post-test blocks. A single dose of the intervention was administered to the participant after block 1 and 30-minutes prior to block 2. A registered nurse assessed heart rate (HR) and blood pressure of the participant before the start of each testing block with a non-invasive, commercially available electronic-blood pressure cuff (Omron Healthcare, Lake Forest, IL). Mean arterial pressure (MAP) was calculated from systolic and diastolic values.

The protocol for testing session #2 was identical to the previous testing session, except the alternative intervention was administered.

**Experimental set-up.** Prior to each experimental session, the skin over the right tibialis anterior (TA) and right soleus (SOL) was shaved, abraded with high-grit sandpaper, and cleansed with water. One 64-channel high-density electrode array (8mm inter-electrode distance, 5 columns x 13 rows, ELSCH064NM2; OT Bioelettronica; Turin, Italy) was coated with conductive adhesive paste (AC Cream; Spes Medica; Genova, Italy) and placed on the skin over the muscle and secured with medical tape (3M Transpore; St. Paul, MN). Specifically, the medial border of the TA HDsEMG array was placed parallel with and aligned to the anterior tibial crest, the center of the array was positioned on the largest part of the muscle belly approximately in the upper 2/3 of the lower right leg. The SOL HDsEMG array was placed on the right leg, medial to the Achilles tendon and distal to the gastrocnemius. Participants were seated in an isokinetic

dynamometer (Biodex; Shirley, NY) and secured with straps across the torso and thigh in a comfortable position of 60-90° hip flexion and 15° knee flexion. The ankle was secured to a footplate achieving 15° degrees of plantarflexion and affixed to a six degrees of freedom load cell (JR3; Woodland, CA). The ankle's axis of rotation was centered to the load cell in this position. Real-time feedback of torque output was provided on a large format monitor positioned directly in front of the participant, approximately 5 ft (1.5 m) from the subject, to assist task performance.

**Isolated joint contractions.** Prior to each testing session, participants performed three maximal volitional isometric contractions (MVIC) in each direction (dorsiflexion and plantarflexion) to establish the participants maximum effort. Strong verbal encouragement was provided by the experimenter during each attempt. Each MVIC consisted of a 3s increase to maximum, a 3s sustained maximal, and a 3s decrease to rest. Each MVIC was separated by at least two minutes of rest.

For the purpose of EMG decomposition and subsequent motor unit analysis, a series of submaximal isometric contractions were utilized, in which the force output could be controlled, to ensure relatively similar levels of effort were achieved between groups and within-subjects. During this time, MN activity was recorded with HDsEMG. For this protocol two types of contractions were performed. The first, a symmetrical isolated joint torque up to 20% MVIC, conducted at a consistent rate of torque development (10s up and 10s down) (**RAMP**). During each testing block participants completed two sets of three repetitions of 20% RAMP contractions, 10 seconds between each repetition and two minutes between sets was observed to mitigate the effects of fatigue. The second type of contraction, an isolated joint torque at a fixed percentage, was

performed at two intensities (10% and 20%) of MVIC (**HOLD**). Each type of HOLD contraction was held for a duration of 40 seconds at the target percentage of MVIC. Participants completed two sets of HOLD contractions, the first at 10% MVIC and the second at 20% MVIC with two minutes rest between each contraction.

**Data collection.** During isolated joint contractions, differential HDsEMG data was recorded using the OTBioLab software (OT Bioelettronica; Turin, Italy). Torque was baseline corrected and filtered using a 20 Hz low pass filter, and this signal was used for visual feedback of task performance. EMG was amplified at 150x, filtered at 20-900 Hz, and collected at 2048 Hz using a 16-bit A/D converter (Quattrocento, OT Bioelettronica; Turin, Italy), simultaneously with the torque data.

**Motor unit decomposition and processing.** All monopolar channels of the HDsEMG array recordings were individually inspected offline and isolated for subsequent processing. The selected HDsEMG array channels were then decomposed into the discharge of individual motor units using a convolutive blind source separation algorithm (Negro et al., 2016). This algorithm has been extensively validated and provides an accurate method for decomposing motor unit spike trains (Thompson et al., 2018). A semi-automated motor unit cleaning process was performed by an experienced investigator, who remained blinded to intervention type, to ensure the accurate detection of each spike of each motor unit, similar to previous reports (Afsharipour et al., 2020; Hassan et al., 2021; Taylor et al., 2022). All remaining motor unit spike trains were identified and incorporated into the subsequent data set for further analysis. The mean discharge rate (DR) and coefficient of variation (CoV) of the inter-spike intervals (ISI) of each motor unit were calculated from the motor unit data 2 seconds after

the start of and 2 seconds prior to the end of the torque plateau from each HOLD contraction (ensuring that only the isolated steady-state firing of each motor unit, during stable torque levels, were considered for analysis). Recruitment thresholds for each motor unit were defined as the torque (% of MVIC) at which each motor unit's first identified spike occurred during RAMP contractions.

**Motor unit tracking.** In order to identify and track the same motor units across the entire testing session, all valid and available motor unit action potential (MUAP) waveform profiles within each subjects' block were cross-correlated with each other in a "daisy-chain" manner (*i.e.*, comparing the MUAPs in block one to block two, then block two to block three, and block three to block four). Motor unit action potential (MUAP) waveforms across the array were calculated by spike-triggered averaging the HDsEMG data using the discharge of each motor unit. Normalized cross-correlations higher than 0.85 between MUAPs of two blocks were considered a match and were given a unique identifier, tracked longitudinally across subsequent blocks, and ultimately utilized in the future motor unit analysis methods. Motor unit tracking was only done within the same type of contraction (*e.g.*, the motor units identified in the 10% HOLD were *not* explicitly tracked within 20% HOLD trials). On rare occasions, multiple matches with cross-correlation values greater than 0.85 were identified, the highest value of cross-correlation source was selected, and all other duplicates were removed from future analysis.

**Delta-F ( $\Delta F$ ).** To estimate the effect of persistent inward current (PIC) activity, and as a measure of MN excitability, the paired motor unit technique was utilized (Gorassini et al., 2002a). In this approach, the time at which a higher threshold unit is recruited and derecruited is found and normalized to the firing frequency of a low-

threshold motor unit (*i.e.*, the estimated synaptic current). Under high levels of PIC activity, the synaptic current needed to reach threshold will be lowered and a lower derecruitment threshold will be observed and the change in discharge rate (*i.e.*,  $\Delta F$ ) will be calculated.

At each timepoint a single RAMP set with the highest motor unit yield was chosen for  $\Delta F$  calculations, and subsequent motor unit tracking. Further, to mitigate time- and repetition-dependent effects on  $\Delta F$  calculations, only the first RAMP contraction of these high-yield sets was utilized in subsequent analysis. To ensure accurate representation of PIC amplitude, from  $\Delta F$  calculations, the following restrictions were applied to limit invalid motor unit comparisons: the low threshold (control) unit was recruited at least 1 second before the higher threshold unit, and the low threshold unit was de-recruited at least 1.5 seconds after the high threshold unit (Hassan et al., 2020).

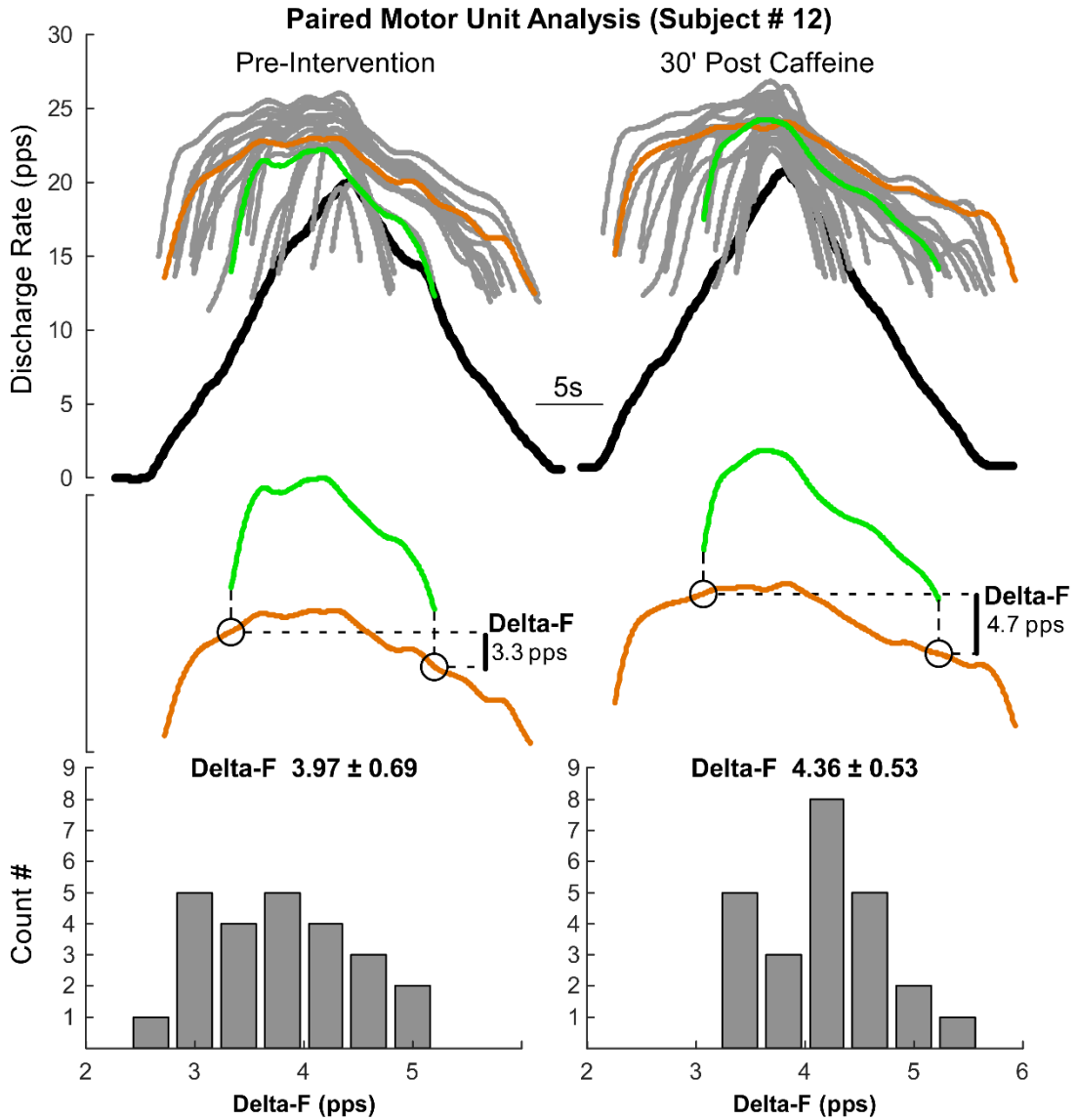


Figure 4.2. Paired Motor Unit Analysis of Tracked MUs. All data is from a single subject, within the CAF condition. The left pane is from PRE time point and the right pane is from data collection 30 minutes after the ingestion of 3mg/kg caffeine. Top: Torque (black line) and tracked motor units (grey) during a single RAMP contraction. Middle: a select pair of unique motor units (green as test unit; orange as control unit) utilized for one Delta-F calculation in each condition. Bottom: Histogram of all comparisons of tracked motor unit Delta-F. The mean and standard deviation of each time point are displayed in text, above the histogram.

**Coherence.** To estimate the common synaptic input to motoneurons, we calculated a pooled coherence (Laine et al., 2015) between all unique pairs of simultaneously active motor unit spike trains, within the active motor pool. This technique provides a normalized value of the correlation in the frequency of synaptic inputs shared between the unique pairs of motoneurons. Here, all valid motor units from the motor pool of interest are assessed to ensure sustained repetitive firing throughout the steady-state portion of each HOLD contraction. Units without sustained repetitive firing during this period were removed and the remaining individual spike trains were concatenated into two long spike trains of consecutive unique pairs. Coherence was then calculated on the two concatenated spike trains in consecutive non-overlapping 1s segments with the cross-spectra of the two uniquely paired units normalized by the pairings combined auto-spectra (Halliday et al., 1995, 1999; Laine et al., 2015; Zaback et al., 2022). To compare these coherence measures across conditions, coherence values at each frequency were converted to standard Z-scores, based on the number of segments contained in the concatenated spike trains, and the area under the curve was calculated in the following frequency bins: Delta band (0-5 Hz), Alpha band (5-15 Hz), Beta band (15-35 Hz).

**Statistical analysis.** The linear mixed effects models (LMEM) were constructed and analyzed with R v4.2.2 (R Core Team, 2012), all other statistical analysis, data manipulation, and visualization were performed using MATLAB 2019b (MathWorks, Natick, USA), and significance was accepted at the  $p \leq 0.05$ . Descriptive statistics are reported as mean ( $\pm$  standard deviation) or estimated margin mean and [standard error].

Trial based outcome measures such as: MAP, HR, and torque at 100% MVICs were assessed for changes over time utilizing a repeated measures analysis of variance (RM-ANOVA), including 2 factors (CAF vs DE) (*ranova*; MATLAB 2019b). Results are reported as ( $F(df_{\text{time}}, df_{\text{error}}) = F\text{-value}, p = p\text{-value}$ ). If significant interactions were found, a post-hoc Tukey's test was used to assess the relationship between variables of interest (*multcompar*; MATLAB 2019b).

Due to the heterogeneity within the tracked motoneuron variables, LMEM were used to analyze these data. This technique ensures appropriate weighting of data from each subject despite the variable amount of motor units contributed for each trial. We utilized *lme4* (Bates et al., 2015) to perform a LMEM analysis of the relationship between motor unit variables of interest (*e.g.*,  $\Delta F$ , MaxDR) and the fixed effects of *Condition* (CAF vs DE), *Time* (pre, post-30', post-60', post-90'), *Muscle* (TA vs Sol) and their interactions, with random effect of *unique motor unit* nested within *Subject*, random intercepts were created for each subject for the effect of condition type (1|Subject/UniqueMotorUnit). For the LMEM variables that rely on by-trial calculations, and not by-motor-unit (*e.g.*, Coherence), *unique motor unit* was removed from the nested random effect. Visual inspection of residual diagnostic plots for each model did not reveal any obvious deviations from homoscedasticity or normality. Main effects of LMEM are reported as  $X^2 = \text{chi-square}, p = \text{statistical significance}$ . Group estimated marginal means were computed with *emmeans* (Lenth et al., 2023). To assess statistical significance and pairwise comparisons across time, *p*-values were obtained by applying Satterthwaite's method for degrees of freedom (*ImerTest* R package; Kuznetsova et al., 2017). Bonferroni correction method was utilized for multiple comparisons. Effect size

(Cohen's  $d$ ) was calculated to determine the standardized magnitude of the effect of condition type from the estimated means.

## Results

In total 4,638 data points (837 from RAMP and 3,801 from HOLD contractions) from 1,452 tracked motor units, across 4 time points, were utilized for the LMEM analysis (see **Tables 2-5** for details). One subject (caffeine naïve) failed to complete the last 90-minute post-CAF assessment due to muscle cramping and restlessness, resulting in missing motor unit data for that time point. A small number of baseline trials ( $n=6/120$ ) failed to yield any valid, trackable, motor units via decomposition from either condition. The majority of these (5/6) were from SOL RAMP contractions. In lieu of motor unit data from these instances, the remaining data (*e.g.*, Torque, MAP, HR, etc.) from these trials were utilized in subsequent analysis.

Baseline differences in motor unit discharge rate variables between motor pools (TA vs SOL) were present and estimates are provided in **Tables 2-5**, however, elucidating these muscle-dependent differences in baseline motor unit behavior extends beyond the intended purpose of this study. For reference, these muscle-dependent differences are well-documented elsewhere (Connelly et al., 1999; Kallio et al., 2013). For brevity, significant by-*Muscle* interactions are not reported below, as the main purpose of the study was to investigate the *Condition\*Time* and *Condition\*Time\*Muscle* interactions within each group.

**Cardiovascular physiology.** A RM-ANOVA revealed a statistically significant effect of *Condition\*Time* interaction in MAP ( $F(3, 114) = 12.69, p < 0.001$ ) with significant differences observed between groups at post-30' ( $p = 0.01$ ), post-60' ( $p =$

0.01), and post-90' ( $p < 0.001$ ). Additionally, there was also a statistically significant effect of *Condition\*Time* interaction on HR ( $F(3, 114) = 7.02, p < 0.001$ ), significant differences were observed between groups at post-30' ( $p < 0.05$ ) (**Figure 4.3**).

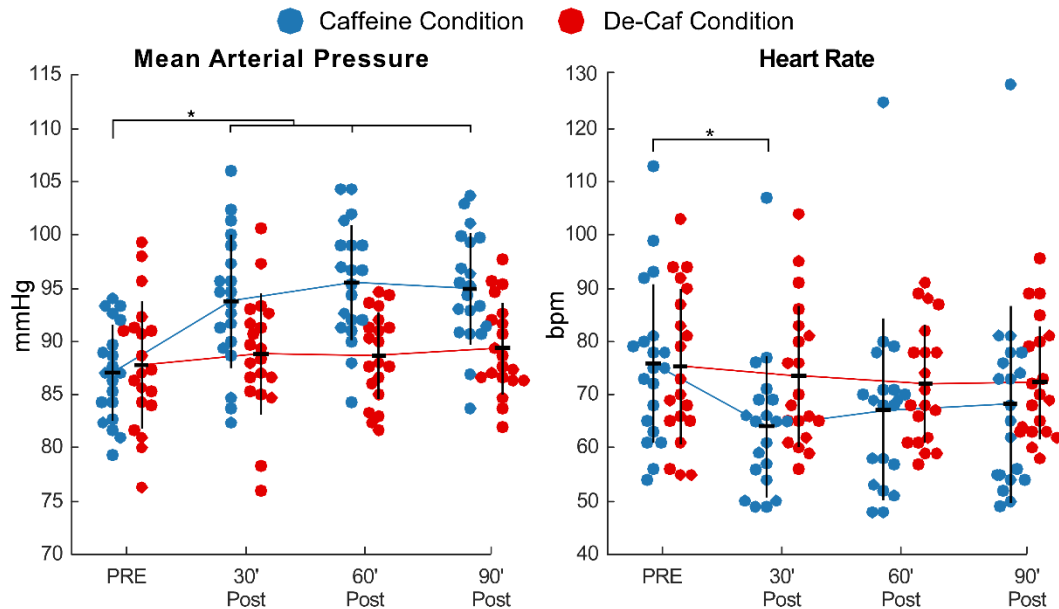


Figure 4.3. Cardiovascular Response to Caffeine. Dots represent individual subject data, from both CAF and DE conditions, across the experiment. (\*) Represent statistically significant ( $p < 0.05$ ) differences between PRE- and select time point.

**MVIC and torque characteristics.** Maximum volitional isometric contractions (100% MVIC), completed before the start of each testing block, did not significantly differ between conditions over the course of the experiment for TA ( $F(3, 114) = 0.66, p = 0.58$ ) or SOL ( $F(3, 114) = 0.66, p = 0.66$ ) (see **Table 1**). This finding suggests 100% MVIC levels remained stable, for both conditions, throughout the experiment (**See Appendix D**). The percentage of MVIC (relative intensity) at the peak of RAMP contractions did not significantly differ between conditions over the course of the experiment for TA ( $F(3, 108) = 0.81, p = 0.48$ ) or SOL ( $F(3, 108) = 0.40, p = 0.75$ ). Similarly, the average percentage of MVIC (relative intensity) during the steady-state

portion of HOLD contractions did not significantly differ between conditions over the course of the experiment for 20% MVIC TA ( $F(3, 108) = 1.69, p = 0.17$ ), 20% MVIC SOL ( $F(3, 108) = 0.14, p = 0.93$ ), 10% MVIC TA ( $F(3, 108) = 0.86, p = 0.46$ ), 10% MVIC SOL ( $F(3, 108) = 0.29, p = 0.84$ ).

The CoV of torque during the steady-state portion of HOLD contractions did not significantly differ between conditions over the course of the experiment for 20% MVIC TA ( $F(3, 108) = 1.0, p = 0.35$ ), 20% MVIC SOL ( $F(3, 108) = 0.39, p = 0.75$ ), 10% MVIC TA ( $F(3, 108) = 0.90, p = 0.44$ ), 10% MVIC SOL ( $F(3, 108) = 0.76, p = 0.51$ ). These findings suggest neither maximum strength, relative trial intensity, nor torque variability changed as an effect of condition type or fatigue.

**Motor unit RAMP variables.** During 20% MVIC RAMP contractions, 201 unique motor units were initially tracked within the TA motor pool and 69 were tracked within SOL. A significant interaction between  $\Delta F$  and *Condition\*Time\*Muscle* ( $X^2 = 18.9, p < 0.001$ ) was observed. Estimated marginal means are displayed in **Table 2**, with a moderate-large effect size within the TA ( $d=0.40-1.23$ ; between baseline and significant time points), indicating an increase in  $\Delta F$  within the TA. This effect was not statistically significant within the SOL.

A significant interaction between MaxDR and *Condition\*Time* ( $X^2 = 14.45, p = 0.002$ ) was observed. Estimated marginal means are displayed in **Table 2**, with a moderate-large effect size within the TA ( $d=0.39-1.11$ ; between baseline and significant time points), indicating an increase in MaxDR within the TA. This effect was not statistically significant within the SOL.

Across both muscles, no significant interaction was found between *Condition\*Time* and Initial DR ( $X^2 = 1.96, p = 0.59$ ), Final DR ( $X^2 = 2.02, p = 0.57$ ), Recruitment ( $X^2 = 4.34, p = 0.22$ ), and De-Recruitment Thresholds ( $X^2 = 2.14, p = 0.54$ ).

### Tracked MU Discharge Characteristics - RAMPs

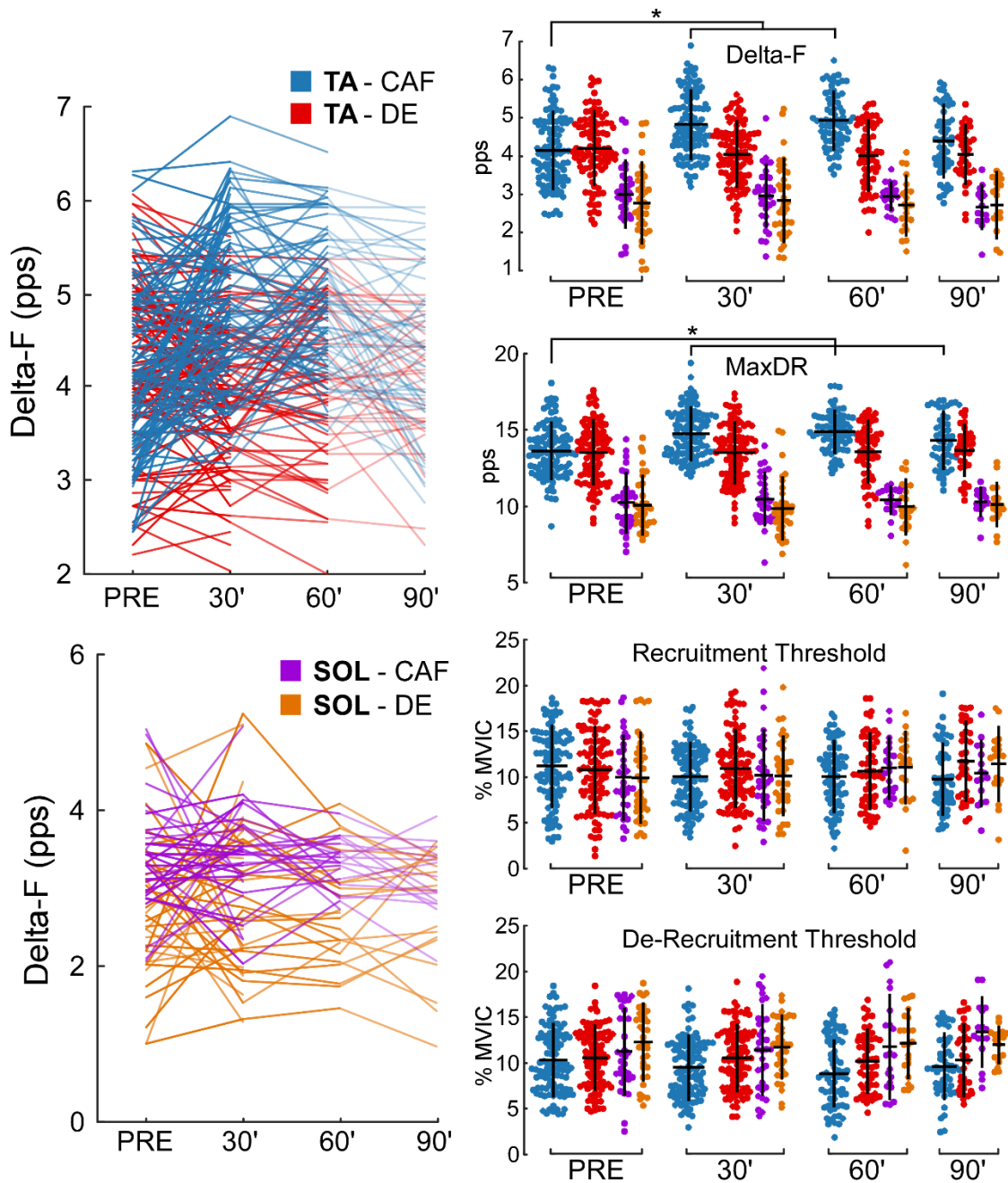


Figure 4.4. Tracked MU Discharge Characteristics – RAMPs. Left: Line plots of Delta-F over time, between TA and SOL motor pools. Each line represents the change observed within each unique MU. Right: Bee-swarm plots of all tracked MUs within each condition. Black lines represent mean (horizontal) and standard deviation (vertical) of each group. (\*) Represent statistically significant ( $p < 0.05$ ) differences between PRE- and select time point as a result of LMEM marginal means contrast comparisons.

**Motor unit HOLD variables.** During 20% HOLDS, 489 unique motor units were initially tracked within the TA and 152 were tracked within the SOL motor pool. During 10% HOLDS, 376 unique motor units were initially tracked within the TA and 165 were tracked within the SOL motor pool (See Figure 4.5).

A significant interaction between Mean DR and *Condition\*Time\*Muscle* was observed within 20% ( $X^2 = 11.50, p = 0.009$ ) and 10% ( $X^2 = 28.58, p < 0.001$ ) MVIC HOLD contractions. Estimated marginal means are displayed in **Table 3**, with a large effect size within the TA ( $d=0.69-0.94$ ; between baseline and significant time points), indicating an increase in mean DR within the TA. This effect was not statistically significant within the SOL (**Table 5**).

A significant interaction between CoV ISI and *Condition\*Time\*Muscle* was observed within 20% MVIC HOLD contractions ( $X^2 = 8.62, p = 0.035$ ). Estimated marginal means are displayed in **Table 3**, with a moderate effect size within the TA ( $d=0.62$ ), between time point 1 and time point 2, indicating an increase in CoV ISI within the TA. This effect was not statistically significant within the SOL or 10% TA HOLDS (**Table 5**).

No significant interaction was found between *Condition\*Time* and the delta-band coherence at 20% MVIC ( $X^2 = 1.76, p = 0.62$ ) and 10% MVIC ( $X^2 = 3.10, p = 0.36$ ); alpha-band coherence at 20% MVIC ( $X^2 = 1.12, p = 0.77$ ) and 10% MVIC ( $X^2 = 0.34, p = 0.95$ ); or beta-band coherence 20% MVIC ( $X^2 = 2.26, p = 0.52$ ) and 10% MVIC ( $X^2 = 0.91, p = 0.82$ ) during HOLD contractions (**Table 3 & 5**)

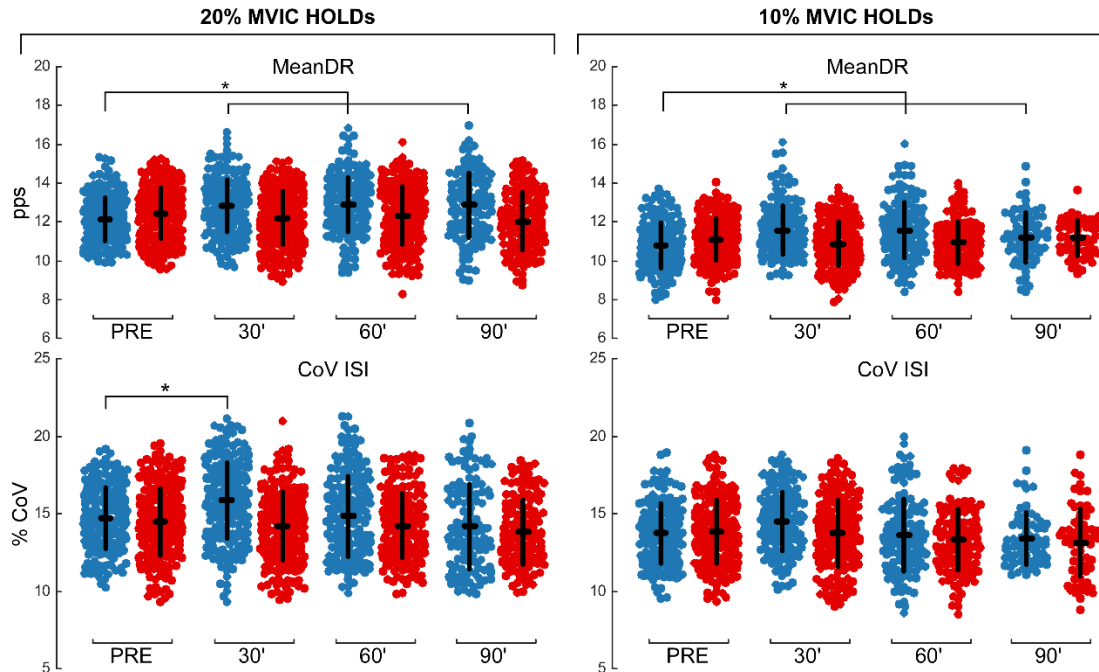


Figure 4.5. Tracked MU Discharge Characteristics – HOLDS. Bee swarm plots of all tracked MUs from 20% and 10% MVIC HOLD contractions of the TA motor pool. Blue represents CAF and red represents DE conditions. Black lines represent mean (horizontal) and standard deviation (vertical) of each group. (\*) Represent statistically significant ( $p < 0.05$ ) differences between PRE and select time point as a result of LMEM marginal means contrast comparisons.

## Discussion

In this study, we assessed the effects of caffeine on the behavior and excitability of human motoneurons within the TA and SOL motor pools. Utilizing novel methods, we show the effects of caffeine on hundreds of active human motoneurons, tracked over the duration of the experiment. Similar to previous work (De Giuseppe et al., 2019; Xu et al., 2021), we observed a significant change in cardiovascular physiology (MAP and HR) over time within the CAF group, with no coincidental changes observed within the DE group. Congruent with our hypothesis, we observed a significant increase in  $\Delta F$  within the TA motor pool after the administration of 3mg/kg of caffeine. However, no similar

changes were observed within the SOL motor pool, suggesting it may be invariant to the effects of caffeine. Further, we observed an increase in maximum discharge rate during RAMP contractions and an increase in mean discharge rate and CoV of the ISI during HOLD contractions, within the TA motor pool after the consumption of caffeine.

**Cardiovascular effects.** Previous studies investigating the use of caffeine as a performance enhancing supplement in exercise physiology and sport science have recommend doses between 3-9 mg/kg (Guest et al., 2021; Spriet, 2014) with a majority of studies utilizing the top end of that range to assess muscular strength and endurance performance outcomes (Grgic et al., 2018; Grgic & Pickering, 2019; Pasmán et al., 1995; Pickering & Kiely, 2018). The intention of the current study was to investigate the effects of an ecologically valid and relatable dose of caffeine on the human neuromotor system. Here, we utilized a dose similar to what most American coffee drinkers consume daily (*i.e.*, ~210 mg for a 70 kg subject) (Fulgoni et al., 2015). Despite this modest dose, we observed a significant change in blood pressure and heart rate of the subjects after the consumption of coffee, suggesting the response from CAF was sufficient to alter subjects' physiology to clinically meaningful degree. No significant cardiovascular changes were observed within the DE group. Curiously, the CAF group had a concomitant reduction in heart rate as their blood pressure increased, this reciprocal reduction in HR was unexpected but may be a compensatory response to control for increased cardiac output provided by increased cardio-inotropic, stroke volume, and vascular resistance changes from the effects of caffeine (Green et al., 1996; McClaran & Wetter, 2007; Nayler, 1963; Whitsett et al., 1984).

**Effects on motoneuron discharge properties.** Our findings show the TA motor pool was affected by CAF through increases in  $\Delta F$ , maximum discharge rate, CoV of the ISI, and mean discharge rate of tracked motor units. To date, few studies have explored the use of psychoactive drugs, such as caffeine, to modulate the effects of monoamines on human motor unit output. Similar to our findings, Udina and colleagues (2010), observed significant increases in  $\Delta F$  (~2.3 pps increase), after subjects received oral administration of amphetamine. While the current study did observe a moderate-strong effect size for change in  $\Delta F$  with the CAF intervention, the magnitude of this change was only estimated at +0.77 pps (at post-60' intervention). This observed variance (between studies) is likely due to differences in drug, dose, and pharmacodynamics, as amphetamines have been shown to act with more potency in the release of monoamines than caffeine (Rank et al., 2007; Udina et al., 2010). Further, the dose utilized by Udina and colleagues' (20-25 mg) exceeds the typical dosage of amphetamine used for commonly prescribed, USFDA approved, disorders (such as 5-20 mg/day; Attention Deficit Disorder, Narcolepsy; (Daughton & Kratochvil, 2009; Skidmore-Roth, 2023.) juxtapose to a fairly ubiquitous dose of caffeine utilized in the current study. Future studies should investigate the dose-dependent relationship of caffeine on motoneuron behavior.

The current study observed a significant increase in the maximum discharge rate and mean discharge rate of tracked motor units of the TA, after CAF intervention. Unfortunately, the previously mentioned studies (Udina et al., 2010; Walton et al., 2002) investigating the effects of drugs (caffeine and amphetamine) on motoneuron excitability, varied in their methods, and did not explicitly report changes in mean or peak discharge

rates. Kalmar and colleagues (1999) are one of few, with similar research questions, to explicitly measure motor unit discharge rates as they are affected by CAF (6mg/kg) with intramuscular EMG. They observed no change in mean discharge rate or H-Reflex amplitude of the SOL motor pool after CAF intervention but did observe significant changes in peripheral muscular characteristics (reflected by an increase in time to fatigue of 50% MVIC hold contractions). While Kalmar's results suggest central neuromuscular characteristics (such as MN discharge rate and excitability) are invariant to CAF, the totality of these findings may represent a muscle-dependent difference in the effects of CAF on motor pools, as the current study also failed to show changes within the SOL (see below - *Differential responses from motor pools*). Others exploring caffeine's effects on strength and fatigue have yielded mixed results utilizing proxy measures of motor unit discharge rate such as sEMG amplitude (Bazzucchi et al., 2011; Duncan et al., 2014; Madigan & Willems, 2011) and mechanomyography (Peterson et al., 2019). While these surrogate measures of motor unit activity provide important data to investigate broad changes in motor unit behavior, they may not be accurate enough to observe changes in rate coding and recruitment of individual motor units (Farina, 2006; Farina et al., 2014; Vigotsky et al., 2018). The use of HDsEMG and motor unit decomposition in the current study allows for the accurate identification of these changes with the ability to track the same motor units over time. We suggest the findings of the current study reflect an amplification in PIC activity in response to the caffeine intervention, resulting in higher rates of discharge within the TA motor pool.

No significant changes were observed in 100% MVIC torque output, CoV Torque, or the relative % MVIC trials were performed at; indicating that subjects

performed contractions at a similar intensity before and after intervention. Given the small dose of caffeine utilized in the current study (3 mg/kg), the expected increase in 100% MVIC torque was minimal, as others have only readily demonstrated small-to-moderate changes in force production with relatively large doses of caffeine (e.g., 5-9 mg/kg) (Grgic et al., 2018, 2019). However, we did observe a significant increase in the CoV ISI in the TA after CAF administration. Additionally, a non-significant trend of increased CoV Torque was observed in parallel to changes in CoV ISI during CAF conditions. The observed changes may be attributed to afferent feedback mechanisms, alterations in peripheral neuromuscular properties, or modifications in volitional control, attempting to throttle the force output for task success under CAF conditions with amplified motor gain. Others have shown CoV Torque may be influenced by motor unit discharge rate and CoV ISI, but only at very low contraction intensities (<5% MVIC) (Dideriksen et al., 2012). Additionally, others have shown CoV of torque is dependent on a number of factors (not just motor unit DR) such as: contraction intensity, number of synergist muscles contributing to the task, and the relative number of motor units recruited (Moritz et al., 2005; Taylor et al., 2003). Lastly, the lack of similar changes within the SOL motor pool may reflect muscle-dependent differences in motor unit behavior – as it has additional synergists which aid in plantarflexion tasks.

Motor unit recruitment and derecruitment thresholds, after CAF intervention, did not significantly change. These findings contrast other studies (Udina et al., 2010; Walton et al., 2002), which suggest the effects of monoaminergic drugs (like caffeine and amphetamine) on motoneuron excitability ( $\Delta F$  and probability of eliciting self-sustained firing, respectively) are likely driven by a reduction in recruitment and/or de-recruitment

thresholds of motor units. Reduction in these thresholds could be contributed to an increase in motoneuron excitability through the activation of PICs (Udina et al., 2010). While our results do not share these findings, there does appear to be a non-significant trend (within the TA motor pool) for a decrease in recruitment and derecruitment thresholds after CAF intervention that likely contributed a small amount to the significant changes observed in  $\Delta F$ . Further, the physiological range of change among recruitment and derecruitment thresholds may be naturally smaller between conditions, resulting in less statistical power when observing differences in these variables. Lastly, the quantification of recruitment and derecruitment thresholds may have been affected by our method of tracking motor units. For example, “newly” recruited motor units over the course of the experiment, are systematically excluded from analysis and we are unable to quantify their thresholds for (de)activation, since they were not observed within the first session, resulting in a selection bias from the set of motor units we first acquired (and thus tracked throughout the experiment). While the techniques utilized in the current study allows for the high-fidelity observation of many concurrently active motoneurons, it may not capture the totality of physiological changes within the entire motor pool, future studies utilizing similar HDsEMG motor unit tracking techniques should consider this.

No significant changes in pooled intra-muscular coherence were observed in response to the CAF intervention. To our knowledge no other study has attempted to quantify how this measure may change in human motor units in response to caffeine (or any other similar monoaminergic stimulant). This finding suggests CAF does not alter the common synaptic drive within each motor pool. If the concomitant increases in  $\Delta F$  and

discharge rate are not being driven through an overt change in intensity or quality of descending synaptic input, it is likely these observed changes are a result of intrinsic changes at the level of the MN.

Lastly, the effects from the CAF intervention appear to be time-dependent and trend towards baseline levels at ~90 minutes post-consumption. Most studies utilizing caffeine as an ergogenic aid for exercise supplementation suggest the optimal consumption time is ~30-60 minutes pre-workout, depending on the type of drug-vehicle utilized (*i.e.*, pill, beverage powder, coffee; Guest et al., 2021), our findings extend this notion to the level of the motoneuron. Future studies should investigate the potential dose- and time-dependent interactions of caffeine on motor unit behavior.

**Differential responses from motor pools.** Contrary to our hypothesis, we observed differential effects of CAF on the TA and SOL motor pools during RAMP and HOLD contractions. We suspect these findings may be a result of a number of physiological or methodological reasons. Firstly, the increased heterogeneity and sparsity of the SOL data set may have contributed to these observations. The overall motor unit yield for SOL was much lower than TA. Additionally, the SOL motor pool comprised the majority (5/6) of the missing baseline trials that failed to yield any valid, trackable, motor units via decomposition. This disparity in data collected from each motor pool may have contributed to the differential responses from each motor pool. Further, the mean discharge rates between these motor pools differ (TA (12.3 pps); SOL (8.2 pps) at 20% MVIC), however, these baseline differences alone should not greatly influence the statistical outcome of the LMEM analysis. However, unlike baseline differences, there may be a diminishing effect on the calculation of  $\Delta F$  in motor pools with lower frequency

of discharge, as the magnitude of  $\Delta F$  is dependent (and limited to) the discharge rates of units within the motor pool it is being calculated for (Taylor et al., 2020).

Alternatively, the observed changes (or lack thereof) within SOL may reflect physiological differences in the ways in which PICs are regulated and controlled. For instance, SOL PICs may already be so large they are at or near saturation and additional input yields little to no change in  $\Delta F$ . Conversely, SOL PICs may be so small the effects are diminished. Others have reported a similar lack of change in measures of excitability within the SOL motor pool. Phillips and colleagues (2022) recently demonstrated oral administration of  $\alpha$ -lactalbumin (40 g), an amino acid precursor of serotonin synthesis, failed to modify  $\Delta F$  or motor unit DR within the SOL motor pool. While  $\alpha$ -lactalbumin does not act as a central nervous system stimulant nor does it share the same potency of psychoactive effects as caffeine,  $\alpha$ -lactalbumin has been shown to raise brain serotonin levels, making it a potential vector to manipulate PICs in humans (Layman et al., 2018; Orosco et al., 2004). Others have also demonstrated a lack of physiological change within the SOL motor pool after the administration of caffeine (6mg/kg), using H-reflex amplitude as a surrogate measure of MN excitability (Kalmar & Cafarelli, 1999; Mesquita et al., 2020). This may further support the inter-muscular differences observed in the current study.

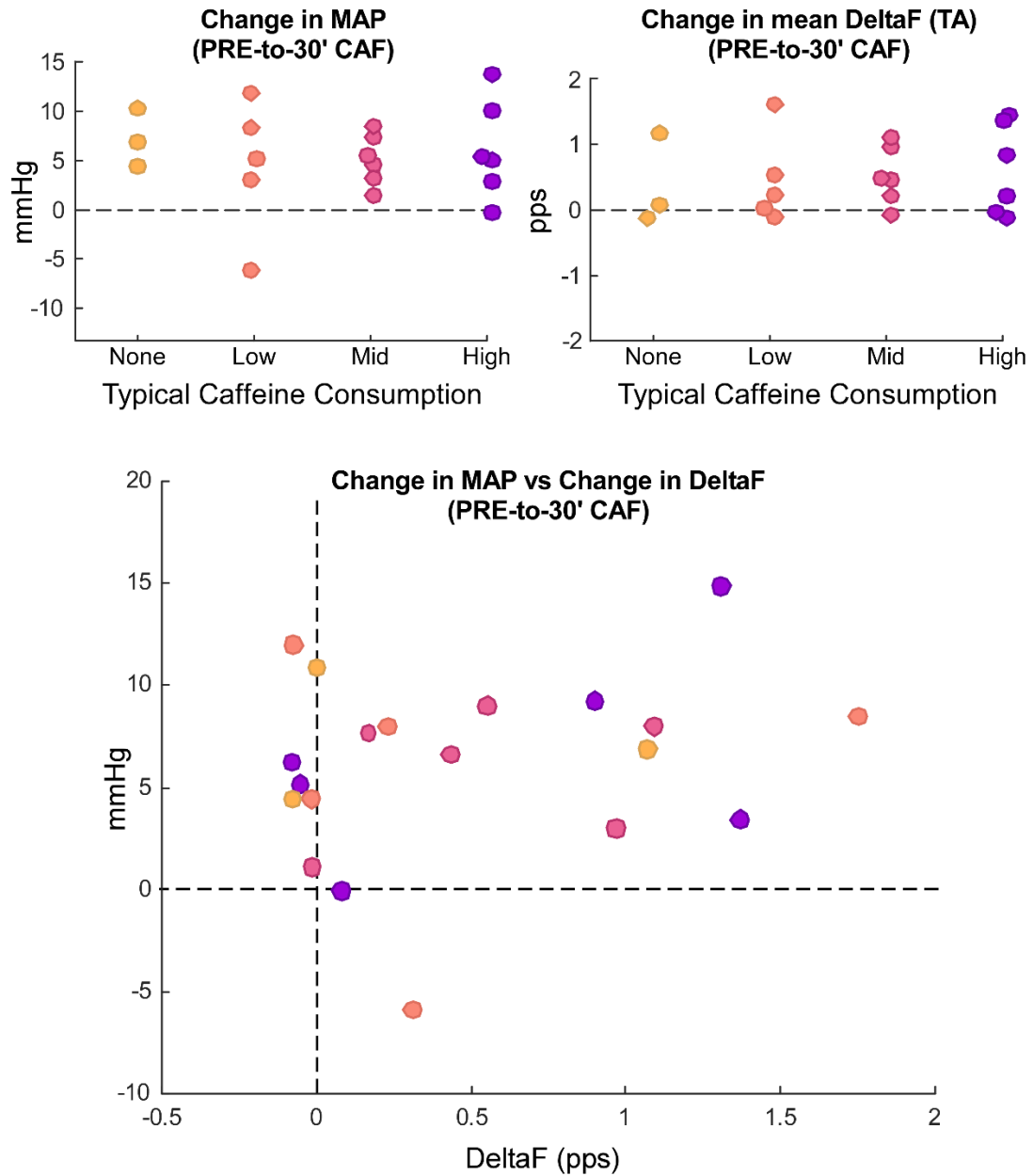


Figure 4.6. Impact of CAF Consumption on MAP and Delta-F. Each dot represents a single subject, stratified by typical caffeine consumption (Bühler et al., 2014). Top: Vertical axis represents the change in MAP and mean Delta-F from block 1 (PRE) to block 2 (30'-Post) during the CAF condition. Bottom: Blue line represents Pearson's product-moment correlation (0.175) between change in MAP vs change in Delta-F ( $t=0.753$ ;  $df=18$ ;  $p\text{-value}=0.461$ ).

**Individual and sex differences.** Individual differences in pharmacokinetics, particularly with respect to the rate of caffeine metabolism vary greatly from person to person, especially depending on the activity of the cytochrome P450 1A2 (CYP1A2) gene, encoding the enzyme that metabolizes caffeine (Gandhi et al., 2004). Without the ability to perform genetic and metabolic profiles on each subject, the current study initially attempted to stratify subjects by baseline caffeine consumption (questionnaire; Bühler et al., 2014), however, the inclusion of this fixed effect did not improve the fit of linear effects models and thus was not included in the final analysis. Additionally, a post hoc analysis of the relationship between baseline caffeine consumption and the effects of CAF on cardiovascular (HR/BP) and motor unit discharge characteristics failed to reveal significant correlations (**See Appendix A**). Others have also observed that individual baseline caffeine tolerance and/or typical caffeine consumption is independent of ergogenic gains acquired through acute caffeine consumption (Grgic et al., 2018; Tarnopolsky & Cupido, 2000).

Sex-related differences observed in the CYP450 isoforms may also explain differential effects of caffeine tolerance between subjects (Robertson et al., 2018; Urry et al., 2016). However, in the current study, the inclusion of *Sex* as a fixed factor did not improve the fit of the LMEM. Further, the inclusion of *Subject* as a nested random effect should account for some of these potential individual differences, as separate intercepts were calculated for each subject within the model. Additionally, as shown in previous studies, there may also be sex-related differences in neuromuscular control and rate coding of motor pools (Taylor et al., 2022). Indeed, the current study also observed a sex-related trend in mean DR during baseline 20% MVIC TA HOLD contractions (females

(12.57 pps) and males (12.10 pps)), although these observations should be interpreted with caution as these values are not a result of estimated marginal mean calculations and represent data that was not a priori considered within the LMEM modeling parameters. Teasing apart sex-related differences in neuromuscular physiology represents an important research initiative within our field (Jenz et al., 2022; Lulic-Kuryllo & Inglis, 2022), however these potential differential effects of caffeine on motor unit behavior extends beyond the scope of this study and future research is required in this domain.

**Limitations.** The current study investigated the effects of caffeine on motoneurons within two motor pools. As demonstrated here within the TA and SOL motor pools, there may be differential effects of caffeine depending on the motor pool, future studies should consider this. Similarly, the lack of varying contraction type and MVIC intensity may limit the generalizability of these findings within the motor pools studied. As observed with most drug interactions, the individual response may vary and accounting for these nuances is difficult. However, utilizing *Subject* and *unique motor unit* as a nested random effect within the LMEM, allows for some of the individual variation between subjects observed in the current study. Some particularly relevant individualistic limitations that may require future investigation are sex-related differences, caffeine tolerance, typical daily consumption, genetic predisposition in the metabolism of caffeine, and establishing a dose-dependent relationship to caffeine at the level of the motoneuron. Lastly, since caffeine is a fairly ubiquitous drug with well-known effects it is possible the placebo and nocebo effects may affect our outcome measures, however, subject and experimenter bias were mitigated through the use of double-blinding procedures.

## Conclusion

Despite caffeine's widespread use and commonly understood ergogenic properties, the mechanisms in which it interacts with the motoneuron in humans are underexplored. Here, we demonstrate a moderate dose of caffeine, similar to a large cup of coffee, can cause profound changes in cardiovascular and central neuromuscular physiology. Utilizing a double-blind, inactive placebo-controlled, crossover study design, we observed the effects of caffeine (3 mg/kg) on 1,452 human motor neurons, before and over the course of 90+ minutes after the consumption of caffeine. We observed an increase in motoneuron excitability ( $\Delta F$ ) and discharge rate within the TA motor pool. Conversely, the motor neurons within the SOL motor pool did not significantly alter their discharge properties in response to CAF. These findings may have important considerations for pharmacological interventions that alter monoamines within humans, as their role in regulating motor control and PICs have become more understood. Lastly, if a substance as innocuous and ubiquitous as a cup of coffee has the propensity to alter the underlying features of motor control, we must truly appreciate the body's ability to adapt and provide flexible control for human movement.

Table 4.1. Torque and Torque Variability

Outcome Variable			Pre (T1)	30' Post (T2)	60' Post (T3)	90' Post (T4)
100% MVIC (% MVIC)	TA	CAF	-	-2.21 (± 6.63)	-2.18 (± 5.38)	-1.98 (± 5.17)
		DE	-	-5.53 (± 4.54)	-5.36 (± 3.87)	-3.75 (± 3.31)
	SOL	CAF	-	-4.94 (± 7.60)	-3.33 (± 5.56)	-3.08 (± 5.32)
		DE	-	-5.51 (± 8.89)	-5.46 (± 7.77)	-3.75 (± 5.35)
RAMP Torque (% MVIC)	TA	CAF	20.56 (± 1.80)	20.92 (± 2.12)	21.10 (± 1.18)	20.92 (± 1.37)
		DE	21.01 (± 2.01)	21.15 (± 2.13)	21.03 (± 2.16)	20.83 (± 2.20)
	SOL	CAF	20.82 (± 0.87)	20.85 (± 0.79)	20.82 (± 0.91)	21.05 (± 0.68)
		DE	20.23 (± 1.33)	20.47 (± 1.23)	20.34 (± 1.27)	20.50 (± 1.18)
20% HOLD (% MVIC)	TA	CAF	20.86 (± 1.91)	20.92 (± 2.09)	21.01 (± 2.02)	20.99 (± 2.49)
		DE	21.40 (± 1.82)	20.93 (± 1.93)	22.14 (± 1.79)	21.17 (± 1.84)
	SOL	CAF	20.20 (± 2.03)	20.42 (± 2.80)	20.36 (± 1.98)	20.01 (± 2.28)
		DE	20.42 (± 2.05)	20.46 (± 1.70)	20.40 (± 1.80)	20.59 (± 1.85)
10% HOLD (% MVIC)	TA	CAF	11.30 (± 1.81)	11.61 (± 1.88)	11.51 (± 1.99)	11.71 (± 1.72)
		DE	11.78 (± 1.61)	11.01 (± 1.63)	11.21 (± 1.57)	11.61 (± 1.67)
	SOL	CAF	10.05 (± 2.03)	10.49 (± 1.75)	10.67 (± 1.89)	10.88 (± 1.78)
		DE	10.37 (± 1.77)	10.39 (± 1.57)	10.24 (± 1.58)	10.48 (± 1.69)
CoV-T, 20%	TA	CAF	1.80 (± 0.65)	1.93 (± 0.48)	1.96 (± 0.80)	1.73 (± 0.72)
		DE	1.82 (± 0.91)	1.66 (± 0.72)	1.64 (± 0.66)	1.52 (± 0.57)
	SOL	CAF	1.85 (± 0.79)	1.71 (± 0.84)	1.55 (± 0.79)	1.72 (± 0.90)
		DE	1.55 (± 0.75)	1.40 (± 0.66)	1.36 (± 0.59)	1.31 (± 0.55)
CoV-T, 10%	TA	CAF	2.15 (± 0.88)	2.33 (± 0.83)	2.54 (± 0.99)	2.37 (± 1.12)
		DE	2.24 (± 0.95)	2.24 (± 1.11)	2.25 (± 0.92)	2.02 (± 0.73)
	SOL	CAF	2.08 (± 1.01)	1.94 (± 0.54)	1.87 (± 0.72)	1.89 (± 0.88)
		DE	1.86 (± 0.90)	1.68 (± 0.62)	1.85 (± 0.47)	1.54 (± 0.63)

Table 4.1. Torque and Torque Variability. Descriptive statistics of torque characteristics. 100% MVIC outcome represents the % change in MVIC of each testing block relative to each subjects known 100% maximum. Abbreviations: Tibialis anterior (TA); Soleus (SOL); maximum volitional isometric contraction (MVIC); coefficient of variation of torque during the steady-state portion of HOLD contractions (CoV-T).

Table 4.2. LMEM Marginal Means Results from TA RAMPs

Outcome Variable		Pre (T1)	30' Post (T2)	60' Post (T3)	90' Post (T4)
Tracked MU, #	CAF	103	103	73	52
	DE	98	98	60	35
Delta-F ( $\Delta F$ ), pps	CAF	4.13 [0.15]	<b>4.81 [0.14]*</b>	<b>4.90 [0.15]*</b>	4.41 [0.16]
	DE	4.19 [0.13]	4.04 [0.13]	4.01 [0.14]	3.98 [0.16]
InitialDR, pps	CAF	5.01 [0.17]	5.11 [0.17]	5.30 [0.15]	4.94 [0.18]
	DE	4.79 [0.13]	4.82 [0.13]	4.90 [0.16]	4.95 [0.20]
MaxDR, pps	CAF	13.51 [0.27]	<b>14.63 [0.28]*</b>	<b>14.81 [0.29]*</b>	<b>14.55 [0.31]*</b>
	DE	13.53 [0.27]	13.49 [0.28]	13.54 [0.29]	13.66 [0.33]
FinalDR, pps	CAF	3.12 [0.10]	3.13 [0.10]	3.09 [0.12]	3.16 [0.13]
	DE	3.18 [0.10]	3.14 [0.11]	3.11 [0.12]	3.01 [0.16]
Recruit, %	CAF	11.40 [0.56]	10.30 [0.56]	10.70 [0.60]	10.71 [0.64]
	DE	11.00 [0.56]	11.21 [0.55]	11.05 [0.62]	11.59 [0.68]
De-Recruit, %	CAF	10.23 [0.47]	9.43 [0.48]	9.21 [0.51]	9.81 [0.56]
	DE	10.70 [0.26]	10.68 [0.26]	10.30 [0.53]	10.39 [0.61]

Table 4.2. LMEM Marginal Mean Results from TA RAMPs. Estimated marginal means [standard error] and statistics from linear mixed effects model analysis (Condition x Time contrasts). Abbreviations: Motor unit (MU); pulses per second (pps); percentage of maximum volitional contraction torque (%); discharge rate (DR). Statistically significant p-values (<0.05; \*) are provided from linear mixed effects model estimates from T1 to T2-T4 contrast comparisons.

Table 4.3. LMEM Marginal Mean Results from TA HOLDS

Outcome Variable			Pre (T1)	30' Post (T2)	60' Post (T3)	90' Post (T4)
Tracked MU (#)	20%	CAF	231	231	193	128
		DE	258	258	212	149
	10%	CAF	178	178	140	71
		DE	198	198	147	71
Mean DR (pps)	20%	CAF	12.14 [0.12]	<b>12.84 [0.12]*</b>	<b>12.91 [0.13]*</b>	<b>12.88 [0.13]*</b>
		DE	12.40 [0.11]	12.17 [0.11]	12.24 [0.12]	12.10 [0.13]
	10%	CAF	10.77 [0.15]	<b>11.54 [0.15]*</b>	<b>11.52 [0.16]*</b>	<b>11.30 [0.18]*</b>
		DE	10.97 [0.15]	10.72 [0.15]	10.78 [0.16]	11.08 [0.19]
CoV ISI (pps)	20%	CAF	14.90 [0.27]	<b>16.01 [0.27]*</b>	15.11 [0.28]	14.73 [0.29]
		DE	14.82 [0.26]	14.59 [0.26]	14.63 [0.27]	14.44 [0.28]
	10%	CAF	14.12 [0.27]	14.80 [0.29]	14.04 [0.28]	13.88 [0.33]
		DE	14.20 [0.27]	14.14 [0.27]	13.89 [0.28]	13.6 [0.33]
Delta (Z-score)	20%	CAF	1.89 [0.10]	1.75 [0.10]	1.68 [0.10]	1.63 [0.11]
		DE	1.97 [0.10]	1.66 [0.11]	1.70 [0.10]	1.62 [0.10]
	10%	CAF	1.63 [0.11]	1.46 [0.11]	1.54 [0.11]	1.62 [0.11]
		DE	1.63 [0.11]	1.65 [0.11]	1.47 [0.11]	1.54 [0.11]
Alpha (Z-score)	20%	CAF	0.98 [0.09]	0.96 [0.09]	0.93 [0.09]	0.92 [0.09]
		DE	0.99 [0.08]	0.88 [0.08]	0.89 [0.09]	0.89 [0.09]
	10%	CAF	0.80 [0.06]	0.86 [0.07]	0.83 [0.06]	0.82 [0.06]
		DE	0.75 [0.06]	0.80 [0.06]	0.79 [0.06]	0.77 [0.06]
Beta (Z-score)	20%	CAF	0.99 [0.13]	0.84 [0.13]	0.79 [0.13]	0.81 [0.13]
		DE	0.88 [0.13]	0.90 [0.13]	0.88 [0.13]	0.91 [0.13]
	10%	CAF	0.96 [0.10]	0.97 [0.11]	0.94 [0.11]	0.89 [0.10]
		DE	0.97 [0.10]	0.95 [0.10]	0.98 [0.10]	0.96 [0.10]

Table 4.3. LMEM Marginal Mean Results from TA HOLDS. Estimated marginal means [standard error] and statistics from linear mixed effects model analysis (Condition x Time contrasts). Abbreviations: Discharge rate (DR); Coefficient of variation of the inter-spike interval (CoV ISI); Delta, Alpha, and Beta reflect bandwidth values for pooled coherence (0-5, 5-15, 15-35 Hz, respectively). Statistically significant p-values (<0.05; \*) are provided from linear mixed effects model estimates from T1 to T2-T4 contrast comparisons.

Table 4.4. LMEM Marginal Mean Results from SOL RAMPs

Outcome Variable		Pre (T1)	30' Post (T2)	60' Post (T3)	90' Post (T4)
Tracked MU, #	CAF	33	33	20	16
	DE	36	36	22	18
Delta-F ( $\Delta F$ ), pps	CAF	2.99 [0.17]	2.95 [0.17]	2.96 [0.19]	2.67 [0.21]
	DE	2.78 [0.16]	2.85 [0.16]	2.76 [0.18]	2.82 [0.19]
InitialDR, pps	CAF	3.91 [0.20]	3.65 [0.20]	4.10 [0.25]	3.96 [0.28]
	DE	3.81 [0.19]	3.78 [0.19]	3.82 [0.24]	3.96 [0.26]
MaxDR, pps	CAF	10.35 [0.35]	10.59 [0.35]	10.36 [0.40]	10.23 [0.42]
	DE	10.21 [0.33]	9.99 [0.33]	10.07 [0.37]	10.29 [0.39]
FinalDR, pps	CAF	2.69 [0.16]	2.57 [0.16]	2.60 [0.19]	2.67 [0.21]
	DE	2.59 [0.15]	2.54 [0.15]	2.67 [0.18]	2.42 [0.20]
Recruit, %	CAF	10.81 [0.77]	11.03 [0.77]	11.92 [0.89]	11.21 [0.95]
	DE	10.20 [0.71]	10.48 [0.71]	11.35 [0.82]	11.71 [0.87]
De-Recruit, %	CAF	12.01 [0.68]	12.19 [0.68]	11.78 [0.80]	12.96 [0.86]
	DE	12.50 [0.62]	11.95 [0.62]	12.10 [0.73]	11.84 [0.78]

Table 4.4. LMEM Marginal Mean Results from SOL RAMPs. Estimated marginal means [standard error] and statistics from linear mixed effects model analysis (Condition x Time contrasts). Abbreviations: Motor unit (MU); pulses per second (pps); percentage of maximum volitional contraction torque (%); discharge rate (DR).

Table 4.5. LMEM Marginal Mean Results from SOL RAMPs

Outcome Variable			Pre (T1)	30' Post (T2)	60' Post (T3)	90' Post (T4)
Tracked MU #	20%	CAF	70	70	59	23
		DE	82	82	65	23
	10%	CAF	75	75	56	24
		DE	90	90	50	27
Mean DR pps	20%	CAF	7.89 [0.17]	7.86 [0.17]	7.95 [0.18]	8.03 [0.26]
		DE	8.39 [0.15]	8.25 [0.15]	8.10 [0.16]	8.70 [0.24]
	10%	CAF	7.86 [0.18]	7.61 [0.18]	8.01 [0.19]	7.90 [0.24]
		DE	8.14 [0.16]	7.98 [0.16]	8.01 [0.18]	8.13 [0.21]
CoV ISI pps	20%	CAF	15.62 [0.34]	15.61 [0.34]	15.27 [0.35]	15.45 [0.48]
		DE	15.24 [0.32]	15.04 [0.32]	15.12 [0.33]	14.78 [0.47]
	10%	CAF	13.76 [0.32]	13.05 [0.32]	13.03 [0.35]	13.01 [0.47]
		DE	13.64 [0.31]	13.13 [0.31]	12.65 [0.36]	12.78 [0.43]
Delta Z-score	20%	CAF	1.19 [0.10]	1.07 [0.10]	1.00 [0.10]	1.12 [0.11]
		DE	1.04 [0.10]	0.94 [0.10]	1.04 [0.10]	1.11 [0.11]
	10%	CAF	1.10 [0.11]	0.96 [0.11]	0.88 [0.11]	0.92 [0.11]
		DE	1.00 [0.11]	1.05 [0.11]	0.88 [0.11]	0.88 [0.11]
Alpha Z-score	20%	CAF	0.67 [0.08]	0.58 [0.08]	0.53 [0.08]	0.60 [0.09]
		DE	0.64 [0.08]	0.55 [0.08]	0.56 [0.08]	0.51 [0.08]
	10%	CAF	0.46 [0.06]	0.40 [0.06]	0.48 [0.06]	0.47 [0.06]
		DE	0.39 [0.06]	0.37 [0.06]	0.36 [0.06]	0.40 [0.06]
Beta Z-score	20%	CAF	1.01 [0.12]	0.89 [0.13]	0.85 [0.12]	0.86 [0.13]
		DE	0.88 [0.13]	0.77 [0.13]	0.89 [0.13]	0.81 [0.13]
	10%	CAF	0.87 [0.11]	0.61 [0.11]	0.64 [0.11]	0.68 [0.11]
		DE	0.76 [0.10]	0.62 [0.10]	0.62 [0.10]	0.67 [0.10]

Table 4.5. LMEM Marginal Mean Results from SOL RAMPs. Estimated marginal means [standard error] and statistics from linear mixed effects model analysis (Condition x Time contrasts). Abbreviations: Discharge rate (DR); Coefficient of variation of the inter-spike interval (CoV ISI); Delta, Alpha, and Beta reflect bandwidth values for pooled coherence (0-5, 5-15, 15-35 Hz, respectively).

## CHAPTER 5

### CONCLUSIONS

#### **Review of Specific Aims**

The aim of this dissertation was to investigate how human MNs behave in response to muscle-, task-, and neuromodulation-dependent state changes. The adaptability and plasticity of MNs in response to these types of states was previously unknown in humans. A comprehensive understanding of MN behavior is essential to elucidating the structure and function of the human neuromuscular system. Furthermore, mapping the magnitude of PICs within and across motor pools may guide diagnostic, prognostic, and therapeutic implications for neuromotor pathology with known PIC disruptions. To best achieve these aims, a series of three experiments were conducted utilizing HDsEMG and MU decomposition algorithms, to observe the discharge characteristics of entire populations of MNs. The specific aims of these three experiments are summarized below.

- 1) Assess human spinal MN behavior and excitability within functionally varying motor pools. We hypothesized that maximal MN discharge rate within the first dorsal interosseous motor pool would differ from the tibialis anterior motor pool. Further, MN excitability ( $\Delta F$ ) would differ between the first dorsal interosseous motor pool and the tibialis anterior motor pool.
- 2) Observe alterations in neuromotor control of a single motor pool in response to varying volitional motor commands. We hypothesized that MN excitability ( $\Delta F$ ) within the biceps brachii motor pool would remain invariant, despite different volitional motor commands (i.e., flexion and supination). Further, intra-muscular

coherence within the biceps brachii motor pool would differ between flexion and supination motor commands.

- 3) Assess the effects of exogenous neuromodulation on the human spinal motoneurons. We hypothesized that MN excitability ( $\Delta F$ ) would increase after the administration of orally ingested caffeine (3mg/kg). Further, intra-muscular coherence would decrease after the administration of orally ingested caffeine.

### **Summary of Results**

**Aim 1 Summary.** During a series of submaximal (20% MVIC) isometric RAMP contractions, 1,638 MU spike trains were identified from 4 subjects and were utilized for subsequent analysis. Consistent with our hypothesis, significantly higher maximum MU discharge rates were observed within the FDI motor pool, when compared to the TA. Similarly,  $\Delta F$  within the TA motor pool was significantly higher than in the FDI. These findings suggest two functionally diverse muscles are controlled in fundamentally different ways by the central nervous system to achieve task dependent outcomes.

This evidence supports the notion that motor pools may be functionally tuned to their environmental demands. Because of the nonlinear ways in which PICs can augment motor unit behavior, it may be possible that the nervous system may utilize these organizational differences to transform the motor command between motor pools, to facilitate complex motor tasks. For example, the TA, predominantly a postural control muscle, is utilized constantly for stability and locomotion. As such, its MNs may have a biophysical benefit to higher levels of excitability ( $\Delta F$ ), this would lower the effective activation threshold of the motor pool to assist in repetitive tasks. In contrast, the FDI is

almost exclusively utilized for fine control in grasping. As such, its MNs may benefit from a reduced level of excitability when executing controlled, fine motor tasks, in which prolonged MN activation may increase the difficulty of controlling a precise movement.

**Aim 2 Summary.** The Biceps Brachii, a muscle with more than one biomechanical function, offers a unique opportunity to observe functional changes in MU behavior between its two primary joint actions (e.g., elbow flexion and forearm supination). Here, we observed the MU discharge characteristics of the biceps brachii from 10 subjects during submaximal isometric contractions, at similar levels of intensity, between these two different modes of activation.

We observed that the MU discharge rate, inter-spike interval variability (CoV ISI), MUAP morphology, torque variability, and estimated MN excitability ( $\Delta F$ ), did not differ between supination and flexion tasks. However, despite homogenous MU discharge characteristics between modes of activation, we did observe a significant increase in coherence during supination within the alpha (5-15Hz) and beta (15-35Hz) bandwidths. We suggest these changes may reflect task-specific alterations in synaptic input to the biceps brachii motor pool, during conditions where additional kinematic information is needed to complete motor tasks.

These data support our hypothesis that the synaptic drive to bicep brachii motoneurons may differ during these modes of activation, however, the excitability and MU discharge characteristics of the motor pool remains invariant to differential functional tasks.

**Aim 3 Summary.** Serotonin and norepinephrine (monoamines) are responsible for the modulation of MNs through the activation of PICs. The resultant activity of MNs,

through the modulation of PICs, causes state-dependent and non-linear behavior. Despite early pioneering studies in animal studies (Hounsgaard et al., 1988; Hounsgaard & Kiehn, 1989), the effects of exogenous neuromodulation via monoamines in humans have been underexplored. The lack of human-based studies in this genre is largely due to the inability to accurately observe MN membrane properties in humans. However, the novel techniques described in this dissertation now allow for such observations.

Caffeine, a central nervous system stimulant, achieves its performance-enhancing effect by acting as a competitive antagonist to adenosine and by stimulating the release of norepinephrine and serotonin. Despite caffeine's widespread use and commonly understood ergogenic properties, the mechanisms in which it interacts with the MN in humans are underexplored.

Consistent with our hypothesis, we demonstrate a moderate dose of caffeine (3 mg/kg), similar to a large cup of coffee, can cause profound changes in cardiovascular and central neuromuscular physiology. Utilizing a double-blind, inactive placebo-controlled, crossover study design, we observed the effects of caffeine on 1,452 human MNs. These unique MNs were identified and tracked before, and over the course of 90+ minutes after the consumption of caffeine.

We observed a significant increase in MN excitability ( $\Delta F$ ) and discharge rate within the TA motor pool, after caffeine consumption. Coincidental to these changes, within the TA, significant inter-spike interval variability (CoV ISI) was also observed. However, in contrast to our hypothesis, intra-muscular coherence remained invariant to caffeine within the TA and SOL motor pools. Furthermore, the MNs within the SOL motor pool did not significantly alter their discharge characteristics or  $\Delta F$  in response to

CAF, suggesting the observed effects of caffeine on MN behavior may be muscle dependent.

### **Limitations**

There are some limitations that should be considered for future investigations. As demonstrated within AIM 1, MN discharge properties and PIC magnitude can vary greatly when compared across different motor pools. Currently, HDsEMG studies often utilize motor pool targets of convenience, for instance muscles that are easily accessible and have a history of generating high MU decomposition yields (*e.g.*, tibialis anterior). While the MU decomposition algorithms can produce very impressive results in some motor pools (resulting in 40+ unique MU spike trains), other motor pools may be intentionally avoided by investigators fearful of small sampling size. While the logistics of experimental design are important to consider, this practice is likely to provide a skewed view of MN behavior, given the variability observed between motor pools. However, it should be mentioned that even under suboptimal conditions, these techniques (HDsEMG/MU decomposition), are often capable of yielding a higher number of observed MUs than alternative methods, such as intra-muscular EMG. It is important to continue efforts mapping the behavior and PIC activity of lesser studied motor pools, for a full understanding of their functional implications.

Another limitation and logistical consideration for future studies is the effects of repeated contractions within the structure of data collection. Historically, it is common to include multiple repetitions of RAMP contractions within a single set, with each set separated by multiple minutes to mitigate effects of fatigue. The inclusion of multiple RAMP contractions separated by ~20s – 60s, within a single set of repetitions, appears to

aid in the accuracy and yield of MU decomposition algorithm as well as create a robust data set for subsequent analysis. The use of submaximal intensities mitigates the effects of muscular fatigue; however, the time-dependent effects of PIC activation may cause non-linear and unexpected outcomes when using these methods. For instance, the effects of repeated contractions may obfuscate  $\Delta F$  values, creating a misrepresentation of a MN's intrinsic excitability. This phenomenon was observed within AIM 3 (see Appendix B). The effects of repeated contractions caused a global reduction in MU recruitment and derecruitment thresholds (as seen in states of high excitability), however, due to the dependency on rate coding for the paired motor unit analysis the resultant  $\Delta F$  value were considerably lower with each repetition. This is contrary, to the understanding that the intrinsic excitability should be increased with repeated contractions (Gorassini et al., 2002b). For the consistency of analysis and to mitigate these effects on the results of AIM 3, the formal analysis was only conducted on the first repetition of each set. Future research is necessary to explore the intricacies of how the paired motor unit analysis may be affected by repeated contractions.

Lastly, the study of MN behavior with HDsEMG and MU decomposition techniques has been largely limited to highly controlled, isometric, contractions. This rigorous experimental control is considered necessary to the analysis of MNs, under such conditions. However, it is important to mention the lack of varying contraction types (not just RAMP and HOLD shapes) and MVIC intensity may limit the generalizability of the findings presented here. Similarly, these findings may not accurately represent naturalistic and ecologically valid motor behaviors, as we are rarely in such restricted situations throughout normal everyday life. The results of this dissertation do provide

powerful information on the basic behavior of MNs. Indeed, these results highlight the nuanced and state-dependent behavior of MUs, which were once thought to be just passive instruments of the nervous system. However, as cautiously demonstrated here, more research is necessary in order to bridge the gap from the foundational models of motor control to understanding the highly complex behavior of MNs.

### **Concluding Remarks**

The novel findings presented here demonstrate the tremendous ability for the human motor system to adapt to various states, both internal and external. Aim 1 demonstrates that not all motor pools behave similarly, with respect to the MN discharge characteristics necessary to accomplish force generation. Aim 2 demonstrates that a muscle with more than one biomechanical function does not necessarily rely on changes of MN discharge characteristics to alter its functional outcome, but instead may utilize changes in synaptic input to do so. Lastly within AIM 3, through exogenous neuromodulation, we demonstrate that a cup of coffee has the ability to alter fundamental motor control mechanisms. Astonishingly, all of these observed state-dependent alterations in motor control largely happen without conscious effort or detection, further emphasizing the subtle adaptability of the nervous system.

## REFERENCES CITED

- Adrian, E., & Bronk, D. (1929). The discharge of impulses in motor nerve fibres: Part II. The frequency of discharge in reflex and voluntary contractions. *67*(2).
- Afsharipour, B., Manzur, N., Duchcherer, J., Fenrich, K. F., Thompson, C. K., Negro, F., Quinlan, K. A., Bennett, D. J., & Gorassini, M. A. (2020). Estimation of self-sustained activity produced by persistent inward currents using firing rate profiles of multiple motor units in humans. *Journal of Neurophysiology*, *124*(1), 63–85. <https://doi.org/10.1152/jn.00194.2020>
- Ammon, H., Bieck, P., Mandalaz, D., & Verspohl, E. (1983). Adaptation of blood pressure to continuous heavy coffee drinking in young volunteers. A double-blind crossover study. *British Journal of Clinical Pharmacology*, *15*(6), 701–706. <https://doi.org/10.1111/j.1365-2125.1983.tb01553.x>
- Aston-Jones, G., Rajkowski, J., & Cohen, J. (2000). Locus coeruleus and regulation of behavioral flexibility and attention. In *Progress in Brain Research* (Vol. 126, pp. 165–182). Elsevier. [https://doi.org/10.1016/S0079-6123\(00\)26013-5](https://doi.org/10.1016/S0079-6123(00)26013-5)
- Athwal, G. S., Steinmann, S. P., & Rispoli, D. M. (2007). The distal biceps tendon: Footprint and relevant clinical anatomy. *The Journal of Hand Surgery*, *32*(8), 1225–1229. <https://doi.org/10.1016/j.jhssa.2007.05.027>
- Baker, S. N., Olivier, E., & Lemon, R. N. (1997). Coherent oscillations in monkey motor cortex and hand muscle EMG show task-dependent modulation. *The Journal of Physiology*, *501*(Pt 1), 225–241.
- Bashford, J., Mills, K., & Shaw, C. (2020). The evolving role of surface electromyography in amyotrophic lateral sclerosis: A systematic review. *Clinical Neurophysiology*, *131*(4), 942–950. <https://doi.org/10.1016/j.clinph.2019.12.007>
- Bates, D., Mächler, M., Bolker, B., & Walker, S. (2015). Fitting Linear Mixed-Effects Models Using lme4. *Journal of Statistical Software*, *67*, 1–48. <https://doi.org/10.18637/jss.v067.i01>
- Bättig, K., & Buzzi, R. (1986). Effect of Coffee on the Speed of Subject-Paced Information Processing. *Neuropsychobiology*, *16*(2–3), 126–130. <https://doi.org/10.1159/000118312>
- Bazzucchi, I., Felici, F., Montini, M., Figura, F., & Sacchetti, M. (2011). Caffeine improves neuromuscular function during maximal dynamic exercise. *Muscle & Nerve*, *43*(6), 839–844. <https://doi.org/10.1002/mus.21995>

- Beavo, J. A., Rogers, N. L., Crofford, O. B., Hardman, J. G., Sutherland, E. W., & Newman, E. V. (1970). Effects of Xanthine Derivatives on Lipolysis and on Adenosine 3',5'-Monophosphate Phosphodiesterase Activity. *Molecular Pharmacology*, 6(6), 597–603.
- Bennett, D. J., Hultborn, H., Fedirchuk, B., & Gorassini, M. (1998). Synaptic Activation of Plateaus in Hindlimb Motoneurons of Decerebrate Cats. *Journal of Neurophysiology*, 80(4), 2023–2037. <https://doi.org/10.1152/jn.1998.80.4.2023>
- Berkowitz, B. A., & Spector, S. (1971). The effect of caffeine and theophylline on the disposition of brain serotonin in the rat. *European Journal of Pharmacology*, 16(3), 322–325. [https://doi.org/10.1016/0014-2999\(71\)90034-3](https://doi.org/10.1016/0014-2999(71)90034-3)
- Bernstein. (1966). The co-ordination and regulation of movements. *The Co-Ordination and Regulation of Movements*. <https://cir.nii.ac.jp/crid/1571698599600323072>
- Bianchi, C. P. (1961). The Effect of Caffeine on Radiocalcium Movement in Frog Sartorius. *Journal of General Physiology*, 44(5), 845–858. <https://doi.org/10.1085/jgp.44.5.845>
- Bianchi, C. P. (1968). Pharmacological actions on excitation-contraction coupling in striated muscle. *Federation Proceedings*, 27(1), 126–131.
- Bühler, E., Lachenmeier, D. W., & Winkler, G. (2014). Development of a tool to assess caffeine intake among teenagers and young adults. *Ernahrungs Umschau*, 61 (4), 58–63. <https://doi.org/10.4455/eu.2014.011>
- Burke, D., Gandevia, S. C., & McKeon, B. (1984). Monosynaptic and oligosynaptic contributions to human ankle jerk and H-reflex. *Journal of Neurophysiology*, 52(3), 435–448. <https://doi.org/10.1152/jn.1984.52.3.435>
- Burke, R. E., Levine, D. N., Tsairis, P., & Zajac III, F. E. (1973). Physiological types and histochemical profiles in motor units of the cat gastrocnemius. *The Journal of Physiology*, 234(3), 723–748. <https://doi.org/10.1113/jphysiol.1973.sp010369>
- Butcher, R. W., & Sutherland, E. W. (1962). Adenosine 3',5'-Phosphate in Biological Materials: I. PURIFICATION AND PROPERTIES OF CYCLIC 3',5'-NUCLEOTIDE PHOSPHODIESTERASE AND USE OF THIS ENZYME TO CHARACTERIZE ADENOSINE 3',5'-PHOSPHATE IN HUMAN URINE. *Journal of Biological Chemistry*, 237(4), 1244–1250. [https://doi.org/10.1016/S0021-9258\(18\)60316-3](https://doi.org/10.1016/S0021-9258(18)60316-3)
- Castronovo, A. M., Negro, F., Conforto, S., & Farina, D. (2015). The proportion of common synaptic input to motor neurons increases with an increase in net excitatory input. *Journal of Applied Physiology* (Bethesda, Md.: 1985), 119(11), 1337–1346. <https://doi.org/10.1152/jappphysiol.00255.2015>

- Clamann, H. P., Gillies, J. D., Skinner, R. D., & Henneman, E. (1974). Quantitative measures of output of a motoneuron pool during monosynaptic reflexes. *Journal of Neurophysiology*, 37(6), 1328–1337. <https://doi.org/10.1152/jn.1974.37.6.1328>
- Connelly, D. M., Rice, C. L., Roos, M. R., & Vandervoort, A. A. (1999). Motor unit firing rates and contractile properties in tibialis anterior of young and old men. *Journal of Applied Physiology*, 87(2), 843–852. <https://doi.org/10.1152/jappl.1999.87.2.843>
- Conway, B. A., Hultborn, H., Kiehn, O., & Mintz, I. (1988). Plateau potentials in alpha-motoneurons induced by intravenous injection of L-dopa and clonidine in the spinal cat. *The Journal of Physiology*, 405(1), 369–384. <https://doi.org/10.1113/jphysiol.1988.sp017337>
- Cotel, F., Antri, M., Barthe, J.-Y., & Orsal, D. (2009). Identified Ankle Extensor and Flexor Motoneurons Display Different Firing Profiles in the Neonatal Rat. *The Journal of Neuroscience*, 29(9), 2748–2753. <https://doi.org/10.1523/JNEUROSCI.3462-08.2009>
- Crone, C., Hultborn, H., Kiehn, O., Mazieres, L., & Wigström, H. (1988). Maintained changes in motoneuronal excitability by short-lasting synaptic inputs in the decerebrate cat. *The Journal of Physiology*, 405, 321–343. <https://doi.org/10.1113/jphysiol.1988.sp017335>
- Daughton, J. M., & Kratochvil, C. J. (2009). Review of ADHD Pharmacotherapies: Advantages, Disadvantages, and Clinical Pearls. *Journal of the American Academy of Child & Adolescent Psychiatry*, 48(3), 240–248. <https://doi.org/10.1097/CHI.0b013e318197748f>
- de Beer, E. L., Grundeman, R. L., Wilhelm, A. J., Caljouw, C. J., Klepper, D., & Schiereck, P. (1988). Caffeine suppresses length dependency of Ca<sup>2+</sup> sensitivity of skinned striated muscle. *American Journal of Physiology-Cell Physiology*, 254(4), C491–C497. <https://doi.org/10.1152/ajpcell.1988.254.4.C491>
- De Giuseppe, R., Di Napoli, I., Granata, F., Mottolise, A., & Cena, H. (2019). Caffeine and blood pressure: A critical review perspective. *Nutrition Research Reviews*, 32(2), 169–175. <https://doi.org/10.1017/S0954422419000015>
- De Luca, C. J. (1997). The Use of Surface Electromyography in Biomechanics. *Journal of Applied Biomechanics*, 13(2), 135–163. <https://doi.org/10.1123/jab.13.2.135>
- De Luca, C. J., & Erim, Z. (1994). Common drive of motor units in regulation of muscle force. *Trends in Neurosciences*, 17(7), 299–305. [https://doi.org/10.1016/0166-2236\(94\)90064-7](https://doi.org/10.1016/0166-2236(94)90064-7)

- de Souza, L. M. L., da Fonseca, D. B., Cabral, H. da V., de Oliveira, L. F., & Vieira, T. M. (2017). Is myoelectric activity distributed equally within the rectus femoris muscle during loaded, squat exercises? *Journal of Electromyography and Kinesiology: Official Journal of the International Society of Electrophysiological Kinesiology*, 33, 10–19. <https://doi.org/10.1016/j.jelekin.2017.01.003>
- Del Vecchio, A., Holobar, A., Falla, D., Felici, F., Enoka, R. M., & Farina, D. (2020). Tutorial: Analysis of motor unit discharge characteristics from high-density surface EMG signals. *Journal of Electromyography and Kinesiology*, 53, 102426. <https://doi.org/10.1016/j.jelekin.2020.102426>
- Denier van der Gon, J. J., ter Haar Romeny, B. M., & van Zuylen, E. J. (1985). Behaviour of motor units of human arm muscles: Differences between slow isometric contraction and relaxation. *The Journal of Physiology*, 359, 107–118.
- Dideriksen, J. L., Negro, F., Enoka, R. M., & Farina, D. (2012). Motor unit recruitment strategies and muscle properties determine the influence of synaptic noise on force steadiness. *Journal of Neurophysiology*, 107(12), 3357–3369. <https://doi.org/10.1152/jn.00938.2011>
- Doherty, M., & Smith, P. M. (2005). Effects of caffeine ingestion on rating of perceived exertion during and after exercise: A meta-analysis. *Scandinavian Journal of Medicine & Science in Sports*, 15(2), 69–78. <https://doi.org/10.1111/j.1600-0838.2005.00445.x>
- Doherty, M., Smith, P. M., Hughes, M. G., & Davison, R. R. (2004). Caffeine lowers perceptual response and increases power output during high-intensity cycling. *Journal of Sports Sciences*, 22(7), 637–643. <https://doi.org/10.1080/02640410310001655741>
- Duchateau, J., & Enoka, R. M. (2011). Human motor unit recordings: Origins and insight into the integrated motor system. *Brain Research*, 1409, 42–61. <https://doi.org/10.1016/j.brainres.2011.06.011>
- Duncan, M. J., Thake, C. D., & Downs, P. J. (2014). Effect of caffeine ingestion on torque and muscle activity during resistance exercise in men. *Muscle & Nerve*, 50(4), 523–527. <https://doi.org/10.1002/mus.24179>
- Eccles, J. C. (1964). The Excitatory Responses of Spinal Neurones. In *Progress in Brain Research* (Vol. 12, pp. 1–34). Elsevier. [https://doi.org/10.1016/S0079-6123\(08\)60614-7](https://doi.org/10.1016/S0079-6123(08)60614-7)
- ElBasiouny, S. M., Schuster, J. E., & Heckman, C. J. (2010). Persistent inward currents in spinal motoneurons: Important for normal function but potentially harmful after spinal cord injury and in amyotrophic lateral sclerosis. *Clinical Neurophysiology*, 121(10), 1669–1679. <https://doi.org/10.1016/j.clinph.2009.12.041>

- Enoka, R. M. (2019). Physiological validation of the decomposition of surface EMG signals. *Journal of Electromyography and Kinesiology: Official Journal of the International Society of Electrophysiological Kinesiology*, 46, 70–83. <https://doi.org/10.1016/j.jelekin.2019.03.010>
- Enoka, R. M., & Duchateau, J. (2017). Rate Coding and the Control of Muscle Force. *Cold Spring Harbor Perspectives in Medicine*, 7(10), a029702. <https://doi.org/10.1101/cshperspect.a029702>
- Farina, D. (2006). Interpretation of the Surface Electromyogram in Dynamic Contractions. *Exercise and Sport Sciences Reviews*, 34(3), 121.
- Farina, D., & Holobar, A. (2016). Characterization of Human Motor Units From Surface EMG Decomposition. *Proceedings of the IEEE*, 104(2), 353–373. <https://doi.org/10.1109/JPROC.2015.2498665>
- Farina, D., Holobar, A., Merletti, R., & Enoka, R. M. (2010). Decoding the neural drive to muscles from the surface electromyogram. *Clinical Neurophysiology: Official Journal of the International Federation of Clinical Neurophysiology*, 121(10), 1616–1623. <https://doi.org/10.1016/j.clinph.2009.10.040>
- Farina, D., Merletti, R., & Enoka, R. M. (2014). The extraction of neural strategies from the surface EMG: An update. *Journal of Applied Physiology*, 117(11), 1215–1230. <https://doi.org/10.1152/jappphysiol.00162.2014>
- Farina, D., & Negro, F. (2015). Common synaptic input to motor neurons, motor unit synchronization, and force control. *Exercise and Sport Sciences Reviews*, 43(1), 23–33. <https://doi.org/10.1249/JES.0000000000000032>
- Fisone, G., Borgkvist, A., & Usiello, A. (2004). Caffeine as a psychomotor stimulant: Mechanism of action. *Cellular and Molecular Life Sciences (CMLS)*, 61(7–8), 857–872. <https://doi.org/10.1007/s00018-003-3269-3>
- Fleshman, J. W., Munson, J. B., Sybert, G. W., & Friedman, W. A. (1981). Rheobase, input resistance, and motor-unit type in medial gastrocnemius motoneurons in the cat. *Journal of Neurophysiology*, 46(6), 1326–1338. <https://doi.org/10.1152/jn.1981.46.6.1326>
- Fryer, M. W., & Neering, I. R. (1989). Actions of caffeine on fast- and slow-twitch muscles of the rat. *The Journal of Physiology*, 416(1), 435–454. <https://doi.org/10.1113/jphysiol.1989.sp017770>
- Fulgoni, V. L., III, Keast, D. R., & Lieberman, H. R. (2015). Trends in intake and sources of caffeine in the diets of US adults: 2001–2010. *The American Journal of Clinical Nutrition*, 101(5), 1081–1087. <https://doi.org/10.3945/ajcn.113.080077>

- Funase, K., Imanaka, K., & Nishihira, Y. (1994). Excitability of the soleus motoneuron pool revealed by the developmental slope of the H-reflex as reflex gain. *Electromyography and Clinical Neurophysiology*, 34(8), 477–489.
- Gandhi, M., Aweeka, F., Greenblatt, R. M., & Blaschke, T. F. (2004). Sex Differences in Pharmacokinetics and Pharmacodynamics. *Annual Review of Pharmacology and Toxicology*, 44(1), 499–523. <https://doi.org/10.1146/annurev.pharmtox.44.101802.121453>
- Georgopoulos, A. P., Kalaska, J. F., Caminiti, R., & Massey, J. T. (1982). On the relations between the direction of two-dimensional arm movements and cell discharge in primate motor cortex. *Journal of Neuroscience*, 2(11), 1527–1537. <https://doi.org/10.1523/JNEUROSCI.02-11-01527.1982>
- Georgopoulos, A. P., Schwartz, A. B., & Kettner, R. E. (1986). Neuronal Population Coding of Movement Direction. *Science*, 233(4771), 1416–1419. <https://doi.org/10.1126/science.3749885>
- Goldstein, E., Jacobs, P. L., Whitehurst, M., Penhollow, T., & Antonio, J. (2010). Caffeine enhances upper body strength in resistance-trained women. *Journal of the International Society of Sports Nutrition*, 7, 18. <https://doi.org/10.1186/1550-2783-7-18>
- Gorassini, M. A., Knash, M. E., Harvey, P. J., Bennett, D. J., & Yang, J. F. (2004). Role of motoneurons in the generation of muscle spasms after spinal cord injury. *Brain*, 127(10), 2247–2258. <https://doi.org/10.1093/brain/awh243>
- Gorassini, M., Yang, J. F., Siu, M., & Bennett, D. J. (2002a). Intrinsic Activation of Human Motoneurons: Possible Contribution to Motor Unit Excitation. *Journal of Neurophysiology*, 87(4), 1850–1858. <https://doi.org/10.1152/jn.00024.2001>
- Gorassini, M., Yang, J. F., Siu, M., & Bennett, D. J. (2002b). Intrinsic Activation of Human Motoneurons: Reduction of Motor Unit Recruitment Thresholds by Repeated Contractions. *Journal of Neurophysiology*, 87(4), 1859–1866. <https://doi.org/10.1152/jn.00025.2001>
- Gordon, T., Tyreman, N., Rafuse, V. F., & Munson, J. B. (1999). Chapter 17 Limited Plasticity of Adult Motor Units Conserves Recruitment Order and Rate Coding. In M. D. Binder (Ed.), *Progress in Brain Research* (Vol. 123, pp. 191–202). Elsevier. [https://doi.org/10.1016/S0079-6123\(08\)62856-3](https://doi.org/10.1016/S0079-6123(08)62856-3)
- Graham, T. E. (2001). Caffeine and Exercise. *Sports Medicine*, 31(11), 785–807. <https://doi.org/10.2165/00007256-200131110-00002>
- Green, P. J., Kirby, R., & Suls, J. (1996). The effects of caffeine on blood pressure and heart rate: A review. *Annals of Behavioral Medicine: A Publication of the Society of Behavioral Medicine*, 18(3), 201–216. <https://doi.org/10.1007/BF02883398>

- Grgic, J., Mikulic, P., Schoenfeld, B. J., Bishop, D. J., & Pedisic, Z. (2019). The Influence of Caffeine Supplementation on Resistance Exercise: A Review. *Sports Medicine*, 49(1), 17–30. <https://doi.org/10.1007/s40279-018-0997-y>
- Grgic, J., & Pickering, C. (2019). The effects of caffeine ingestion on isokinetic muscular strength: A meta-analysis. *Journal of Science and Medicine in Sport*, 22(3), 353–360. <https://doi.org/10.1016/j.jsams.2018.08.016>
- Grgic, J., Trexler, E. T., Lazineca, B., & Pedisic, Z. (2018). Effects of caffeine intake on muscle strength and power: A systematic review and meta-analysis. *Journal of the International Society of Sports Nutrition*, 15(1), 11. <https://doi.org/10.1186/s12970-018-0216-0>
- Guest, N. S., VanDusseldorp, T. A., Nelson, M. T., Grgic, J., Schoenfeld, B. J., Jenkins, N. D. M., Arent, S. M., Antonio, J., Stout, J. R., Trexler, E. T., Smith-Ryan, A. E., Goldstein, E. R., Kalman, D. S., & Campbell, B. I. (2021). International society of sports nutrition position stand: Caffeine and exercise performance. *Journal of the International Society of Sports Nutrition*, 18(1), 1. <https://doi.org/10.1186/s12970-020-00383-4>
- Halliday, D. M., Conway, B. A., Farmer, S. F., & Rosenberg, J. R. (1999). Load-Independent Contributions From Motor-Unit Synchronization to Human Physiological Tremor. *Journal of Neurophysiology*, 82(2), 664–675. <https://doi.org/10.1152/jn.1999.82.2.664>
- Halliday, D. M., Rosenberg, J. R., Amjad, A. M., Breeze, P., Conway, B. A., & Farmer, S. F. (1995). A framework for the analysis of mixed time series/point process data—Theory and application to the study of physiological tremor, single motor unit discharges and electromyograms. *Progress in Biophysics and Molecular Biology*, 64(2–3), 237–278. [https://doi.org/10.1016/s0079-6107\(96\)00009-0](https://doi.org/10.1016/s0079-6107(96)00009-0)
- Harvey, P. J., Li, X., Li, Y., & Bennett, D. J. (2006). Endogenous monoamine receptor activation is essential for enabling persistent sodium currents and repetitive firing in rat spinal motoneurons. *Journal of Neurophysiology*, 96(3), 1171–1186. <https://doi.org/10.1152/jn.00341.2006>
- Hassan, A. S., Fajardo, M. E., Cummings, M., McPherson, L. M., Negro, F., Dewald, J. P. A., Heckman, C. J., & Pearcey, G. E. P. (2021). Estimates of persistent inward currents are reduced in upper limb motor units of older adults. *The Journal of Physiology*, 599(21), 4865–4882. <https://doi.org/10.1113/JP282063>
- Hassan, A., Thompson, C. K., Negro, F., Cummings, M., Powers, R. K., Heckman, C. J., Dewald, J. P. A., & McPherson, L. M. (2020). Impact of parameter selection on estimates of motoneuron excitability using paired motor unit analysis. *Journal of Neural Engineering*, 17(1), 016063. <https://doi.org/10.1088/1741-2552/ab5eda>

- Heckman, C. J. (1994). Computer simulations of the effects of different synaptic input systems on the steady-state input-output structure of the motoneuron pool. *Journal of Neurophysiology*, 71(5), 1727–1739. <https://doi.org/10.1152/jn.1994.71.5.1727>
- Heckman, C. j., & Enoka, R. M. (2012). Motor Unit. In *Comprehensive Physiology* (pp. 2629–2682). John Wiley & Sons, Ltd. <https://doi.org/10.1002/cphy.c100087>
- Heckman, C. J., Gorassini, M. A., & Bennett, D. J. (2005). Persistent inward currents in motoneuron dendrites: Implications for motor output. *Muscle & Nerve*, 31(2), 135–156. <https://doi.org/10.1002/mus.20261>
- Heckman, C. J., Johnson, M., Mottram, C., & Schuster, J. (2008). Persistent inward currents in spinal motoneurons and their influence on human motoneuron firing patterns. *The Neuroscientist: A Review Journal Bringing Neurobiology, Neurology and Psychiatry*, 14(3), 264–275. <https://doi.org/10.1177/1073858408314986>
- Heckman, C. J., Lee, R. H., & Brownstone, R. M. (2003). Hyperexcitable dendrites in motoneurons and their neuromodulatory control during motor behavior. *Trends in Neurosciences*, 26(12), 688–695. <https://doi.org/10.1016/j.tins.2003.10.002>
- Heckman, C. J., Mottram, C., Quinlan, K., Theiss, R., & Schuster, J. (2009). Motoneuron excitability: The importance of neuromodulatory inputs. *Clinical Neurophysiology: Official Journal of the International Federation of Clinical Neurophysiology*, 120(12), 2040–2054. <https://doi.org/10.1016/j.clinph.2009.08.009>
- Henneman, E. (1957). Relation between Size of Neurons and Their Susceptibility to Discharge. *Science*, 126(3287), 1345–1347. <https://doi.org/10.1126/science.126.3287.1345>
- Henneman, E., Clamann, H. P., Gillies, J. D., & Skinner, R. D. (1974). Rank order of motoneurons within a pool: Law of combination. *Journal of Neurophysiology*, 37(6), 1338–1349. <https://doi.org/10.1152/jn.1974.37.6.1338>
- Henneman, E., & Mendell, L. M. (1981). Functional Organization of Motoneuron Pool and its Inputs. In R. Terjung (Ed.), *Comprehensive Physiology* (1st ed., pp. 423–507). Wiley. <https://doi.org/10.1002/cphy.cp010211>
- Herrmann, U., & Flanders, M. (1998). Directional Tuning of Single Motor Units. *The Journal of Neuroscience*, 18(20), 8402–8416. <https://doi.org/10.1523/JNEUROSCI.18-20-08402.1998>
- Holobar, A., Minetto, M. A., Botter, A., Negro, F., & Farina, D. (2010). Experimental analysis of accuracy in the identification of motor unit spike trains from high-density surface EMG. *IEEE Transactions on Neural Systems and Rehabilitation Engineering: A Publication of the IEEE Engineering in Medicine and Biology Society*, 18(3), 221–229. <https://doi.org/10.1109/TNSRE.2010.2041593>

- Holtermann, A., Mork, P. J., Andersen, L. L., Olsen, H. B., & Sjøgaard, K. (2010). The use of EMG biofeedback for learning of selective activation of intra-muscular parts within the serratus anterior muscle: A novel approach for rehabilitation of scapular muscle imbalance. *Journal of Electromyography and Kinesiology: Official Journal of the International Society of Electrophysiological Kinesiology*, 20(2), 359–365. <https://doi.org/10.1016/j.jelekin.2009.02.009>
- Holtermann, A., & Roeleveld, K. (2006). EMG amplitude distribution changes over the upper trapezius muscle are similar in sustained and ramp contractions. *Acta Physiologica (Oxford, England)*, 186(2), 159–168. <https://doi.org/10.1111/j.1748-1716.2005.01520.x>
- Holtermann, A., Roeleveld, K., & Karlsson, J. S. (2005). Inhomogeneities in muscle activation reveal motor unit recruitment. *Journal of Electromyography and Kinesiology*, 15(2), 131–137. <https://doi.org/10.1016/j.jelekin.2004.09.003>
- Houngaard, J., Hultborn, H., Jespersen, B., & Kiehn, O. (1988). Bistability of alpha-motoneurons in the decerebrate cat and in the acute spinal cat after intravenous 5-hydroxytryptophan. *The Journal of Physiology*, 405(1), 345–367. <https://doi.org/10.1113/jphysiol.1988.sp017336>
- Houngaard, J., & Kiehn, O. (1989). Serotonin-induced bistability of turtle motoneurons caused by a nifedipine-sensitive calcium plateau potential. *The Journal of Physiology*, 414(1), 265–282. <https://doi.org/10.1113/jphysiol.1989.sp017687>
- Hug, F., Avrillon, S., Ibáñez, J., & Farina, D. (2023). Common synaptic input, synergies and size principle: Control of spinal motor neurons for movement generation. *The Journal of Physiology*, 601(1), 11–20. <https://doi.org/10.1113/JP283698>
- Hug, F., Del Vecchio, A., Avrillon, S., Farina, D., & Tucker, K. (2021). Muscles from the same muscle group do not necessarily share common drive: Evidence from the human triceps surae. *Journal of Applied Physiology*, 130(2), 342–354. <https://doi.org/10.1152/jappphysiol.00635.2020>
- Hynghstrom, A. S., Johnson, M. D., Miller, J. F., & Heckman, C. J. (2007). Intrinsic electrical properties of spinal motoneurons vary with joint angle. *Nature Neuroscience*, 10(3), 363–369. <https://doi.org/10.1038/nn1852>
- Jahanmiri-Nezhad, F., Barkhaus, P. E., Rymer, W. Z., & Zhou, P. (2014). Sensitivity of fasciculation potential detection is dramatically reduced by spatial filtering of surface electromyography. *Clinical Neurophysiology: Official Journal of the International Federation of Clinical Neurophysiology*, 125(7), 1498–1500. <https://doi.org/10.1016/j.clinph.2013.11.033>
- Jensen, C., & Westgaard, R. H. (1997). Functional subdivision of the upper trapezius muscle during low-level activation. *European Journal of Applied Physiology and Occupational Physiology*, 76(4), 335–339. <https://doi.org/10.1007/s004210050257>

- Jenz, S. T., Beauchamp, J. A., Gomes, M. M., Negro, F., Heckman, C. J., & Pearcey, G. E. P. (2022). The effects of biological sex on estimates of persistent inward currents in the human lower limb [Preprint]. *Neuroscience*.  
<https://doi.org/10.1101/2022.10.09.511486>
- Kallio, J., Sjøgaard, K., Avela, J., Komi, P. V., Selänne, H., & Linnamo, V. (2013). Motor Unit Firing Behaviour of Soleus Muscle in Isometric and Dynamic Contractions. *PLOS ONE*, 8(2), e53425. <https://doi.org/10.1371/journal.pone.0053425>
- Kalmar, J. M., & Cafarelli, E. (1999). Effects of caffeine on neuromuscular function. *Journal of Applied Physiology* (Bethesda, Md.: 1985), 87(2), 801–808.  
<https://doi.org/10.1152/jappl.1999.87.2.801>
- Kandel, E., Schwartz, J., Jessel, T., Siegelbaum, S., & Hudspeth, A. J. (2012). *Principles of Neural Science* (5th ed.). McGraw-hill.
- Kaplan, G. B., Greenblatt, D. J., Ehrenberg, B. L., Goddard, J. E., Cotreau, M. M., Harmatz, J. S., & Shader, R. I. (1997). Dose-dependent pharmacokinetics and psychomotor effects of caffeine in humans. *Journal of Clinical Pharmacology*, 37(8), 693–703. <https://doi.org/10.1002/j.1552-4604.1997.tb04356.x>
- Kernell, D., & Zwaagstra, B. (1981). Input conductance, axonal conduction velocity and cell size among hindlimb motoneurons of the cat. *Brain Research*, 204(2), 311–326. [https://doi.org/10.1016/0006-8993\(81\)90591-6](https://doi.org/10.1016/0006-8993(81)90591-6)
- Khurram, O. U., Negro, F., Heckman, C. J., & Thompson, C. K. (2021). Estimates of persistent inward currents in tibialis anterior motor units during standing ramped contraction tasks in humans. *Journal of Neurophysiology*, 126(1), 264–274.  
<https://doi.org/10.1152/jn.00144.2021>
- Kilner, J. M., Baker, S. N., Salenius, S., Jousmäki, V., Hari, R., & Lemon, R. N. (1999). Task-dependent modulation of 15-30 Hz coherence between rectified EMGs from human hand and forearm muscles. *The Journal of Physiology*, 516 ( Pt 2)(Pt 2), 559–570. <https://doi.org/10.1111/j.1469-7793.1999.0559v.x>
- Kim, E. H., Wilson, J. M., Thompson, C. K., & Heckman, C. J. (2020). Differences in estimated persistent inward currents between ankle flexors and extensors in humans. *Journal of Neurophysiology*, 124(2), 525–535.  
<https://doi.org/10.1152/jn.00746.2019>
- Kleine, B., Boekestein, W., Arts, I., Zwarts, M., Schelhaas, H. J., & Stegeman, D. (2012). Fasciculations and their F-response revisited: High-density surface EMG in ALS and benign fasciculations. *Clinical Neurophysiology : Official Journal of the International Federation of Clinical Neurophysiology*, 123(2).  
<https://doi.org/10.1016/j.clinph.2011.06.032>

- Knikou, M. (2008). The H-reflex as a probe: Pathways and pitfalls. *Journal of Neuroscience Methods*, 171(1), 1–12. <https://doi.org/10.1016/j.jneumeth.2008.02.012>
- Kuznetsova, A., Brockhoff, P. B., & Christensen, R. H. B. (2017). lmerTest Package: Tests in Linear Mixed Effects Models. *Journal of Statistical Software*, 82, 1–26. <https://doi.org/10.18637/jss.v082.i13>
- Laine, C. M., Martinez-Valdes, E., Falla, D., Mayer, F., & Farina, D. (2015). Motor Neuron Pools of Synergistic Thigh Muscles Share Most of Their Synaptic Input. *The Journal of Neuroscience: The Official Journal of the Society for Neuroscience*, 35(35), 12207–12216. <https://doi.org/10.1523/JNEUROSCI.0240-15.2015>
- Lawrence, J. H., & De Luca, C. J. (1983). Myoelectric signal versus force relationship in different human muscles. *Journal of Applied Physiology: Respiratory, Environmental and Exercise Physiology*, 54(6), 1653–1659. <https://doi.org/10.1152/jappl.1983.54.6.1653>
- Layman, D. K., Lönnerdal, B., & Fernstrom, J. D. (2018). Applications for  $\alpha$ -lactalbumin in human nutrition. *Nutrition Reviews*, 76(6), 444–460. <https://doi.org/10.1093/nutrit/nuy004>
- Lee, R. H., & Heckman, C. J. (1996). Influence of voltage-sensitive dendritic conductances on bistable firing and effective synaptic current in cat spinal motoneurons in vivo. *Journal of Neurophysiology*, 76(3), 2107–2110. <https://doi.org/10.1152/jn.1996.76.3.2107>
- Lee, R. H., & Heckman, C. J. (1998). Bistability in Spinal Motoneurons In Vivo: Systematic Variations in Rhythmic Firing Patterns. *Journal of Neurophysiology*, 80(2), 572–582. <https://doi.org/10.1152/jn.1998.80.2.572>
- Lee, R. H., & Heckman, C. J. (1999). Enhancement of bistability in spinal motoneurons in vivo by the noradrenergic  $\alpha$ 1 agonist methoxamine. *Journal of Neurophysiology*, 81(5), 2164–2174. <https://doi.org/10.1152/jn.1999.81.5.2164>
- Lee, R. H., Kuo, J. J., Jiang, M. C., & Heckman, C. J. (2003). Influence of Active Dendritic Currents on Input-Output Processing in Spinal Motoneurons In Vivo. *Journal of Neurophysiology*, 89(1), 27–39. <https://doi.org/10.1152/jn.00137.2002>
- Lemon, R. N. (2008). Descending Pathways in Motor Control. *Annual Review of Neuroscience*, 31(1), 195–218. <https://doi.org/10.1146/annurev.neuro.31.060407.125547>
- Lenth, R. V., Buerkner, P., Giné-Vázquez, I., Herve, M., Jung, M., Love, J., Miguez, F., Riebl, H., & Singmann, H. (2023). emmeans: Estimated Marginal Means, aka Least-Squares Means (1.8.4-1). <https://CRAN.R-project.org/package=emmeans>

- Lulic-Kuryllo, T., & Inglis, J. G. (2022). Sex differences in motor unit behaviour: A review. *Journal of Electromyography and Kinesiology*, 66, 102689. <https://doi.org/10.1016/j.jelekin.2022.102689>
- Mackay Phillips, K., Orssatto, L. B. R., Polman, R., Van der Pols, J. C., & Trajano, G. S. (2022). The effects of  $\alpha$ -lactalbumin supplementation and handgrip contraction on soleus motoneuron excitability. *European Journal of Applied Physiology*. <https://doi.org/10.1007/s00421-022-05101-3>
- Madigan, D. J., & Willems, M. E. T. (2011). Effect of Caffeine on Fatigue During Submaximal Isometric Contractions at Different Knee Angles. *Medicina Sportiva*, 15(4), 194–200. <https://doi.org/10.2478/v10036-011-0027-8>
- Martinez-Valdes, E., Negro, F., Laine, C. M., Falla, D., Mayer, F., & Farina, D. (2017). Tracking motor units longitudinally across experimental sessions with high-density surface electromyography. *The Journal of Physiology*, 595(5), 1479–1496. <https://doi.org/10.1113/JP273662>
- McAuley, J. H., & Marsden, C. D. (2000). Physiological and pathological tremors and rhythmic central motor control. *Brain: A Journal of Neurology*, 123 ( Pt 8), 1545–1567. <https://doi.org/10.1093/brain/123.8.1545>
- McClaran, S. R., & Wetter, T. J. (2007). Low doses of caffeine reduce heart rate during submaximal cycle ergometry. *Journal of the International Society of Sports Nutrition*, 4, 11. <https://doi.org/10.1186/1550-2783-4-11>
- McKiernan, B. J., Marcario, J. K., Karrer, J. H., & Cheney, P. D. (2000). Correlations between corticomotoneuronal (CM) cell postspike effects and cell-target muscle covariation. *Journal of Neurophysiology*, 83(1), 99–115. <https://doi.org/10.1152/jn.2000.83.1.99>
- McMillan, A. S., & Hannam, A. G. (1992). Task-related behaviour of motor units in different regions of the human masseter muscle. *Archives of Oral Biology*, 37(10), 849–857. [https://doi.org/10.1016/0003-9969\(92\)90119-S](https://doi.org/10.1016/0003-9969(92)90119-S)
- McPherson, J. G., Ellis, M. D., Heckman, C. J., & Dewald, J. P. A. (2008). Evidence for Increased Activation of Persistent Inward Currents in Individuals With Chronic Hemiparetic Stroke. *Journal of Neurophysiology*, 100(6), 3236–3243. <https://doi.org/10.1152/jn.90563.2008>
- Mesquita, R. N. O., Cronin, N. J., Kyröläinen, H., Hintikka, J., & Avela, J. (2020). Effects of caffeine on neuromuscular function in a non-fatigued state and during fatiguing exercise. *Experimental Physiology*, 105(4), 690–706. <https://doi.org/10.1113/EP088265>

- Mesquita, R. N. O., Taylor, J. L., Trajano, G. S., Škarabot, J., Holobar, A., Gonçalves, B. A. M., & Blazevich, A. J. (2022). Effects of reciprocal inhibition and whole-body relaxation on persistent inward currents estimated by two different methods. *The Journal of Physiology*, 600(11), 2765–2787. <https://doi.org/10.1113/JP282765>
- Meyers, B. m., & Cafarelli, E. (2005). Caffeine increases time to fatigue by maintaining force and not by altering firing rates during submaximal isometric contractions. *Journal of Applied Physiology*, 99(3), 1056–1063. <https://doi.org/10.1152/jappphysiol.00937.2004>
- Milner-Brown, H. S., Stein, R. B., & Yemm, R. (1973). Changes in firing rate of human motor units during linearly changing voluntary contractions. *The Journal of Physiology*, 230(2), 371–390. <https://doi.org/10.1113/jphysiol.1973.sp010193>
- Misiaszek, J. (2003). The H-reflex as a tool in neurophysiology: Its limitations and uses in understanding nervous system function. *Muscle & Nerve*, 28(2), 144–160. <https://doi.org/10.1002/mus.10372>
- Monster, A. W., & Chan, H. (1977). Isometric force production by motor units of extensor digitorum communis muscle in man. *Journal of Neurophysiology*, 40(6), 1432–1443. <https://doi.org/10.1152/jn.1977.40.6.1432>
- Moritz, C. T., Barry, B. K., Pascoe, M. A., & Enoka, R. M. (2005). Discharge rate variability influences the variation in force fluctuations across the working range of a hand muscle. *Journal of Neurophysiology*, 93(5), 2449–2459. <https://doi.org/10.1152/jn.01122.2004>
- Mottram, C. J., Suresh, N. L., Heckman, C. J., Gorassini, M. A., & Rymer, W. Z. (2009). Origins of abnormal excitability in biceps brachii motoneurons of spastic-paretic stroke survivors. *Journal of Neurophysiology*, 102(4), 2026–2038. <https://doi.org/10.1152/jn.00151.2009>
- Muceli, S., Poppendieck, W., Negro, F., Yoshida, K., Hoffmann, K. P., Butler, J. E., Gandevia, S. C., & Farina, D. (2015). Accurate and representative decoding of the neural drive to muscles in humans with multi-channel intramuscular thin-film electrodes. *The Journal of Physiology*, 593(17), 3789–3804. <https://doi.org/10.1113/JP270902>
- Murray, G. M., Orfanos, T., Chan, J. Y., Wanigaratne, K., & Klineberg, I. J. (1999). Electromyographic activity of the human lateral pterygoid muscle during contralateral and protrusive jaw movements. *Archives of Oral Biology*, 44(3), 269–285. [https://doi.org/10.1016/s0003-9969\(98\)00117-4](https://doi.org/10.1016/s0003-9969(98)00117-4)

- Murray, K. C., Nakae, A., Stephens, M. J., Rank, M., D'Amico, J., Harvey, P. J., Li, X., Harris, R. L. W., Ballou, E. W., Anelli, R., Heckman, C. J., Mashimo, T., Vavrek, R., Sanelli, L., Gorassini, M. A., Bennett, D. J., & Fouad, K. (2010). Recovery of motoneuron and locomotor function after spinal cord injury depends on constitutive activity in 5-HT<sub>2C</sub> receptors. *Nature Medicine*, 16(6), Article 6. <https://doi.org/10.1038/nm.2160>
- Nawrot, P., Jordan, S., Eastwood, J., Rotstein, J., Hugenholtz, A., & Feeley, M. (2003). Effects of caffeine on human health. *Food Additives and Contaminants*, 20(1), 1–30. <https://doi.org/10.1080/0265203021000007840>
- Nayler, W. G. (1963). Effect of caffeine on cardiac contractile activity and radiocalcium movement. *The American Journal of Physiology*, 204, 969–974. <https://doi.org/10.1152/ajplegacy.1963.204.6.969>
- Negro, F., Holobar, A., & Farina, D. (2009). Fluctuations in isometric muscle force can be described by one linear projection of low-frequency components of motor unit discharge rates. *The Journal of Physiology*, 587(24), 5925–5938. <https://doi.org/10.1113/jphysiol.2009.178509>
- Negro, F., Muceli, S., Castronovo, A. M., Holobar, A., & Farina, D. (2016). Multi-channel intramuscular and surface EMG decomposition by convolutive blind source separation. *Journal of Neural Engineering*, 13(2), 026027. <https://doi.org/10.1088/1741-2560/13/2/026027>
- Nehlig, A., & Debry, G. (1994). Caffeine and Sports Activity: A Review. *International Journal of Sports Medicine*, 15(05), 215–223. <https://doi.org/10.1055/s-2007-1021049>
- Olson, C. B., Carpenter, D. O., & Henneman, E. (1968). Orderly Recruitment of Muscle Action Potentials: Motor Unit Threshold and EMG Amplitude. *Archives of Neurology*, 19(6), 591–597. <https://doi.org/10.1001/archneur.1968.00480060061008>
- Orosco, M., Rouch, C., Beslot, F., Feurte, S., Regnault, A., & Dauge, V. (2004). Alpha-lactalbumin-enriched diets enhance serotonin release and induce anxiolytic and rewarding effects in the rat. *Behavioural Brain Research*, 148(1–2), 1–10. [https://doi.org/10.1016/s0166-4328\(03\)00153-0](https://doi.org/10.1016/s0166-4328(03)00153-0)
- Palmieri, R. M., Ingersoll, C. D., & Hoffman, M. A. (2004). The Hoffmann Reflex: Methodologic Considerations and Applications for Use in Sports Medicine and Athletic Training Research. *Journal of Athletic Training*, 39(3), 268–277.
- Pasman, W. J., van Baak, M. A., Jeukendrup, A. E., & de Haan, A. (1995). The effect of different dosages of caffeine on endurance performance time. *International Journal of Sports Medicine*, 16(4), 225–230. <https://doi.org/10.1055/s-2007-972996>

- Paton, M. E., & Brown, J. M. M. (1994). An electromyographic analysis of functional differentiation in human pectoralis major muscle. *Journal of Electromyography and Kinesiology*, 4(3), 161–169. [https://doi.org/10.1016/1050-6411\(94\)90017-5](https://doi.org/10.1016/1050-6411(94)90017-5)
- Perrier, J.-F. (2005). Synaptic Release of Serotonin Induced by Stimulation of the Raphe Nucleus Promotes Plateau Potentials in Spinal Motoneurons of the Adult Turtle. *Journal of Neuroscience*, 25(35), 7993–7999. <https://doi.org/10.1523/JNEUROSCI.1957-05.2005>
- Peterson, B. M., Brown, L. E., Judelson, D. A., Gallo-Rebert, S., & Coburn, J. W. (2019). Caffeine Increases Rate of Torque Development Without Affecting Maximal Torque. *Journal of Science in Sport and Exercise*, 1(3), 248–256. <https://doi.org/10.1007/s42978-019-00048-y>
- Pickering, C., & Kiely, J. (2018). Are the Current Guidelines on Caffeine Use in Sport Optimal for Everyone? Inter-individual Variation in Caffeine Ergogenicity, and a Move Towards Personalised Sports Nutrition. *Sports Medicine (Auckland, N.Z.)*, 48(1), 7–16. <https://doi.org/10.1007/s40279-017-0776-1>
- Pierrot-Deseilligny, E., Bergego, C., Katz, R., & Morin, C. (1981). Cutaneous depression of Ib reflex pathways to motoneurons in man. *Experimental Brain Research*, 42(3), 351–361. <https://doi.org/10.1007/BF00237500>
- Pierrot-Deseilligny, E., & Mazevet, D. (2000). The monosynaptic reflex: A tool to investigate motor control in humans. Interest and limits. *Neurophysiologie Clinique/Clinical Neurophysiology*, 30(2), 67–80. [https://doi.org/10.1016/S0987-7053\(00\)00062-9](https://doi.org/10.1016/S0987-7053(00)00062-9)
- Powers, R. K., Nardelli, P., & Cope, T. C. (2008). Estimation of the Contribution of Intrinsic Currents to Motoneuron Firing Based on Paired Motoneuron Discharge Records in the Decerebrate Cat. *Journal of Neurophysiology*, 100(1), 292–303. <https://doi.org/10.1152/jn.90296.2008>
- Purves, D., Augustine, G., Fitzpatrick, D., Katz, L., LaMantia, A.-S., McNamara, J., & Williams, S. M. (2001). *Neuroscience* (2nd ed.). Sinauer Associates.
- Rank, M. M., Li, X., Bennett, D. J., & Gorassini, M. A. (2007). Role of endogenous release of norepinephrine in muscle spasms after chronic spinal cord injury. *Journal of Neurophysiology*, 97(5), 3166–3180. <https://doi.org/10.1152/jn.01168.2006>
- Reggiani, C. (2021). Caffeine as a tool to investigate sarcoplasmic reticulum and intracellular calcium dynamics in human skeletal muscles. *Journal of Muscle Research and Cell Motility*, 42(2), 281–289. <https://doi.org/10.1007/s10974-020-09574-7>

- Robertson, T. M., Clifford, M. N., Penson, S., Williams, P., & Robertson, M. D. (2018). Postprandial glycaemic and lipaemic responses to chronic coffee consumption may be modulated by CYP1A2 polymorphisms. *British Journal of Nutrition*, 119(7), 792–800. <https://doi.org/10.1017/S0007114518000260>
- Rudroff, T., Jordan, K., Enoka, J. A., Matthews, S. D., Baudry, S., & Enoka, R. M. (2010). Discharge of biceps brachii motor units is modulated by load compliance and forearm posture. *Experimental Brain Research*, 202(1), 111–120. <https://doi.org/10.1007/s00221-009-2116-7>
- Ruxton, C. H. S. (2008). The impact of caffeine on mood, cognitive function, performance and hydration: A review of benefits and risks. *Nutrition Bulletin*, 33(1), 15–25. <https://doi.org/10.1111/j.1467-3010.2007.00665.x>
- Seki, K., & Narusawa, M. (1996). Firing rate modulation of human motor units in different muscles during isometric contraction with various forces. *Brain Research*, 719(1–2), 1–7. [https://doi.org/10.1016/0006-8993\(95\)01432-2](https://doi.org/10.1016/0006-8993(95)01432-2)
- Sherrington, C. (1904). Correlation of Reflexes and the Principle of the Common Path. 70, 460–466.
- Skidmore-Roth, L. (n.d.). *Mosby's 2023 Nursing Drug Reference—36th Edition*. Elsevier. Retrieved January 30, 2023, from <https://www.elsevier.com/books/mosby%27s-2023-nursing-drug-reference/978-0-323-93072-7>
- Spriet, L. L. (2014). Exercise and Sport Performance with Low Doses of Caffeine. *Sports Medicine (Auckland, N.z.)*, 44(Suppl 2), 175–184. <https://doi.org/10.1007/s40279-014-0257-8>
- Staudenmann, D., Stegeman, D. F., & van Dieën, J. H. (2013). Redundancy or heterogeneity in the electric activity of the biceps brachii muscle? Added value of PCA-processed multi-channel EMG muscle activation estimates in a parallel-fibered muscle. *Journal of Electromyography and Kinesiology: Official Journal of the International Society of Electrophysiological Kinesiology*, 23(4), 892–898. <https://doi.org/10.1016/j.jelekin.2013.03.004>
- Stifani, N. (2014). Motor neurons and the generation of spinal motor neuron diversity. *Frontiers in Cellular Neuroscience*, 8. <https://doi.org/10.3389/fncel.2014.00293>
- Tarnopolsky, M., & Cupido, C. (2000). Caffeine potentiates low frequency skeletal muscle force in habitual and nonhabitual caffeine consumers. *Journal of Applied Physiology (Bethesda, Md.: 1985)*, 89(5), 1719–1724. <https://doi.org/10.1152/jappl.2000.89.5.1719>
- Taylor, A. M., Christou, E. A., & Enoka, R. M. (2003). Multiple Features of Motor-Unit Activity Influence Force Fluctuations During Isometric Contractions. *Journal of Neurophysiology*, 90(2), 1350–1361. <https://doi.org/10.1152/jn.00056.2003>

- Taylor, C. A., Kopicko, B. H., Negro, F., & Thompson, C. K. (2022). Sex differences in the detection of motor unit action potentials identified using high-density surface electromyography. *Journal of Electromyography and Kinesiology*, 65, 102675. <https://doi.org/10.1016/j.jelekin.2022.102675>
- Taylor, C., Kmiec, T., & Thompson, C. (2020). Differences in Human Motoneuron Excitability Between Functionally Diverse Muscles. *CommonHealth*, 1(1), 12–23. <https://doi.org/10.15367/ch.v1i1.300>
- ter Haar Romeny, B. M., Denier van der Gon, J. J., & Gielen, C. C. A. M. (1984). Relation between location of a motor unit in the human biceps brachii and its critical firing levels for different tasks. *Experimental Neurology*, 85(3), 631–650. [https://doi.org/10.1016/0014-4886\(84\)90036-0](https://doi.org/10.1016/0014-4886(84)90036-0)
- Thompson, C. K., Negro, F., Johnson, M. D., Holmes, M. R., McPherson, L. M., Powers, R. K., Farina, D., & Heckman, C. J. (2018). Robust and accurate decoding of motoneuron behaviour and prediction of the resulting force output. *The Journal of Physiology*, 596(14), 2643–2659. <https://doi.org/10.1113/JP276153>
- Udina, E., D'Amico, J., Bergquist, A. J., & Gorassini, M. A. (2010). Amphetamine Increases Persistent Inward Currents in Human Motoneurons Estimated From Paired Motor-Unit Activity. *Journal of Neurophysiology*, 103(3), 1295–1303. <https://doi.org/10.1152/jn.00734.2009>
- Urry, E., Jetter, A., & Landolt, H.-P. (2016). Assessment of CYP1A2 enzyme activity in relation to type-2 diabetes and habitual caffeine intake. *Nutrition & Metabolism*, 13(1), 66. <https://doi.org/10.1186/s12986-016-0126-6>
- van Dusseldorp, M., Smits, P., Thien, T., & Katan, M. B. (1989). Effect of decaffeinated versus regular coffee on blood pressure. A 12-week, double-blind trial. *Hypertension*, 14(5), 563–569. <https://doi.org/10.1161/01.HYP.14.5.563>
- van Zuylen, E. J., Gielen, C. C., & Denier van der Gon, J. J. (1988). Coordination and inhomogeneous activation of human arm muscles during isometric torques. *Journal of Neurophysiology*, 60(5), 1523–1548. <https://doi.org/10.1152/jn.1988.60.5.1523>
- Vigotsky, A. D., Halperin, I., Lehman, G. J., Trajano, G. S., & Vieira, T. M. (2018). Interpreting Signal Amplitudes in Surface Electromyography Studies in Sport and Rehabilitation Sciences. *Frontiers in Physiology*, 8. <https://www.frontiersin.org/articles/10.3389/fphys.2017.00985>
- Walton, C., Kalmar, J., & Cafarelli, E. (2003). Caffeine increases spinal excitability in humans. *Muscle & Nerve*, 28(3), 359–364. <https://doi.org/10.1002/mus.10457>
- Walton, C., Kalmar, J. M., & Cafarelli, E. (2002). Effect of caffeine on self-sustained firing in human motor units. *The Journal of Physiology*, 545(2), 671–679. <https://doi.org/10.1113/jphysiol.2002.025064>

- Wang, L.-J., Yu, X.-M., Shao, Q.-N., Wang, C., Yang, H., Huang, S.-J., & Niu, W.-X. (2020). Muscle Fatigue Enhance Beta Band EMG-EMG Coupling of Antagonistic Muscles in Patients With Post-stroke Spasticity. *Frontiers in Bioengineering and Biotechnology*, 8, 1007. <https://doi.org/10.3389/fbioe.2020.01007>
- Warren, G. L., Park, N. D., Maresca, R. D., Mckibans, K. I., & Millard-Stafford, M. L. (2010). Effect of Caffeine Ingestion on Muscular Strength and Endurance: A Meta-Analysis. *Medicine & Science in Sports & Exercise*, 42(7), 1375–1387. <https://doi.org/10.1249/MSS.0b013e3181cabbd8>
- Watanabe, K., Vieira, T. M., Gallina, A., Kouzaki, M., & Moritani, T. (2021). Novel Insights Into Biarticular Muscle Actions Gained From High-Density Electromyogram. *Exercise and Sport Sciences Reviews*, 49(3), 179–187. <https://doi.org/10.1249/JES.0000000000000254>
- Wei, K., Glaser, J. I., Deng, L., Thompson, C. K., Stevenson, I. H., Wang, Q., Hornby, T. G., Heckman, C. J., & Kording, K. P. (2014). Serotonin Affects Movement Gain Control in the Spinal Cord. *Journal of Neuroscience*, 34(38), 12690–12700. <https://doi.org/10.1523/JNEUROSCI.1855-14.2014>
- Wendt, I. R., & Stephenson, D. G. (1983). Effects of caffeine on Ca-activated force production in skinned cardiac and skeletal muscle fibres of the rat. *Pflügers Archiv*, 398(3), 210–216. <https://doi.org/10.1007/BF00657153>
- Whitsett, T. L., Manion, C. V., & Christensen, H. D. (1984). Cardiovascular effects of coffee and caffeine. *The American Journal of Cardiology*, 53(7), 918–922. [https://doi.org/10.1016/0002-9149\(84\)90525-3](https://doi.org/10.1016/0002-9149(84)90525-3)
- Wilson, J. M., Thompson, C. K., Miller, L. C., & Heckman, C. J. (2015). Intrinsic excitability of human motoneurons in biceps brachii versus triceps brachii. *Journal of Neurophysiology*, 113(10), 3692–3699. <https://doi.org/10.1152/jn.00960.2014>
- Wolf, S. L., Segal, R. L., & English, A. W. (1993). Task-oriented EMG activity recorded from partitions in human lateral gastrocnemius muscle. *Journal of Electromyography and Kinesiology*, 3(2), 87–94. [https://doi.org/10.1016/1050-6411\(93\)90003-F](https://doi.org/10.1016/1050-6411(93)90003-F)
- Wood, S. J., & Slater, C. (2001). Safety factor at the neuromuscular junction. *Progress in Neurobiology*, 64(4), 393–429. [https://doi.org/10.1016/S0301-0082\(00\)00055-1](https://doi.org/10.1016/S0301-0082(00)00055-1)
- Xu, Z., Meng, Q., Ge, X., Zhuang, R., Liu, J., Liang, X., Fan, H., Yu, P., Zheng, L., & Zhou, X. (2021). A short-term effect of caffeinated beverages on blood pressure: A meta-analysis of randomized controlled trails. *Journal of Functional Foods*, 81, 104482. <https://doi.org/10.1016/j.jff.2021.104482>

Yang, Q., Fang, Y., Sun, C.-K., Siemionow, V., Ranganathan, V. K., Khoshknabi, D., Davis, M. P., Walsh, D., Sahgal, V., & Yue, G. H. (2009). Weakening of functional corticomuscular coupling during muscle fatigue. *Brain Research*, 1250, 101–112. <https://doi.org/10.1016/j.brainres.2008.10.074>

Zaback, M., Tiwari, E., Krupka, A. J., Marchionne, F., Negro, F., Lemay, M. A., & Thompson, C. K. (2022). Toward Assessing the Functional Connectivity of Spinal Neurons. *Frontiers in Neural Circuits*, 16. <https://www.frontiersin.org/articles/10.3389/fncir.2022.839521>

## APPENDIX A

### RELATIONSHIP BETWEEN CAFFEINE CONSUMPTION AND OUTCOME VARIABLES

A post hoc analysis of the relationship between baseline caffeine consumption and the effects of CAF on cardiovascular (MAP) and motor unit discharge characteristics failed to reveal significant correlations. These findings suggest previous or preferred caffeine use have no significant correlation with the main outcome measures in Chapter 4/AIM 3 (Below are the results of Pearson's product-moment correlations from R-Studio).

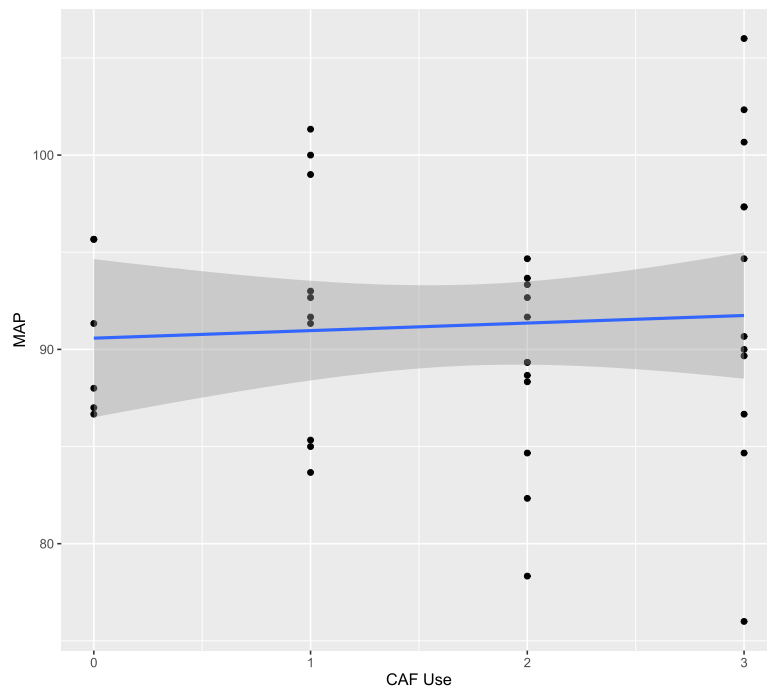


Figure A.1. Mean Arterial Pressure vs Caffeine Use. Data: CAFdata\$MAP and CAFdata\$CAFUSE;  $t = 0.39411$ ,  $df = 38$ ,  $p\text{-value} = 0.6957$ ; 95 percent confidence interval: -0.2527303 0.3679975; sample estimates: cor 0.06380209.

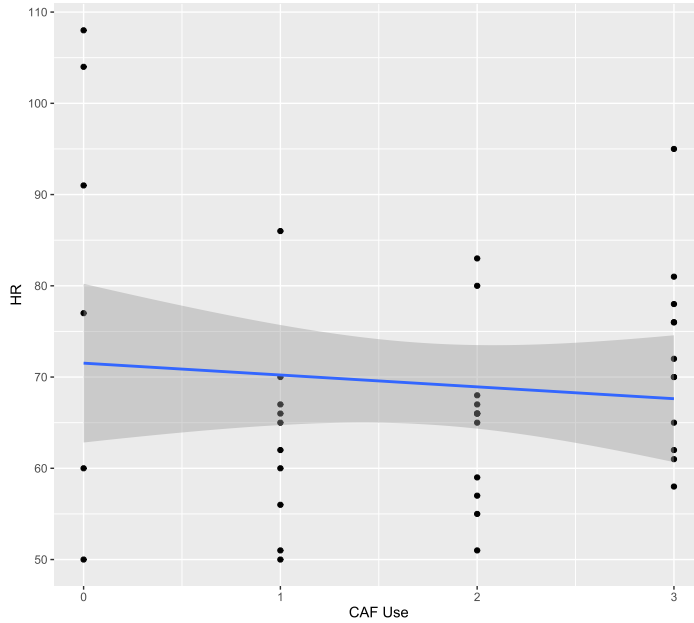


Figure A.2. Hear Rate vs Caffeine Use. Data: CAFdata\$HR and CAFdata\$CAFUSE;  $t = -0.61587$ ,  $df = 38$ ,  $p\text{-value} = 0.5417$ ; 95 percent confidence interval:  $-0.3985787$   $0.2188750$ ; sample estimates:  $\text{cor} -0.09941249$ .

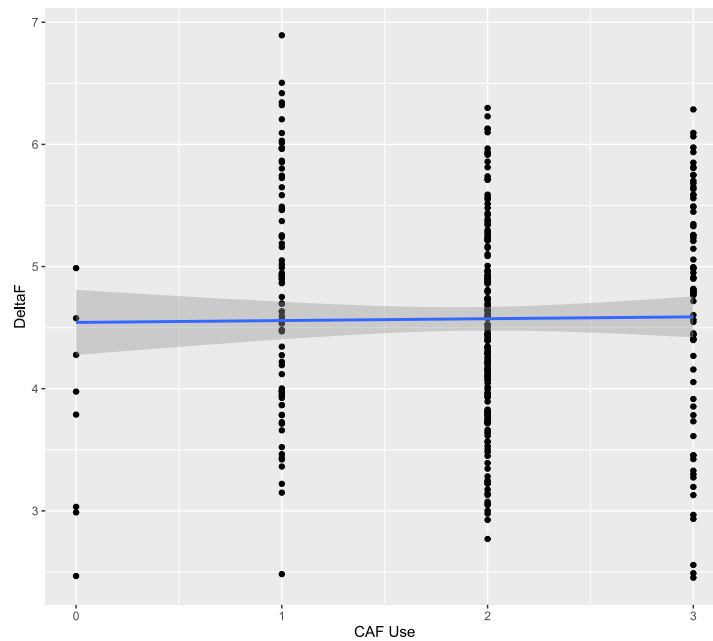


Figure A.3. Delta-F vs Caffeine Use. Data: dataTACAF\$DeltaF and dataTACAF\$CAFUse;  $t = 0.23186$ ,  $df = 329$ ,  $p\text{-value} = 0.8168$ ; 95 percent confidence interval:  $-0.09514968$   $0.12041629$ ; sample estimates:  $\text{cor} 0.01278181$ .

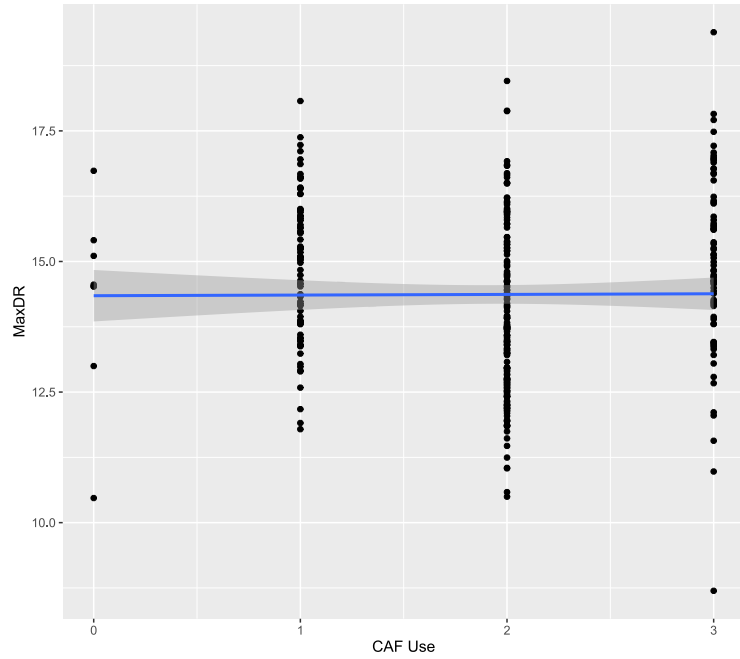


Figure A.4. Maximum DR vs Caffeine Use. Data: dataTACAF\$MaxDR and dataTACAF\$CAFUse;  $t = 0.10223$ ,  $df = 329$ ,  $p\text{-value} = 0.9186$ ; 95 percent confidence interval: -0.1022266 0.1133674; sample estimates: cor 0.005635916

## APPENDIX B

### EFFECTS OF REPEATED CONTRACTIONS

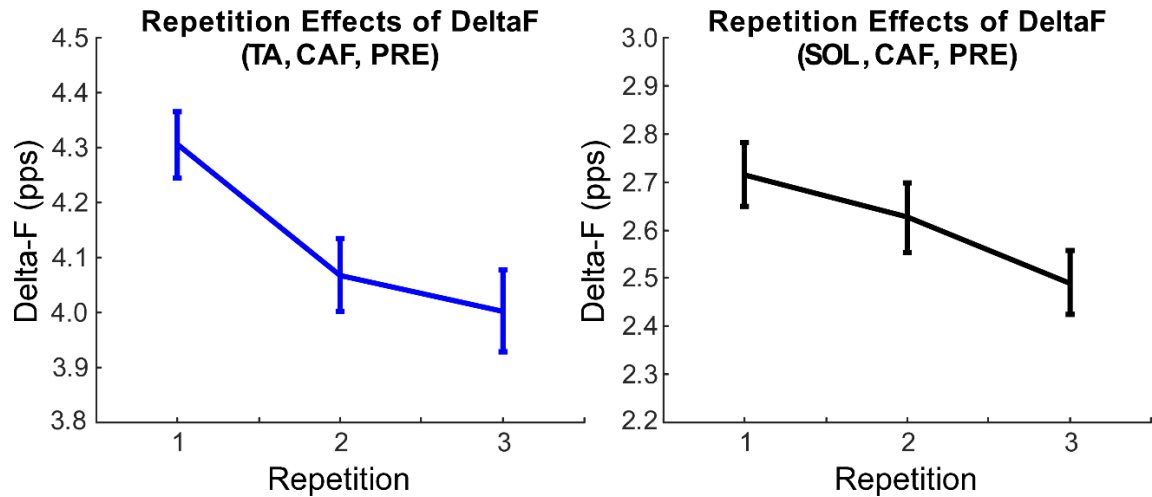


Figure B.1. Effects of Repeated Contractions on Delta-F. Data represents mean and standard error for all available motor units at each timepoint, condition, and motor pool. A global reductions in Delta-F can be observed within sets of repetitions. To mitigate these unintended effects the data from AIM 3 utilized only the first repetition of the highest MU Yield set, per subject, per time point.










## APPENDIX C

### CAFFEINE CONSUMPTION QUESTIONNAIRE

We would like to know how much caffeine you consume












Indicate in the table, how much you drank yesterday.  
Put a line in the box for every cup/glass.  
If you didn't drink the Item, leave the box empty.

Portion sizes:

Small cup 150 mL	Large cup 250 mL	Small glass 150 mL	Large glass 250 mL	Energy Drink Dose 250 mL	Energy drink Dose 500 mL	Energy shot Dose 60 mL	Espresso cup 60 mL	Chocolate bar 20g
								

For example, like this:

	Coffee		Cola, fizzy, soft drink		Chocolate
Breakfast	II	I	I	I	I

	Coffee	Decaffeinated coffee	Espresso	Black-, green, white, mate tea	Cocoa drink	Iced tea, drinks with tea extract	Cola, mixed cola beverages (but not orangeade and lemonade)	Energy drink	Energy shot	Alcopops with energy drink, cola or coffee	Chocolate
											
Breakfast											
Between breakfast and lunch											
lunch											
Between lunch and dinner											
Dinner											
After dinner											

© K. Schlägel, Hochschule Albstadt-Sigmaringen

Figure C.1. Caffeine Consumption Questionnaire. Subjects in AIM 3 completed this questionnaire, in order to stratify baseline caffeine consumption prior to enrollment into the intervention arm.

## APPENDIX D

### CHANGE IN STRENGTH OVER TIME

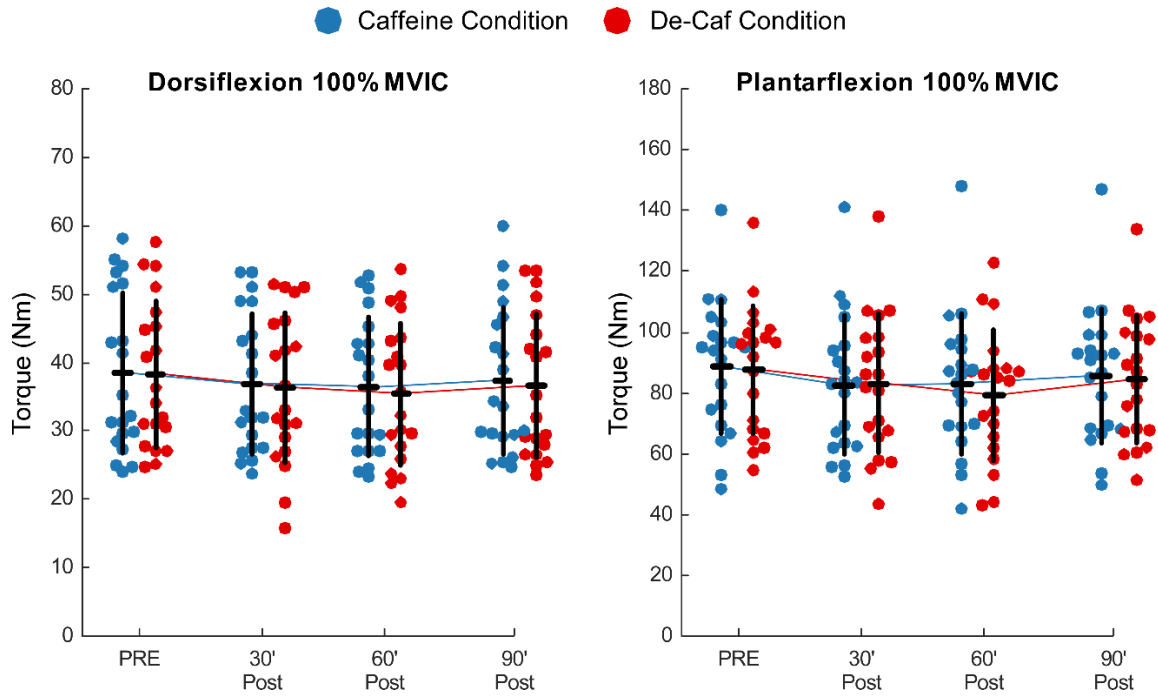


Figure D.1. Change in Maximum Strength. Maximum volitional isometric contraction (MVIC) values for all 20 subjects within AIM 3. No significant effect of time of condition was observed.

## APPENDIX E

### MUSCLE OR DISCHARGE RATE DEPENDENT

Within the final analysis reported in Chapter 4, a muscle-specific effect of caffeine was observed within the TA motor pool. Because the known discharge rates of the TA and SOL vary substantially (TA (12.3 pps) and SOL (8.2 pps) at 20% MVIC during HOLDS), a post hoc analysis was conducted on each motor pool independently, to assess if these effects represent true muscle-specific differences or differences in responsiveness based on the discharge rate of the individual MNs.

LMEMs were created to assess the relationship of *Delta-F* ( $\Delta F$ ) with the fixed effects of *Condition*, *Time*, *MaxDR*, their interactions and random effects of *unique motor unit* nested within *Subject*. This model was created and performed, first on data containing only TA MNs and a second iteration only on SOL MNs. To inspect the influence of MaxDR through the continuum of MNs within a single muscle, the predictor variable (MaxDR) was centered to reduce the correlation between the predictor variable and the intercept. Furthermore, we analyzed the estimated marginal means contrasted for *Time* and *Condition* to observe any changes within each muscle, independently. Lastly, estimated marginal means were plotted and investigated for the effects of CAF, for each muscle, at one standard deviation below the mean of *MaxDR* (-SD), at the mean of *MaxDR*, and at one standard deviation above the mean of *MaxDR* (+SD).

The main effects of *Condition\*Time* (originally observed in chapter 4) were no longer statistically significant. Instead, within both motor pools, a significant main effect of MaxDR was found (TA  $X^2 = 13.7$ ,  $p < 0.001$ ; SOL  $X^2 = 4.7$ ,  $p = 0.034$ ). This indicates

a strong interaction between the *MaxDR* and *Delta-F* variables. Pearson correlation coefficient revealed a positive correlation between *DeltaF* and *MaxDR* (TA:  $r(621)=0.38$ ,  $p < 0.001$ ; SOL:  $r(212)=0.28$ ,  $p = 0.001$ ). This finding is unsurprising as the change in discharge rate of the paired lower threshold MN is explicitly used to quantify Delta-F, and the tracked pairs of MNs used in this method are likely highly correlated themselves. No other main effects achieved statistical significance. However, when comparing estimated marginal means contrasted for *Time* and *Condition*,  $\Delta F$  values significantly differed ( $p < 0.0001$ ;  $d=0.99-1.24$ ) between PRE-to-30-Post and PRE-to-60-Post time points within the CAF condition of the TA only. Lastly, when plotting predicted values of *MaxDR* centered at -SD, mean, and +SD; effects of CAF were only observed in the TA motor pool (see **Figure E.1. & E.2.**).

These findings suggest that the observed effects of caffeine within chapter 4 reflect genuine muscle-specific differences in caffeine responsiveness and amplification of PICs (when comparing TA vs SOL MNs). Further, we demonstrate  $\Delta F$  is correlated with the maximum discharge rate of tracked high threshold units (*MaxDR*). However, through inspection of marginal means contrasted for *Time* and *Condition*, we observe MNs within the TA motor pool, despite this correlation, respond selectively to the effects of CAF across the entire firing profile of the TA motor pool.

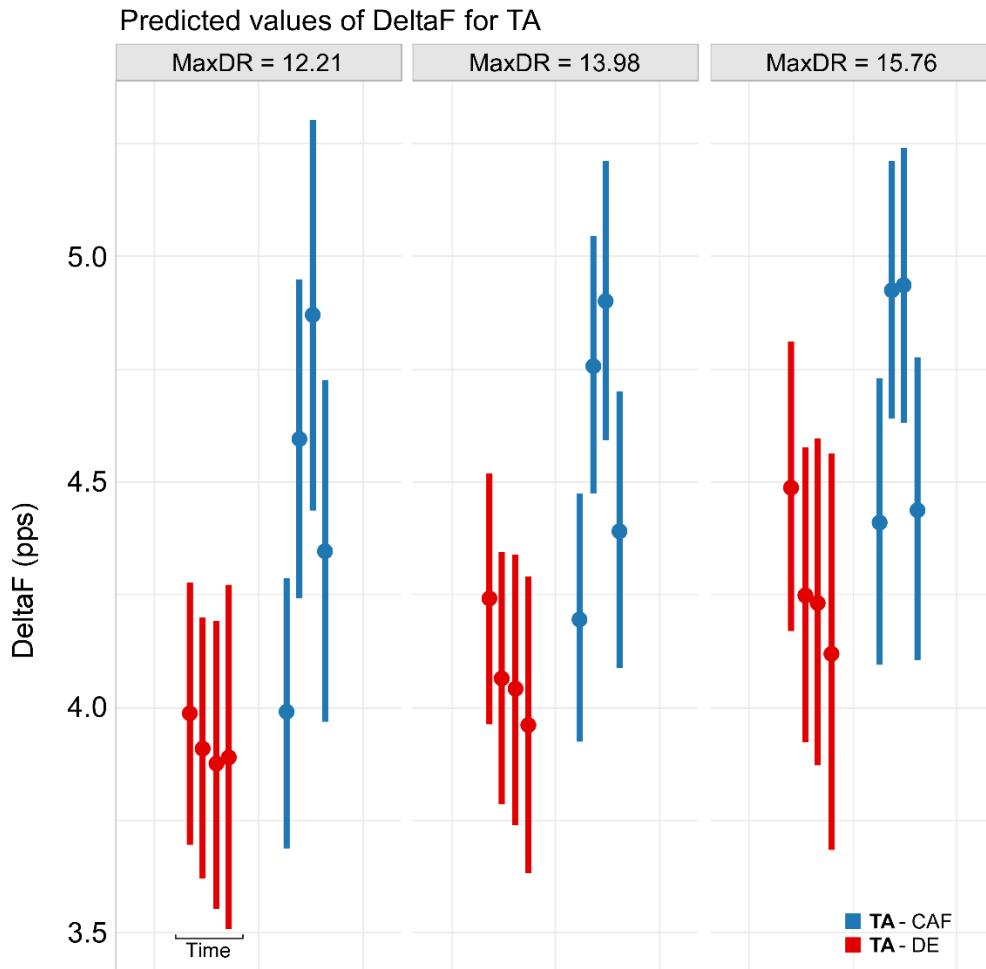


Figure E.1. DeltaF Across MaxDR of TA. Estimated marginal means of TA Delta-F, centered at one standard deviation below the mean (left; -SD; 12.21 pps), mean (middle; 13.98 pps), and one standard deviation above the mean (right; +SD; 15.76 pps), contrasts for Condition (CAF vs DE) and Time (Pre, post-30', post-60', post-90').

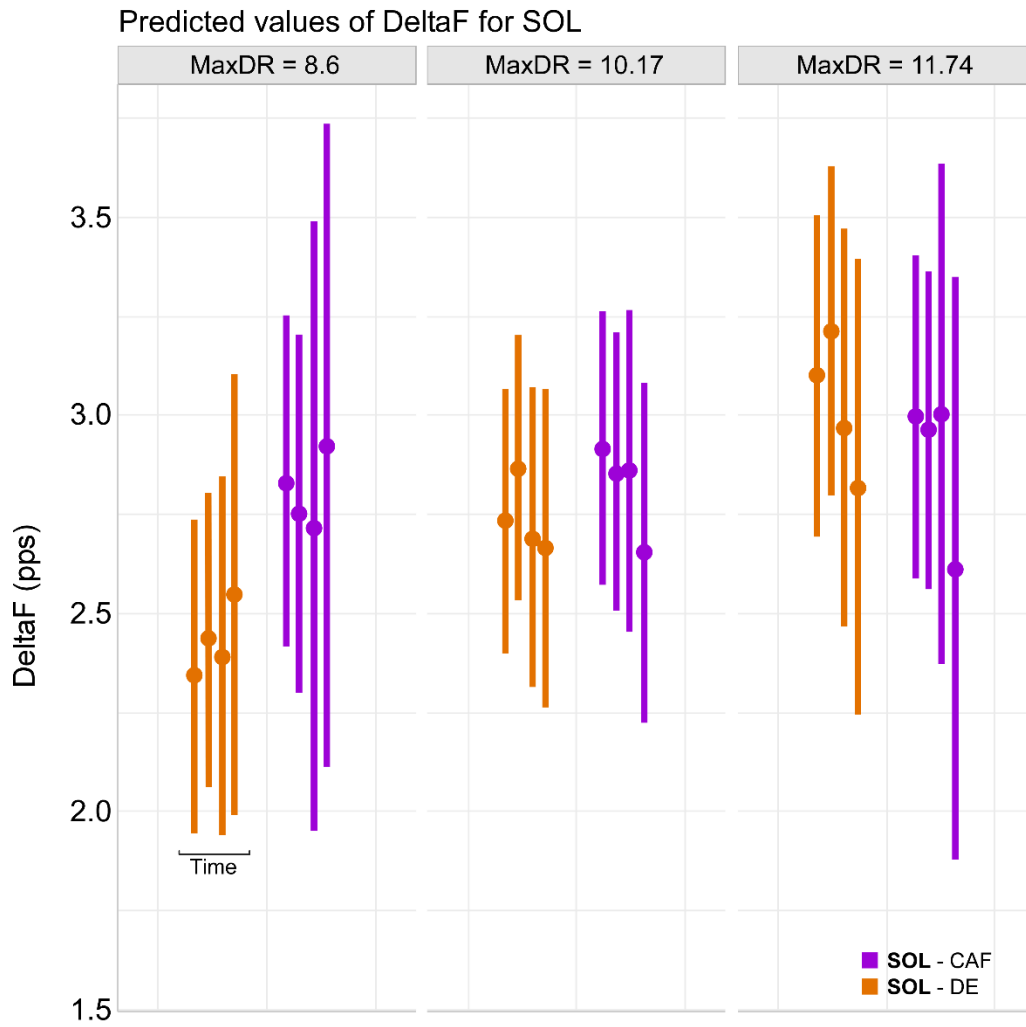


Figure E.2. DeltaF Across MaxDR of SOL. Estimated marginal means of SOL Delta-F, centered at one standard deviation below the mean (left; -SD; 8.6 pps), mean (middle; 10.17 pps), and one standard deviation above the mean (right; +SD; 11.74 pps), contrasts for Condition (CAF vs DE) and Time (Pre, post-30', post-60', post-90').